

**Influence of fiber direction and temperature on the
tribological behavior of carbon reinforced peek for
applications in gas turbine engines**

Marie-Laurence Cliche

A Thesis
in
The Department
of
Mechanical, Industrial and Aerospace Engineering

Presented in Partial Fulfillment of the Requirements
for the Degree of Master of Applied Science (Mechanical Engineering) at
Concordia University
Montréal, Québec, Canada

Mai 2022

© Marie-Laurence Cliche, 2022

Concordia University
School of Graduate Studies

This is to certify that the thesis prepared

By: Marie-Laurence Cliche

Entitled: Influence of fiber direction and temperature on the tribological behavior of carbon reinforced peek for applications in gas turbine engines

And submitted in partial fulfillment of the requirements for the degree of

Master of Applied Science (Mechanical Engineering)

Complies with the regulations of the University and meets the accepted standards with respect to originality and quality.

Signed by final examining committee

_____ Chair

Dr. Carole El Ayoubi

_____ Examiner

Dr. Marc-Antoni Goulet

_____ Examiner

Dr. Carole El Ayoubi

_____ Supervisor

Dr. Pantcho Stoyanov

Approved by _____

Martin D. Pugh, Chair Department of Mechanical, Industrial
and Aerospace Engineering

May 2022

Mourad Debbabi, Dean Gina Cody School of Engineering and
Computer Science

Abstract

Influence of fiber direction and temperature on the tribological behavior of carbon reinforced peek for applications in gas turbine engines

Marie-Laurence Cliche

In order to reduce the emissions of greenhouse gas (GHG), many industries are turning towards more environmentally friendly technologies. The aerospace industry is particularly targeted as gas turbine engines will be required to reduce their CO₂ emissions to net zero. New challenges will arise regarding the conditions in which materials are expected to operate (e.g. high temperatures, high velocities, high pressures) in order to achieve this goal. More conventional metals and alloys currently used in engine manufacturing will most likely be limited by their mechanical and tribological properties and thus, proper selection of materials is primordial to ensure the performance and efficiency of engines. Fiber-Reinforced Polymer (FRP) composites have been widely used in the aerospace industry and is one alternative solution due to their lightweight and high-strength properties. However, when considering FRP for the purpose of gas turbine engines, it is also important to consider the orientation of the fibers. Since there are a lot of moving and contacting mechanical assemblies in the engines where a high quantity of elements such as bearings and seals are present, the orientation of the fibers in FRP play a crucial role in ensuring good tribological behaviour. Many different studies have previously performed extensive characterization of carbon reinforced polymer composites and have demonstrated the impact of the parallel and anti-parallel orientation of the fibers on the mechanical properties and tribological behavior of composites. However, FRP composite with fibers oriented in the normal direction, which have shown improved mechanical properties, have received little attention regarding the impact of orienting vertically the fibers on the tribological properties.

The purpose of this study is to fully capture the influence of the fiber direction (parallel, anti-parallel and normal direction) in fiber-reinforced composite, with an emphasis on carbon fiber/PEEK composite, and the influence on its tribological behavior for the purpose of gas turbine engines. The research performed throughout this study is divided into two parts where the influence of fiber direction in FRP composites on the tribological behaviour have been critically

examined. The main focus of the first study is to identify the influence of fiber orientation on the surface energy and tribological behavior of CF-PEEK systems for the Fan and LPC region of the gas turbine engine (i.e. room temperature). The focus of the second study is to identify the influence of temperature on the tribological behavior of carbon fiber-reinforced PEEK. The tribological tests were performed using a ball-on-disk tribometer where the samples were subjected to different testing parameters to simulate more accurately the operating environment the material would have to go through in the engine. This includes a high loading, an elevated testing temperature, and a high number of cycles. The characterization to obtain the interfacial phenomena of the different worn surfaces and counterfaces was done using Scanning Electron Microscopy (SEM), confocal laser scanning microscopy (CLSM), Energy Dispersive X-ray Spectroscopy (EDS) and Atomic Force Microscope (AFM). Overall, it was found that there is a clear benefit of using CF-PEEK reinforced with fibers in the normal direction since it showcases better tribological properties, a higher reliability and higher potential of integrations within the gas turbine engines.

Table of Contents

List of Figures	viii
List of Tables	xi
Organization of the Thesis	xii
1. Introduction & Scope.....	1
1.1. Introduction	2
1.2. Scope	4
1.3. Methodology	4
1.4. Final remarks.....	7
1.5. References	8
2. Literature Review	11
2.1. Tribology review	12
2.1.1. Why the need of tribological evaluation?	12
2.1.2. Friction.....	13
2.1.3. Wear	15
2.2. Tribology of fiber-reinforced polymer composites.....	16
2.2.1. Fiber-reinforced polymer composites.....	16
2.2.2. Tribological properties of fiber-reinforced polymer composites.....	18
2.2.3. Impact of fiber length & orientation on the tribological properties of fiber-reinforced polymer composites.....	19
2.2.4. Impact of temperature on the tribological properties of fiber-reinforced polymer composites	21
2.3. Statistical Analysis	22
2.4. References	23

3. Influence of fiber direction on the tribological behavior of carbon reinforced PEEK for applications in gas turbine engines	26
3.1. Abstract	27
3.2. Introduction	28
3.3. Experimental procedure	30
3.3.1. Materials	30
3.3.2. Characterization and Tribological Evaluation	32
3.4. Results	34
3.4.1. Friction Behaviour	34
3.4.2. Wear Behaviour	35
3.4.3. Ex Situ Analysis.....	37
3.5. Discussion	44
3.6. Conclusion.....	49
3.7. References	50
4. Influence of temperature and fiber direction on the tribological behavior of carbon reinforced PEEK for applications in gas turbine engines.....	54
4.1. Abstract	55
4.2. Introduction	56
4.3. Materials & methods	58
4.3.1. Materials	58
4.3.2. Tribological Evaluation & Characterization Methods.....	59
4.3.3. Friction Behaviour	61
4.3.4. Wear Behaviour	62
4.3.5. Ex Situ Analysis.....	64
4.4. Discussion	72

4.5.	Conclusion.....	76
4.6.	References	77
5.	Conclusion & Future Work	81
5.1.	Conclusion.....	82
5.2.	Future work	84
5.3.	References	87

List of Figures

Figure 1.1: Gas turbine engine materials and operating temperatures in different sections [4].....	2
Figure 1.2: Top front view of Anton-Paar TRB3 tribometer [29]	5
Figure 1.3: Linear Reciprocating Module with Universal Sample Holder of Anton-Paar TRB3 tribometer [29]	6
Figure 1.4: Temperature LED on left top panel of Anton-Paar TRB3 tribometer [29].....	7
Figure 2.1: Factors influencing tribological properties of materials.....	12
Figure 2.2: Components of sliding friction [3]	14
Figure 2.3: Relationship between operating conditions and type of wear [3]	16
Figure 2.4: Classification of composites [6]	17
Figure 2.5: FRP composite components used in aircraft structures [9].....	17
Figure 2.6: "Areas of influence on the tribological performance of composite materials" [11]...	18
Figure 2.7: Wear mechanism of parallel and anti-parallel FRP [3].....	19
Figure 2.8: "Effect of fiber length on the specific wear rate of epoxy composites" [13]	20
Figure 2.9: Pictorial illustration of the fiber orientation in relation to the sliding direction [13].	20
Figure 2.10: Effect of the increase of temperature on the A) elastic modulus, B) Tensile strength C) fracture strain of PEEK [24]	21
Figure 3.1: 60"-wide ZRT film production line installed at Boston Materials' factory in Billerica MA, USA [26]	29
Figure 3.2: Cross-section of a ZRT composite film	30
Figure 3.3: Samples Fiber Orientation.....	31
Figure 3.4: Schematic Representation of ball-on-disk linear tribometer	32
Figure 3.5: Friction Behaviour of the samples.....	34

Figure 3.6: Wear Measurement for a 18N Load on A) CF-PEEK Normal to the Fiber Direction Sample B) Pure Peek Sample C) CF-PEEK Parallel to the Fiber Direction Sample D) CF-PEEK Anti-parallel to the Fiber Direction Sample.....	35
Figure 3.7: Wear Rate of the Samples	36
Figure 3.8: SEM Analysis of Sample Surface A) CF-PEEK Normal to the Fiber Direction Sample B) Pure Peek Sample C) CF-PEEK Parallel to the Fiber Direction Sample D) CF-PEEK Anti-parallel to the Fiber Direction Sample	37
Figure 3.9: SEM Analysis of Sample Wear Track A) CF-PEEK Normal to the Fiber Direction Sample B) Pure Peek Sample C) CF-PEEK Parallel to the Fiber Direction Sample D) CF-PEEK Anti-parallel to the Fiber Direction Sample.....	38
Figure 3.10: Adhesion Force of the A) Unworn Samples B) Worn Samples Using AFM Spectroscopy	39
Figure 3.11: Estimation of the Nano Hardness of the Unworn (left) and Worn (right) samples Using AFM Spectroscopy	40
Figure 3.12: CF-PEEK Parallel to the Fiber Direction A) Failure due to a Crack on the Surface	41
Figure 3.13: Confocal Images of Counterface for A) CF-PEEK Normal to the Fiber Direction Sample B) Pure Peek Sample	41
Figure 3.14: Transfer Film Formation	42
Figure 3.15:SEM Analysis of Samples Counterfaces A) CF-PEEK normal to the fiber direction Sample B) Pure Peek Sample	43
Figure 3.16: EDS Analysis on the Counterfaces	44
Figure 3.17: Ploughing mechanism	45
Figure 3.18: Shearing Mechanism	46
Figure 4.1: Contacting Mechanical-Assemblies in Cross-Section of Gas Turbine Engine [1]	56
Figure 4.2: Temperature range for polymers materials currently in use [25].....	57
Figure 4.3: ZRT/PEEK film Manufacturing Schema	59

Figure 4.4: Friction Behaviour on Polished Samples at 200°C	62
Figure 4.5: Wear Measurement at 200°C A) CF-PEEK Normal to the Fiber Direction Sample B) Pure Peek Sample C) CF-PEEK Parallel to the Fiber Direction Sample D) CF-PEEK Anti-parallel to the Fiber Direction Sample	63
Figure 4.6: Wear Rate of the Samples at 200°C	64
Figure 4.7: SEM Analysis of Sample Surface at 200°C A) CF-PEEK Normal to the Fiber Direction Sample B) Pure Peek Sample C) CF-PEEK Parallel to the Fiber Direction Sample D) CF-PEEK Anti-parallel to the Fiber Direction Sample.....	65
Figure 4.8: SEM Analysis of Sample Wear Track at 200°C A) CF-PEEK Normal to the Fiber Direction Sample B) Pure Peek Sample C) CF-PEEK Parallel to the Fiber Direction Sample D) CF-PEEK Anti-parallel to the Fiber Direction Sample	66
Figure 4.9: CF-PEEK Parallel to the Fiber Direction Mechanics of Damages at 200°C.....	67
Figure 4.10:EDS Line Analysis of Sample Wear Track at 200°C A) CF-PEEK Normal to the Fiber Direction Sample B) CF-PEEK Parallel to the Fiber Direction Sample C) CF-PEEK Anti-parallel to the Fiber Direction Sample D) Pure Peek Sample.....	68
Figure 4.11: Confocal Images of Counterface at 200°C A) CF-PEEK Normal to the Fiber Direction Sample B) Pure Peek Sample	70
Figure 4.12:SEM Analysis of Samples Counterfaces at 200°C A) CF-PEEK normal to the fiber direction Sample B) Pure Peek Sample C) CF-PEEK Parallel to the Fiber Direction Sample D) CF-PEEK Anti-parallel to Fiber Direction Sample	71
Figure 4.13: EDS Analysis on the Counterfaces at 200°C.....	72
Figure 4.14: Pictorial representation of a transfer film formation on a counterface.....	74
Figure 5.1: Interpretation of contact angle measurement results for hydrophobicity [2]	84
Figure 5.2:Advancing angle measurement A) CF-PEEK (normal) sample B) CF-PEEK (parallel and anti-parallel) sample.....	85
Figure 5.3: Receding angle measurement A) CF-PEEK (normal) sample B) CF-PEEK (parallel and anti-parallel) sample.....	85

Figure 5.4: Critical force for contact line movement..... 86

List of Tables

Table 3-1: Tribometer Testing Parameters 33

Table 4-1: Samples Descriptions 58

Table 4-2: Tribological testing parameters 60

Organization of the Thesis

- Chapter 1 present an introduction as well as the overall scope and purpose of this thesis.
- Chapter 2 present an overview of the fundamentals of tribology, and a literature review of the tribology of fiber-reinforced composite materials.
- Chapter 3 present the tribological study on the influence of fiber direction on the tribological behavior of carbon reinforced PEEK for applications in gas turbine engines. This study was performed at room temperature with high contact conditions and over time to simulate the harsh conditions in which tribological interfaces are subjected to in gas turbine engines.
- Chapter 4 present the tribological study on the influence of temperature and fiber direction on the tribological behavior of carbon reinforced PEEK for applications in gas turbine engines. This study was performed at an elevated temperature of 200°C with again high contact conditions and over time to showcase the potential implementation of carbon fiber PEEK in components situated in the front region of gas turbine engines.
- Chapter 5 present the final conclusions and proposal for future work regarding the use of carbon fiber-reinforced PEEK within the aerospace industry.

Chapter

1. Introduction & Scope

In this chapter...

An introduction as well as the overall scope and the purpose of this thesis is presented.

1.1. Introduction

Whitin the next 30 years, the aerospace industry has set a goal to reduce greenhouse gas (GHG) emissions to net-zero, which will bring several new challenges to the design of gas turbine engines [1] [2] [3]. Such reduction in GHG will only be possible by shifting towards low-carbon technologies in gas turbine engines such as hydrogen fuel cells and low carbon intensity fuels, which will require an increase in thermal efficiency and performance of the engines [2] [4] [5] [6]. However, the implementation of these technologies will create a more challenging environment within the engines, where materials will need to operate under higher velocities, pressure, and temperature and thus, making the selection of materials for specific regions of the engines harder [7] [8] [9]. Currently, in the manufacturing of gas turbine engines, the most common materials that are being employed, as seen in Figure 1.1, are aluminum, titanium, steel, and nickel [10] [11]. The material selection process heavily depends on the operating and temperature conditions of the region within the engines [10] [11]. Typically, in the front of the engine materials operates at lower temperature and in the back of the engine, materials operate at higher temperatures (Figure 1.1) [4]. Therefore, with the new arisen challenges, the option of more conventional metal and alloys, currently used in gas turbine engines, will be limited by their mechanical and tribological properties and consequently, a new generation of aerospace materials will need to be developed in order to fulfill the need of the aerospace industry.

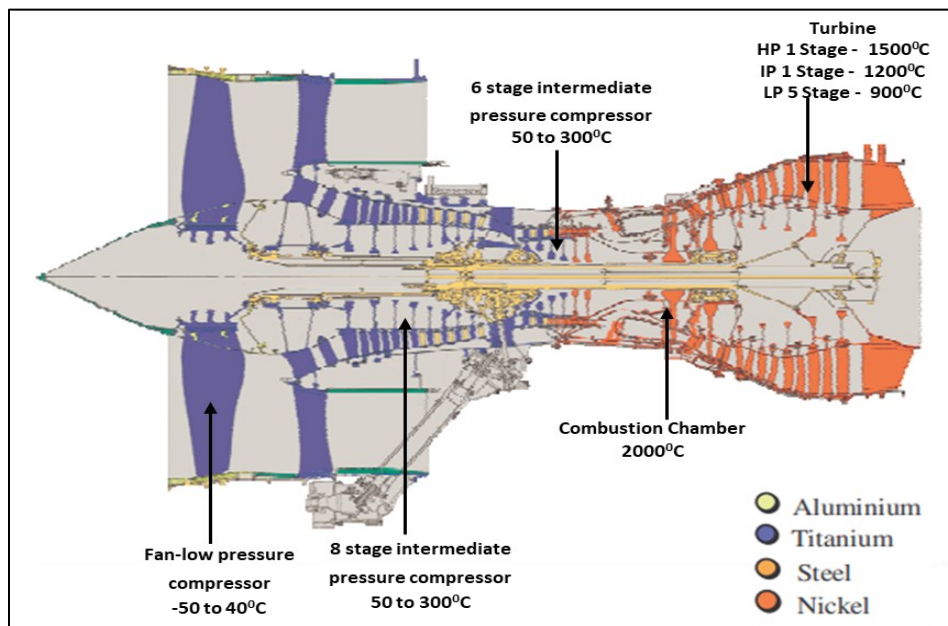


Figure 1.1: Gas turbine engine materials and operating temperatures in different sections [4]

Due their high structural properties and their light weight, fiber-reinforced polymer (FRP) composite could be a cost-effective alternative solution to conventional metals or alloys for certain components in the engine [12] [13]. Although commercially available composites have many advantages and are already widely used in the aerospace industry, there are limitations regarding their usage in load-bearing situations [14] [15] [16] since they often fail prematurely due to delamination and/or fiber breakage [16] [17]. This implies that there persists to be a deficiency in the through-thickness properties of composite materials. Consequently, through-thickness reinforcement of the composite is necessary in order to improve its mechanical properties as well as its interlaminar damage tolerance [18] [19] [20].

Additional factors also need to be considered for the implementation of FRP in gas turbine engines including the choice of polymer matrix and fiber orientation. Due to the higher operating temperature requirements of the region of the front of the engine, typically ranging from -40°C to 300°C [10], the choice of the matrix material is a determining factor since the glass transition temperature of polymers is lower than the fibers [21]. Furthermore, since there are a lot of moving and contacting mechanical assemblies in the engines where a high quantity of elements such as bearings and seals are present [22] [23], the orientation of fibers against the direction of motion in FRP is crucial to ensure good tribological properties [24] [25]. Although studies have already been performed on the tribological characterization of the parallel and anti-parallel fiber orientation in FRP [25] [26] [27], little attention has been given to the characterization of the normal orientation of FRP for the purpose of implementation in long-lasting gas turbine engines.

1.2. Scope

The main objective of this thesis is to provide a better understanding of the influence of the fiber direction on the tribological behavior of fiber-reinforced composite, with an emphasis on carbon fiber/ PEEK composite. The following sub-objectives are addresses throughout this work:

SO1 → Develop a methodology and procedure for evaluating the tribological behavior of carbon fiber/PEEK composite for applications in gas turbine engines

SO2 → Identify the influence of fiber orientation on the surface energy and tribological behavior of CF-PEEK systems for the Fan and LPC region of the gas turbine engine (i.e. room temperature).

SO3 → Identify the influence of temperature on the tribological behavior of carbon fiber PEEK.

1.3. Methodology

To provide a better understanding of the influence of fiber direction and temperature on the tribological properties of carbon fiber/ PEEK composite, tribometer tests were performed using a ball-on-disk linear tribometer (Anton-Paar TRB3 tribometer). The top front view of the tribometer as well as the description of each component is shown in Figure 1.2. In the ball-on-disk linear tribometer, the integrated two friction force sensors and a symmetrical elastic measuring arm allows to record the data from the tribological testing into a modelization software for easy data treatment and more importantly and for the purpose of this study, the obtention of the friction curve [28]. To ensure validity of the data, the calibration of different sections of the tribometer is crucial which includes the calibration of the motor and the calibration of the friction force using different weights can be done through a set of predefined steps provided in the tribometer user software.

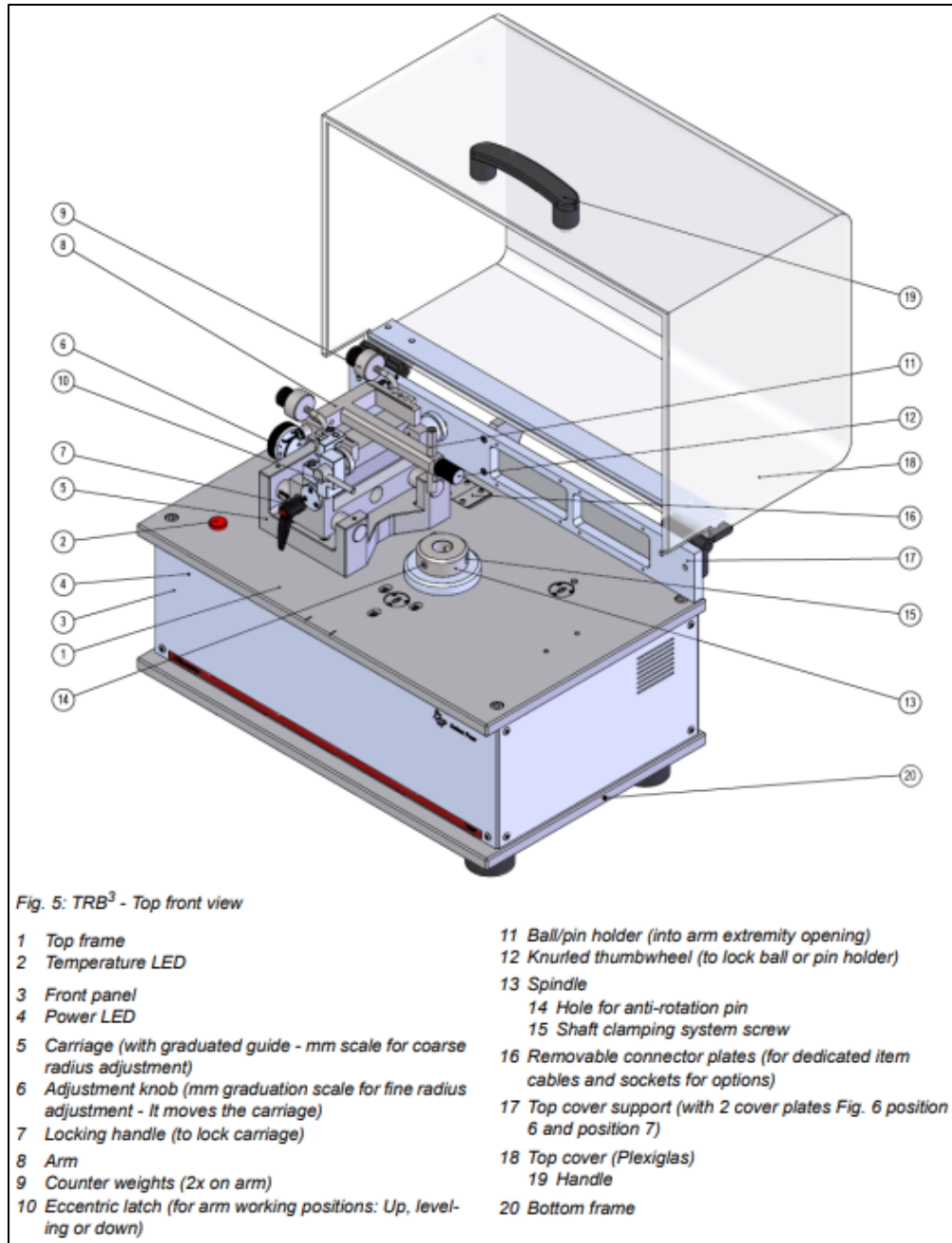


Figure 1.2: Top front view of Anton-Paar TRB3 tribometer [29]

In the Anton-Paar TRB3 ball-on-disk linear tribometer, the sample being tested is held in a universal sample holder attached to a linear assembly which is the fixed based moving in a linear motion provided by the rotation of the motor. The linear distance is predetermined based on the study need and can be adjusted from the cam assembly. The different assemblies are shown in Figure 1.3. Additionally, in the Anton-Paar TRB3 tribometer, the counterface presses stationary

on the surface of the samples and held by the ball/pin holder in the tribometer arm which allows for the recording of the data from the linear displacement of the linear assembly [28].

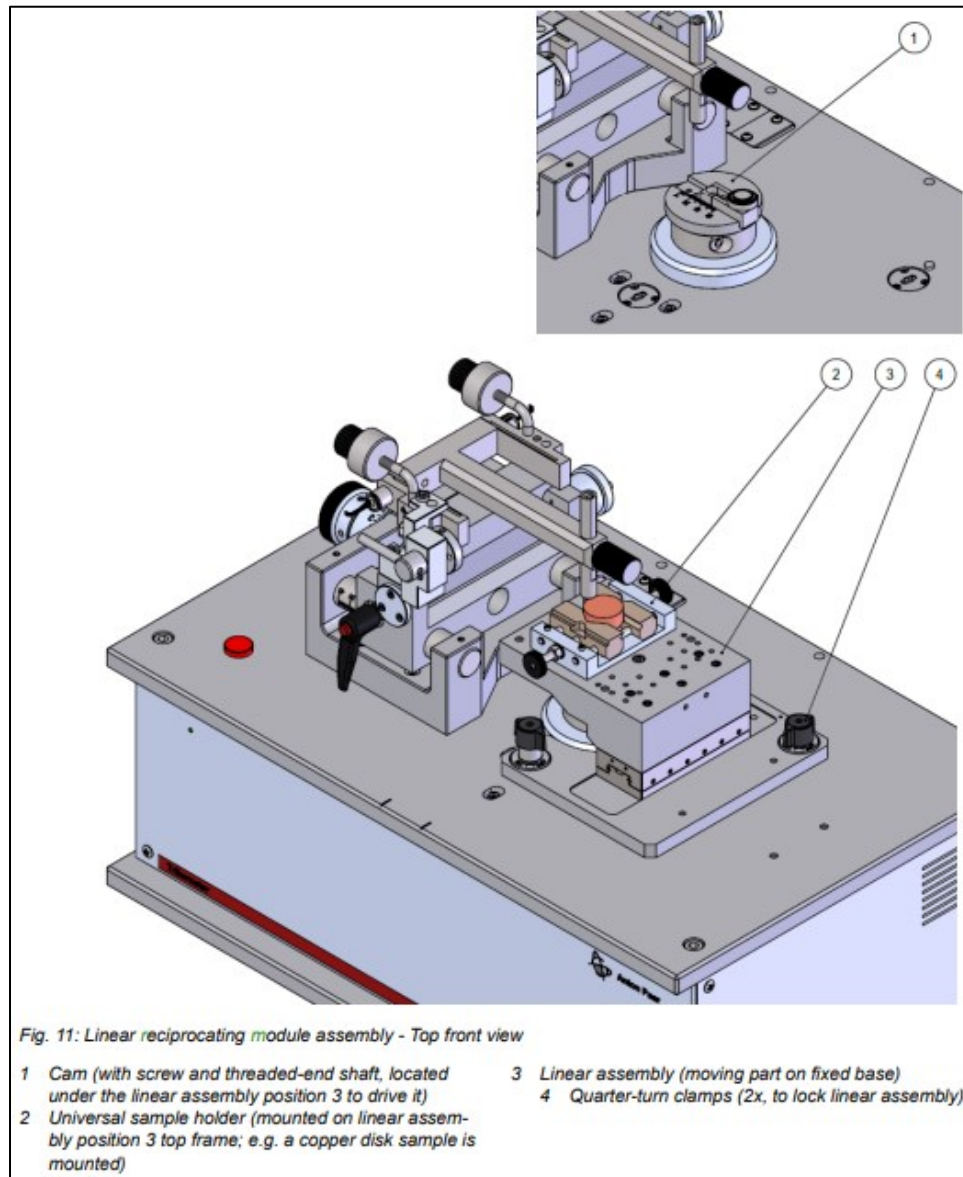


Figure 1.3: Linear Reciprocating Module with Universal Sample Holder of Anton-Paar TRB3 tribometer [29]

Furthermore, the environmental conditions of the tribological testing can also be monitored by different sensors which includes temperature and humidity as shown in Figure 1.4 [28]. It is possible to subject the sample being tested to different temperatures by changing the universal sample holder by the high temperature sample holder which contains a heat source placed directly under the samples. The tribometer testing and recording of the data is done in the same way as for tests at room temperature.

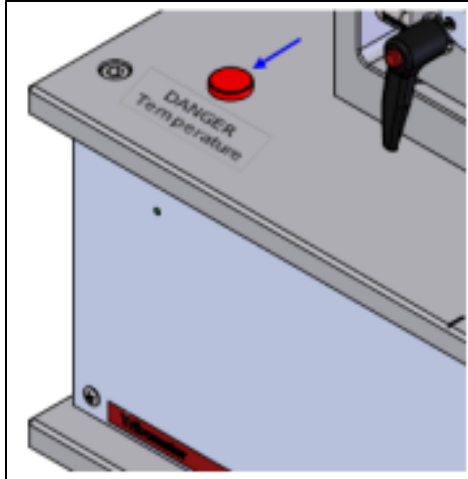


Figure 1.4: Temperature LED on left top panel of Anton-Paar TRB3 tribometer [29]

For the purpose of this study, the carbon fiber/ PEEK composite sample were subjected in a first time with room temperature conditions and in a second time at high temperature conditions. The tribological testing using the Anton-Paar TRB3 ball-on-disk linear tribometer was repeated three times for each of the different fiber orientation (parallel, anti-parallel and normal to the fiber direction) to obtain the variability in the data in between the tests.

1.4. Final remarks

It is to be noted that Chapter three and four of this thesis is in the submission process for publication and thus some information might overlap since the same samples and characterization methods were used.

1.5. References

- [1] E. a. C. C. Canada, "2030 EMISSIONS REDUCTION PLAN Canada's Next Steps for Clean Air and a Strong Economy," Gatineau, 2022.
- [2] T. Canada, "CANADA'S ACTION PLAN to Reduce Greenhouse Gas Emissions from Aviation," Public Works and Government Services Canada, Ottawa, 2012.
- [3] U. D. o. Transportation, "United States 2021 Aviation Climate Action Plan," 2021.
- [4] Z. Wei, S. Zhang, S. Jafari and T. Nikolaidis, "Gas turbine aero-engines real time on-board modelling: A review, research challenges, and exploring the future," *Progress in Aerospace Sciences*, vol. CXXI, no. 1, 2020.
- [5] A. Baroutaji, T. Wilberforce, M. Ramadan and A. Ghani Olabi, "Comprehensive investigation on hydrogen and fuel cell technology in the aviation and aerospace sectors," *Renewable and Sustainable Energy Reviews*, vol. CVI, pp. 31-40, 2019.
- [6] D. Vardon, B. Sherbacow, K. Guan, J. Heyne and Z. Abdullah, "Realizing "net-zero-carbon" sustainable aviation fuel," *Joule*, vol. VI, no. 1, pp. 12-21, 2022.
- [7] M. Hughes, "Challenges for Gas Turbine Engine Components in Power Generation," *Procedia Structural Integrity*, vol. VII, pp. 33-35, 2017.
- [8] D. Chiaramonti, "Sustainable Aviation Fuels: the challenge of decarbonization," *Energy Procedia*, vol. CLVIII, pp. 1202-1207, 2019.
- [9] Z. Pu, G. Zhang, A. Hassanpour, D. W. S. Zheng, S. Liao, Z. Chen and S. Sun, "Regenerative fuel cells: Recent progress, challenges, perspectives and their applications for space energy system," *Applied Energy*, vol. CLXXXIII, p. 116376, 2021.
- [10] P. Spittle, "Gas Trubine Technology," *Physics Education*, vol. XXXVIII, no. 6, pp. 504-511, 2003.
- [11] G. Meetham, "High temperature materials in gas turbine engines," *Materials & Design*, vol. VIII, no. 4, pp. 213-219, 1988.

- [12] M. W. Hyer, *Stress Analysis of Fiber-Reinforced Composite Materials*, Lancaster: DEStech Publications, 2009.
- [13] I. M. Daniel and O. Ishar, *Engineering Mechanics of Composite Materials*, New York: Oxford University Press, 2006.
- [14] P. Mangalgi, "Composite materials for aerospace applications," *Bulletin of Materials Science*, no. 22, pp. 657-664, 1999.
- [15] M. Bellonte, "Composite Materials in the Airbus A380," 2001.
- [16] D. F. Adams, L. A. Carlson and R. B. Pipers, *Experimental Characterization of Advanced Composite*, CRC Press, 2003.
- [17] E. S. Greenhalgh, *Failure Analysis and Fractography of Polymer Composites*, Woodhead Publishing Series in Composites Science and Engineering, 2009, pp. 107-163.
- [18] X. L. P. W. a. D. S. I Gnaba, "Through-the-thickness reinforcement for composite structures: A review," *Journal of Industrial Textiles*, vol. XLIX, no. 1, pp. 71-96, 2019.
- [19] K. Tan, N. Watanabe and Y. Iwahori, "Impact Damage Resistance, Response, and Mechanisms of Laminated Composites Reinforced by Through-Thickness Stitching," *International Journal of Damage Mechanics*, vol. XXI, no. 1, pp. 51-80, 2011.
- [20] G. Pappas, S. Joncas, V. Michaud and J. Botsis, "The influence of through-thickness reinforcement geometry and pattern on delamination of fiber-reinforced composites: Part I – Experimental results," *Composite Structures*, vol. CLXXXIV, pp. 924-934, 2018.
- [21] S. Kurtz, *PEEK biomaterials handbook*, Elvise and William Andrew Applied Science Publishers, 2019.
- [22] P. Stoyanov, K. Harrington and A. Frye, "Insights into the Tribological Characteristic of CU-Based Coatings Under Extreme Contact Conditions," *JOM*, vol. LXXII, p. 2191–2197, 2020.

- [23] X. Centrich, E. Shehab, P. Sydor, T. Mackley, P. John and A. Harrison, "An Aerospace Requirements Setting Model to Improve System Design," *Procedia CIRP*, vol. XXII, pp. 287-292, 2014.
- [24] C. B., J. Gu, Z. Long, Z. Li, S. Ruan and C. Shen, "Effects of temperature and fiber orientation on the tensile behavior of short carbon fiber-reinforced PEEK composites," *Polymer Composites*, no. 42, pp. 597-602, 2021.
- [25] A. Abdelbary and Y. Mohamed, "Chapter 4 - Tribological behavior of fiber-reinforced polymer composites," in *Tribology of Polymer Composites*, Elsevier, 2021, pp. 63-94.
- [26] P. Sarath, R. Reghunath, J. Haponiuk, S. Thomas and S. George, "Tribology of Fiber-reinforced Polymer Composites: Effect of Fiber Length, Fiber Orientation, and Fiber Size," in *Tribological Applications of Composite Materials*, Springer, 2021, pp. 99-117.
- [27] H. Parikh and P. Gohil, "Tribology of fiber-reinforced polymer," *Journal of Reinforced Plastics*, pp. 1-7, 2016.
- [28] A. Paar, "Pin-on-disk tribometer: TRB3," Anton Paar, [Online]. Available: https://www.anton-paar.com/ca-en/products/details/trb3-pin-on-disk-tribometer/?utm_source=google&utm_medium=cpc&utm_campaign=CA_Dynamic.Search_EN&utm_content=C-00049741&gclid=CjwKCAiAlfqOBhAeEiwAYi43F4ZUMnEMxIBJnnZyr6y1ozwG0DrNGhfSinnJM5r0NBcSqDRP97Z3wIRoC. [Accessed 10 01 2022].
- [29] A. Paar, "Instruction Manual and Safety Information," Anton Paar TriTec SA, Switzerland, 2021.

Chapter

2. Literature Review

In this chapter...

An overview of the fundamentals of tribology, and a literature review of the tribology of fiber-reinforced composite materials is presented.

2.1. Tribology review

2.1.1. Why the need of tribological evaluation?

Tribology is generally defined as “the branch of science and technology concerned with interacting surfaces in relative motion and with associated matters” [1]. There exist only few mechanical assemblies where surfaces are not sliding or rolling against each other, which consequently makes tribology the key to understanding interfacial phenomena related to the friction, wear and lubrication. Furthermore, within moving and contacting mechanical assemblies, energy is lost due to the friction of components sliding against each other. Thus, understanding the friction and wear behavior within assemblies can help to minimize the loss of energy and consequently increase the overall efficiency of the system. [1] [2] [3]

With the constant need to provide higher performance and efficiency within machinery, tribology is the key to reduce or control friction and wear which would overall extend the lifetime of components and decrease maintenance and operational cost [3]. There exists a lot of different factors, Figure 2.1, which that can influence the tribological behavior of mechanical assemblies such as the choice of materials, the choice of lubricant, the choice of contact conditions, etc. [2] [4].

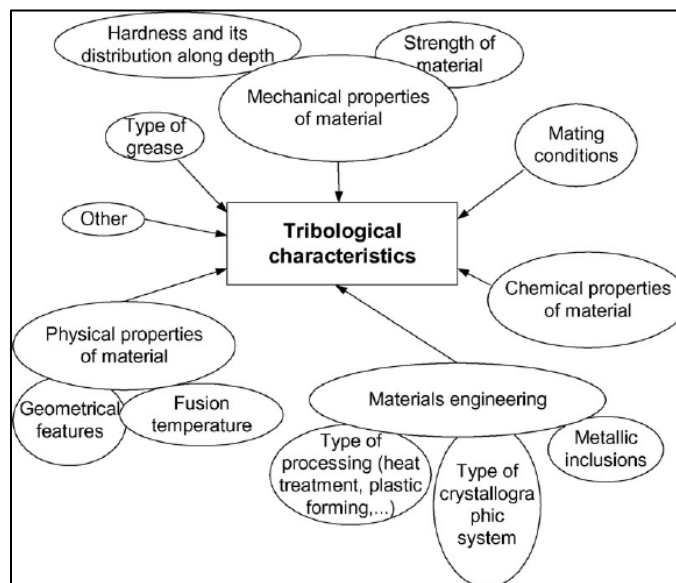


Figure 2.1: Factors influencing tribological properties of materials

The designing of products with a long lifecycle requires experience, especially when it comes to integrating the principles of friction and wear in the design process [2]. In order to simplify the integration of tribology principles in the design cycle to increase the wear life of components within assembly, there exists a comprehensive list of notions that need to be considered and is used by many designers [2]:

- Maintain low contact pressure.
- Maintain low sliding speed.
- Maintain smooth bearing surfaces.
- Prevent high temperature.
- Use hard materials.
- Insure a low coefficient of friction (μ).
- Use a lubricant.

Moreover, as mentioned earlier, the loss of energy due to the friction of components sliding against each other with the combination of material losses due to the wear of components within mechanical assemblies, can increase the operational and maintenance cost [3]. The small energy and material losses within one mechanical assembly might not be high in itself but when the same lost is repeated in millions of mechanical assemblies, the cost becomes very large [3]. This principle is illustrated in Equation 1. Indeed, the need of tribological studies is critical in order to ensure efficient and reliable mechanical designs.

$$\text{Total Tribological Cost/Saving} = \frac{\text{Sum of Individual Machine Cost/Saving} *}{\text{Number of Machines}} \quad (1) [3]$$

2.1.2. Friction

The friction force is defined as “the resistance encountered by one body in moving over another” [5]. There are three governing laws of frictions which can provide useful insights of the frictional behavior of a surface. The three different laws are explained as [1] [5]:

1. In the first law of friction, it is stated that “the friction force is proportional to the normal load” [5]. Thus, the coefficient of friction (μ), Equation 2, is a function of the tangential frictional force (F) divided by the normal load (W) on the contact surface [1].

$$\mu = \frac{F}{W} \quad (2) [1]$$

2. The second law of friction states that “the friction force is independent of the apparent area of contact” [5]. Thus, the second law of friction implies that the friction force (F), Equation 3, is a function of the friction the force due to the adhesion (F_a) between the surfaces, the force due to ploughing (F_p) and the force due to the deformation (F_d) [1]. In addition, Figure 2.2 shows a pictorial representation of the different force components constituting the friction force.

$$F = F_a + F_p + F_d \quad (3) [1]$$

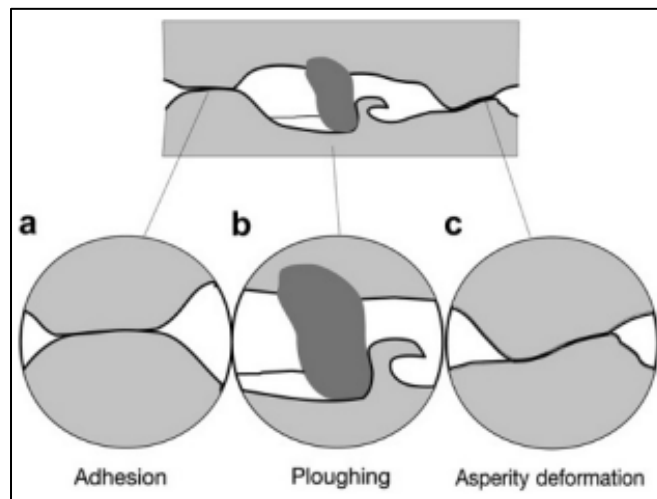


Figure 2.2: Components of sliding friction [3]

3. The third law of friction states that “the friction force is independent of the sliding velocity” [5].

Overall, there are many different parameters that can affect the friction force such as the type or material, the type of contact, the environment, time etc. It thus important to consider all of them in order to obtain an accurate representation of the force of friction to minimize the energy loss in mechanical assemblies [1].

2.1.3. Wear

Wear is defined as “the removal of material from solid surfaces as a result of one contacting surface moving over another” [1]. From literature, there exists different mechanisms of wear that can describe the interfacial phenomena occurring between sliding or rotating components within mechanical assemblies. The four most common mechanisms of wear are [1] [2] [3] [5]:

- Adhesive wear,
 - In this mechanism, the wear is caused by the adhesion between asperities on a surface coming into contact with the asperities of the counter surface and thus forming asperities junction. [1] [2] [3] [5]
- Abrasive wear,
 - In this mechanism, the wear is caused by the contact of surfaces where one of the surfaces is significantly harder than the other one causing the harder surface asperities to be pressed into the softer surface and thus resulting in the flow of softer material around the harder one. [1] [2] [3] [5]
- Fatigue wear,
 - In this mechanism, the wear is caused by fatigue crack growth between the contacting surfaces resulting from high applied loading and unloading of a surface which is increasing the stress level of the materials and thus resulting in large-scale cracking liberating material from the surface which is producing wear debris. [1] [2] [3] [5]
- Chemical wear.
 - In this mechanism, the wear is caused by the influence of the environment and detrimental chemical reactions in the contact between surfaces where followed by rubbing, there is a removal of material and debris formation on the surface. [1] [2] [3] [5]

Figure 2.3 showcases the relationship between the operating conditions of contact surfaces within mechanical assemblies and the procedure to determine the wear mechanism between the surfaces.

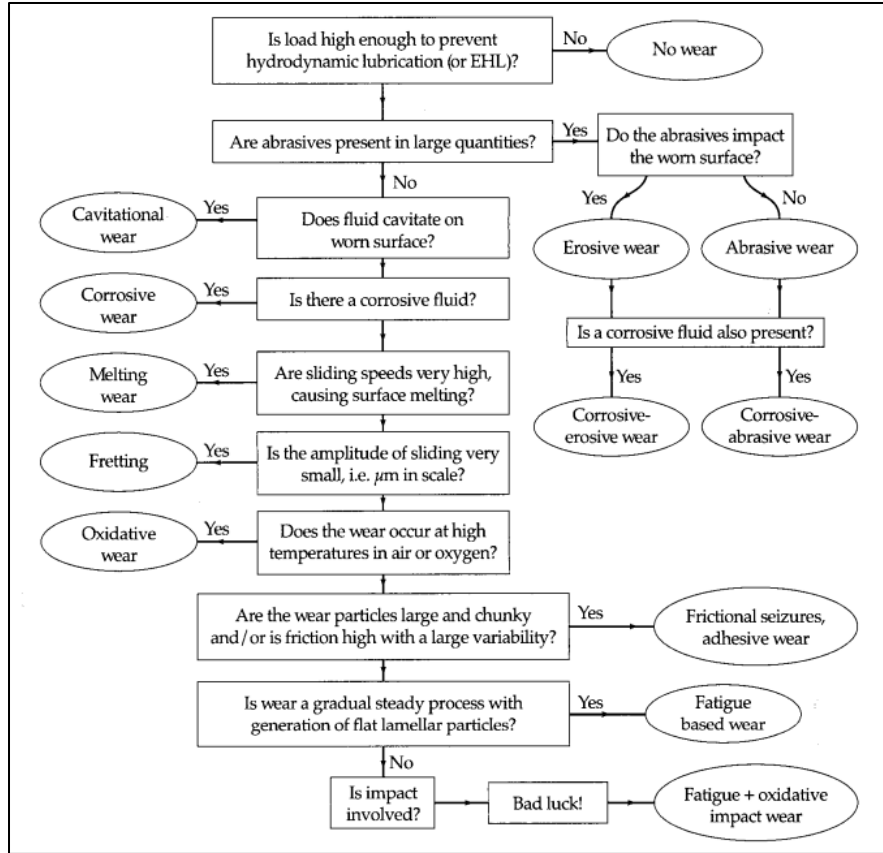


Figure 2.3: Relationship between operating conditions and type of wear [3]

In addition, in order to give a more practical value to describe the amount of wear of a surface, the wear rate can be calculated. The wear rate (K) is a function of the wear volume (V), the applied load (w) and sliding distance (s) which can be seen in Equation 4 [1] :

$$K = \frac{V}{w*s} \quad (4) [1]$$

2.2. Tribology of fiber-reinforced polymer composites

2.2.1. Fiber-reinforced polymer composites

Composites materials can be classified according to their content, as shown in Figure 2.4, and are comprised of a base and filler material [6]. In the case of fiber-reinforced polymer (FRP) composites, the base material is the polymer matrix, and the filler material are the fibers. The role

of the fibers, due to their high strength and stiffness, are to provide reinforcement and structure to a composite so that it can support different loading conditions [7] [8]. On the other hand, the role of the polymer matrix, due to its lower density, is to provide support (alignment of the fibers) and protection to the fibers (act as a stress transfer medium) [7] [8]. Generally, the polymer matrix accounts for 30-40 percent of the composite [8]. When the fibers and the polymer matrix are bounded together to form a composite, its material properties will depend mainly on the fiber content, fiber orientation and length and the type of polymer used.

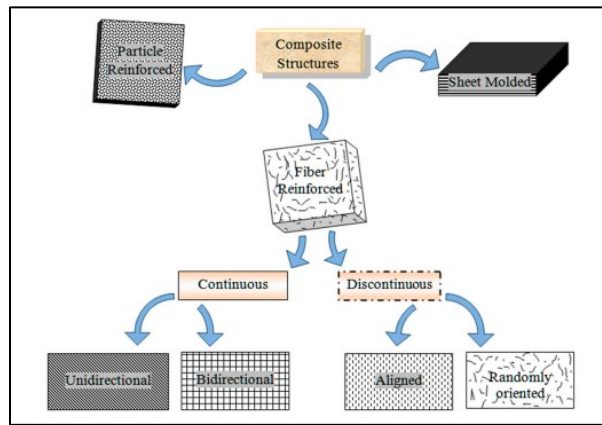


Figure 2.4: Classification of composites [6]

FRP have been widely used for structure of aircraft and spacecraft in the aerospace industry for weight reduction purposes, as shown in Figure 2.5, and have slowly been replacing more conventional materials due to their many structural advantages [9] [10]. FRP are characterized by their high strength and stiffness properties, high fatigue, high toughness and high temperature wear and oxidation resistance [6] [8] [9]. In addition, FRP have good manufacturability that can be customized towards targeted needs which makes it an excellent choice for engineering applications [6] [9].

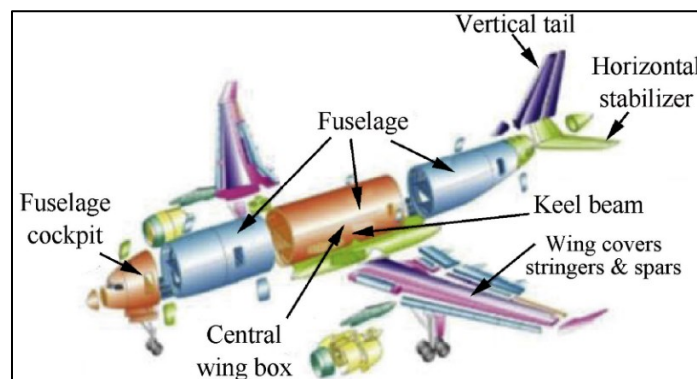


Figure 2.5: FRP composite components used in aircraft structures [9]

2.2.2. Tribological properties of fiber-reinforced polymer composites

There exist many different factors that can influence the tribological properties of fiber-reinforced polymer composites as shown in Figure 2.6 [11] [12]. Usually, polymers are reinforced with fibers in order to enhance their tribological properties which improves their hardness and compressive strength while decreasing their adhesion to the contacting surface [13]. Consequently, the wear and friction mechanisms of FRP are governed by the choice of the polymer matrix material due to its lower stiffness and strength [11] [13]. Tribological properties of fiber-reinforced polymer matrix composites can also be affected by different operating parameters and material parameters such as: fiber orientation, fiber volume fraction, fiber length, surface treatment and operating parameters such as the sliding distance and the temperature [11] [14] [15].

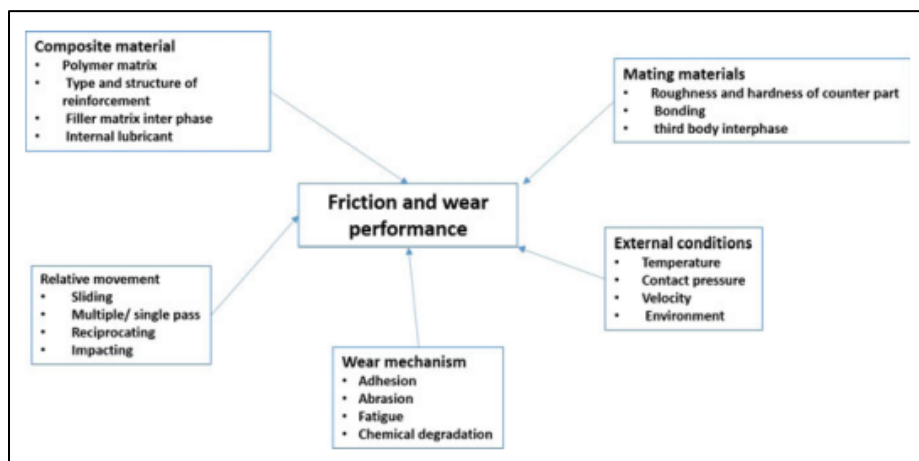


Figure 2.6: "Areas of influence on the tribological performance of composite materials" [11]

The tribological behavior of FRP and corresponding wear mechanisms will also depend on the form of fibers added to the polymer: randomly oriented chopped fibers or unidirectional or woven fibres [3] [16]. In the case of the reinforcement of the polymer using randomly oriented chopped fibres, it has been shown that they are effective for reducing the wear in situations where there is a strong adhesion between the fibers and the matrix [3] [17]. The principals wear mechanisms that observed in polymers reinforced with randomly oriented chopped fibers are the abrasive wear or erosive wear [18] [19]. On the other hand, in the case of reinforcement of polymers using unidirectional or woven fibres, the wear mechanisms of the material will depend on the direction

of sliding of the counterface against the fiber direction [3] [13]. Figure 2.7 illustrates the wear process of the parallel and anti-parallel fiber orientation. Typically, a lower wear rate and better tribological properties can be obtained with FRP and unidirectional or woven fibres [3].

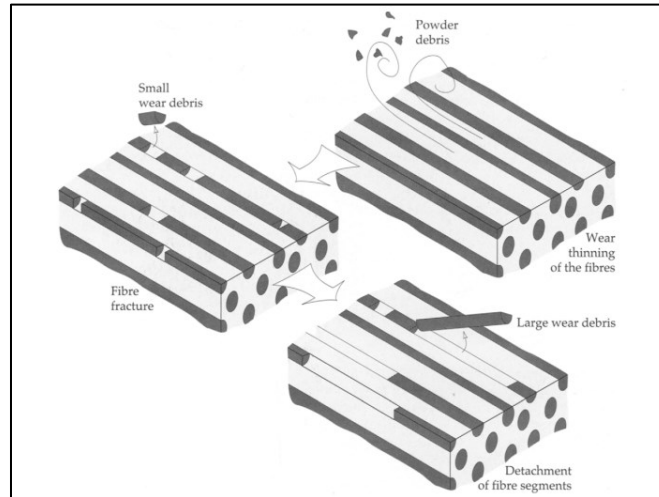


Figure 2.7: Wear mechanism of parallel and anti-parallel FRP [3]

Finally, previous studies have performed extensive characterization and have revealed that FRP composites are extremely particular concerning their good tribological performance and thus should be chosen carefully [3] [13] [20]. FRP exhibits good wear resistance when the contact is smooth between its surface and the counterface with predominant adhesive or fatigue wear mechanisms [3]. Alternatively, when there exists predominance of abrasive or erosive wear mechanisms between the FRP and contacting surface, it has been demonstrated that there is a decrease in wear behavior compared to unreinforced polymers [3] [19].

2.2.3. Impact of fiber length & orientation on the tribological properties of fiber-reinforced polymer composites

The fiber length of the reinforcement fibers of polymers plays a big role in the tribological behaviors of FRP since it is directly related to the creation of interfacial bonding of the matrix and fiber [13] [20] [21]. From literature, it has been shown that continuously long carbon fibers provide improvement in relation of abrasive wear resistance [22] but due to the abrasive particles breaking-off the long fibers, and creating fiber pull-out, the opposite effect can be observed and is seen in

Figure 2.8 [8] [13]. On the other hand, really short fibers can create excessive wear rate of FRP since it does not provide sufficient load carrying capacities [13].

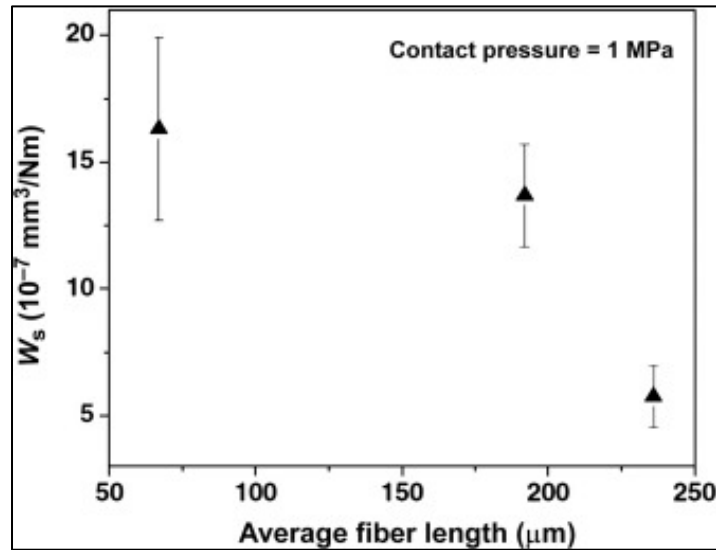


Figure 2.8: "Effect of fiber length on the specific wear rate of epoxy composites" [13]

Additionally, the orientation of the fibers also plays a crucial role in the tribological properties of FRP and especially in the case of short fiber reinforcement [13] [20]. It has been shown that the rate of wear is directly related to the orientation of the fiber axis with the direction of the sliding [8] [13] [23]. The wear rate is typically higher for composites tested in the parallel and anti-parallel direction, due to the peeling off of the fibers, compared to the normal direction where the load carrying capacity of the surface is higher as illustrated in Figure 2.9 [13].

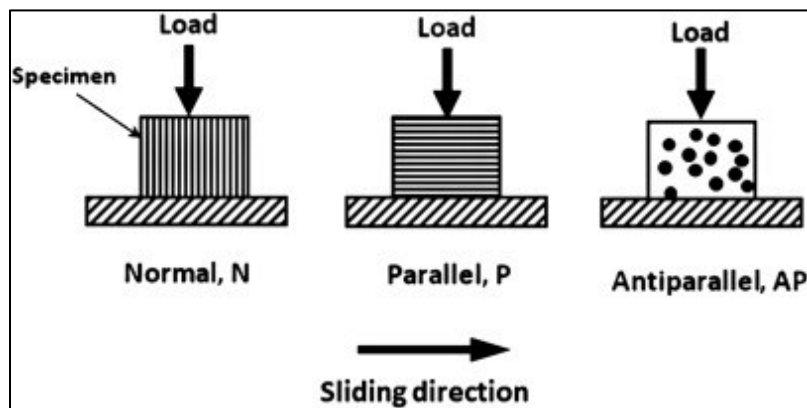


Figure 2.9: Pictorial illustration of the fiber orientation in relation to the sliding direction [13]

2.2.4. Impact of temperature on the tribological properties of fiber-reinforced polymer composites

The temperature is a factor that can have a big impact on the tribological properties of FRP since the polymer matrix has lower glass transition temperatures [24] [25] [26]. The mechanical performance of FRP is thus dependent on the operating temperatures since passed the glass transition temperature, the strength and tensile modulus of the polymers decreases and thus the load-capacity of the material decreases which provides a less stable environment for the fibers [24]. This phenomenon can be seen in Figure 2.10. The decrease in mechanical properties with the increase of the contact temperature of the matrix directly affect the tribological properties of the material as the friction and wear rate is increased. This is also due to the softening of the polymer matrix which accelerates the peeling-off process of the fiber removal, which consequently increase the friction due to de generated debris particle and thus increase the wear rate [25].

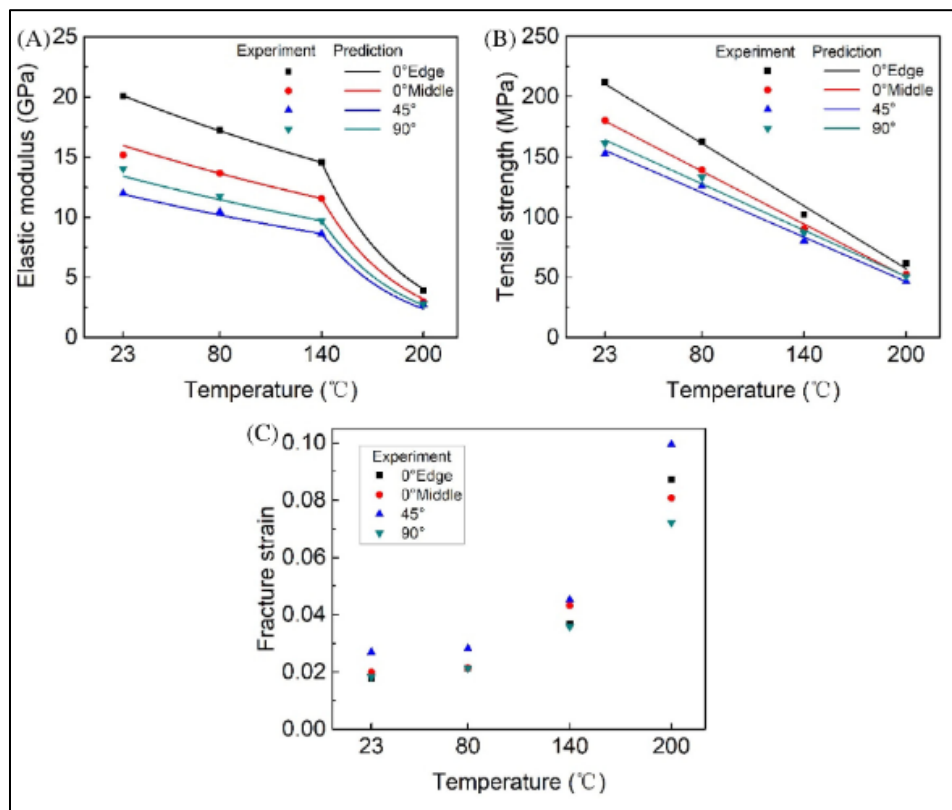


Figure 2.10: Effect of the increase of temperature on the A) elastic modulus, B) Tensile strength C) fracture strain of PEEK [24]

2.3. Statistical Analysis

For the purposes of this study, the influence of fiber direction and temperature on carbon-fiber PEEK composite and their influence on its tribological properties was studied through tribometer testing. It was mentioned in Chapter 1, section 1.3, that the tribological tests were performed three different times for each of the fiber orientation in order to obtain the variability in the data. From the data obtained from the modelization software of the Anton-Paar TRB3 ball-on-disk linear tribometer, the friction curves can be obtained. The statistical error between the different tests can be obtained by calculating the standard deviation from the three different testing and then calculating the standard deviation error. The standard deviation in statistics, σ , is know as the “The positive square root of the variance. The standard deviation is the most widely used measure of variability” [27] and is shown in equation 5 where the variance is denoted as σ^2 . The variance, on the other hand, is described as “A measure of variability defined as the expected value of the square of the random variable around its mean.” [27].

$$\sigma = \sqrt{\sigma^2} \quad (5) [27]$$

Additionally, the error in the standard deviation is defined as the “The standard deviation of the estimator of a parameter. The standard error is also the standard deviation of the sampling distribution of the estimator of a parameter.” [27]. The standard deviation error, σ_χ is the ratio of the standard deviation over the square root of the number of samples and is seen in equation 6 [27].

$$\sigma_\chi = \frac{\sigma}{\sqrt{n}} \quad (6) [27]$$

Statistical analysis was used at several times during this study to showcase the variability in the data and give a better representation of the tribological behaviour of the carbon-fiber PEEK based on the parallel, anti-parallel and normal fiber orientation. Statistical analysis was used for the obtention of the friction behaviour where the standard deviation error was calculated every 500 cycles. Furthermore, the standard deviation was also calculated and shown in the various bar graphs of this study so show the variability in the date. This includes for the wear rate, Atomic Force Microscope (AFM) analysis of the estimated nanohardness and adhesion force, and the Energy Dispersive X-ray Spectroscopy (EDS) analysis of the different samples elemental distributions.

2.4. References

- [1] K. Holmberg and A. Matthews, *Coatings Tribology; Properties, Mechanisms, Techniques and Applications in Surface Engineering Second Edition*, Amsterdam: Elsevier, 2009.
- [2] K. Ludema and O. Ajayi, *Friction, wear, lubrication. A textbook in tribology. Second edition*, CRC Press Taylor & Francis Group, 2019.
- [3] G. Stachowiak and A. Batchelor, *ENGINEERING TRIBOLOGY 3rd edition*, Elsevier Butterworth-Heinemann, 2005.
- [4] T. Lesniewski, "The effect of ball hardness on four-ball wear test results," *Wear*, vol. CCLXIV, no. 7, pp. 552-670, 2008.
- [5] I. Hutchings and I. Shipway, *Tribology. Friction and wear of engineering materials. Second edition*, Butterworth-Heinemann an imprint of Elsevier, 2017.
- [6] D. Rajak, D. Pagar, P. Menezes and E. Linul, "Fiber-Reinforced Polymer Composites: Manufacturing, Properties, and Applications," *Polymers*, no. 11, p. 1167, 2019.
- [7] I. M. Daniel and O. Ishar, *Engineering Mechanics of Composite Materials*, New York: Oxford University Press, 2006.
- [8] M. Hyer, *Stress Analysis of Fiber-Reinforced Composite Materials*, DEStech Publications, Inc., 2009.
- [9] M. Karatas and H. Gokkaya, "A review on machinability of carbon fiber-reinforced polymer (CFRP) and glass fiber-reinforced polymer (GFRP) composite materials," *Defence Technology*, vol. XIV, no. 4, pp. 318-326, 2018.
- [10] C. Soutis, "Fibre reinforced composites in aircraft construction," *Progress in Aerospace Sciences*, vol. XLI, no. 2, pp. 143-151, 2005.
- [11] Mohamed Thariq Hameed Sultan, Mohd Ridzuan Mohd Jamir, Mohd Shukry Abdul Majid, Azwan Iskandar Azmi, Naheed Saba, *Tribological Applications of Composite Materials*, Singapore: Springer Nature Singapore Pte Ltd.

- [12] P. Menezes, P. Rohatgi and M. Lovell, "Studies on the Tribological Behavior of Natural Fiber-reinforced Polymer Composite," in *Green Tribology*, Springer, 2012, pp. 329-345.
- [13] A. Abdelbary and Y. Mohamed, "Chapter 4 - Tribological behavior of fiber-reinforced polymer composites," in *Tribology of Polymer Composites*, Elsevier, 2021, pp. 63-94.
- [14] H. Parik and P. Gohil, "Tribology of fiber-reinforced polymer matrix composites—A review," *Journal of Reinforced Plastics*, vol. XXXIV, no. 16, pp. 1340-1346, 2015.
- [15] K. Friedrich, "Polymer composites for tribological applications," *Advanced Industrial and Engineering Polymer Research*, vol. I, no. 1, pp. 3-39, 2018.
- [16] S. Kumar and K. Singh, "Tribological behaviour of fibre-reinforced thermoset polymer composites: A review," *Journal of Materials: Design and applications*, vol. CCXXXIV, no. 11, pp. 1439-1449, 2020.
- [17] S. Bahadur, "Mechanical and Tribological Behavior of Polyester Reinforced with Short Fibres of Carbon and Aramid," *Lubrication Engineering*, vol. XXXXVII, pp. 661-667, 1991.
- [18] J. Bijwe, C. Logano and U. Tewari, "Influence of Fillers and Fibre Reinforcement on Abrasive Wear Resistance of Some Polymeric Composites," *Wear*, vol. CXXXVIII, pp. 77-92, 1990.
- [19] P. Mathias, W. Wu, K. Goretti, J. Routnort, D. Groppi and K. Karasek, "Solid Particle Erosion of a Graphite-Fibre-Reinforced Bismaleimide Polymer Composite," *Wear*, vol. CXXXV, pp. 161-169, 1989.
- [20] P. Sarath, R. Reghunath, J. Haponiuk, S. Thomas and S. George, "Tribology of Fiber-reinforced Polymer Composites: Effect of Fiber Length, Fiber Orientation, and Fiber Size," in *Tribological Applications of Composite Materials*, Springer, 2021, pp. 99-117.
- [21] H. Zhang, Z. Zhang and K. Friedrich, "Effect of fiber length on the wear resistance of short carbon fiber-reinforced epoxy composites," *Composites Science and Technology*, vol. LXVII, no. 2, pp. 222-230, 2007.
- [22] Z. Zhang, K. Friedrich and K. Velten, "Prediction on tribological properties of short fibre composites using artificial neural networks," *Wear*, vol. CCLII, no. 7, pp. 668-675, 2002.

- [23] H. Parikh and P. Gohil, "Tribology of fiber-reinforced polymer matrix composites—A review".
- [24] B. Chang, J. Gu, Z. Long, Z. Li, S. Ruan and C. Shen, "Effects of temperature and fiber orientation on the tensile behavior of short carbon fiber-reinforced PEEK composites," *Polymer Composites*, no. 42, pp. 597-607, 2020.
- [25] L. Mu, ., X. Feng, J. Zhu, H. Wang, Q. Sun, Y. Shi and X. Lu, "Comparative Study of Tribological Properties of Different Fibers Reinforced PTFE/PEEK Composites at Elevated Temperatures," *Tribology Transactions*, vol. LIII, no. 2, pp. 184-194, 2010.
- [26] J. Gomes, O. Silva, C. Silva and R. Silva, "The effect of sliding speed and temperature on the tribological behaviour of carbon–carbon composites," *Wear*, vol. CCXLIX, no. 3-4, pp. 240-245, 2001.
- [27] D. Montgomery and G. Runger, *Applied Statistics and Probability for Engineers*, John Wiley & Sons, Inc, 2011.

Chapter

3. Influence of fiber direction on the tribological behavior of carbon reinforced PEEK for applications in gas turbine engines

In this chapter...

The identification of the influence of fiber orientation on the surface energy and tribological behavior of CF-PEEK systems for the Fan and LPC region of the gas turbine engine (i.e. room temperature) will be presented.

3.1. Abstract

Proper material selection is crucial within the aerospace industry in order to improve the performance and efficiency of current engines. However, the conditions in which materials are expected to operate in are becoming more demanding (e.g. high temperatures, high pressures), and thus, there is a strong desire for the development and implantation of high-performance materials. Polymer Matrix Composite (PMC) materials are one alternative solution to more conventional metal or alloys due to their light weight and high strength properties. However, in harsh environments PMCs can be limited by their mechanical and tribological properties such as wear and friction. With the recent development, it is practical to produce high-temperature stable PMC, such as those produced using polyether ether ketone (PEEK), with orientation of reinforcing carbon fibers (CF-PEEK) normal to the in-plane fiber direction that is typically found in composites. This technology has shown to be promising for improving tribological applications in gas turbine engines. The CF-PEEK film with fibers normal to the in-plane fiber direction is developed by means of vertically orienting sub-millimeter carbon fibers using a novel process to produce thin composite films with fiber reinforcement that is normal to traditional unidirectionally aligned carbon fibers in a polymer matrix. However, the tribological behaviour of polymer matrix composite with carbon fiber oriented in the normal fiber direction direction have yet to be extensively characterized. The purpose of this study is to better understand of the influence of the fiber orientation on tribological behavior of carbon reinforced polymers. Friction and wear testing was performed on CF-PEEK film with fiber oriented in the normal direction and compared to conventional standard modulus carbon fiber/PEEK unidirectional tape (UD) and unreinforced, pure PEEK film under various contact conditions. The characterization of the worn surfaces was performed through ex situ analysis to reveal the interfacial phenomena by means of Scanning Electron Microscopy (SEM), Energy Dispersive X-ray Spectroscopy (EDS), confocal laser scanning microscopy (CLSM) and Atomic Force Microscope (AFM). A correlation between the orientation of carbon fibers and the wear and friction performance was established based on the different study parameters.

3.2. Introduction

With the rapidly growing advancements and constant need for improvement within the aerospace industry, the conditions in which materials are expected to operate are becoming increasingly more challenging. Increase in capability, affordability, safety, and environmental compatibility are all challenges that can be associated to the development of new materials for the aerospace industry [1] [2] [3] [4] [5] [6]. This is even more important when it comes to the proper material selection for the purpose of long-lasting gas turbine engines. Materials that will be used in future gas turbine engines are expected to withstand more extreme conditions such as increasingly high temperatures, vibrations, etc. in order to increase the performance and efficiency of the engines [7] [8] [9]. The materials currently used for the manufacturing of critical gas turbine engines components such as metal and alloys, will most likely be limited by their mechanical and tribological properties such as friction and wear when subjected to considerable increase in operating temperature [10] [11] [12]. This could lead to a decrease in the lifetime of critical components in gas turbine engines and lead to their failure under creep or fatigue [2] [11]. Thus, there is a clear need for the development of new tribological materials for the purpose of long-lasting gas turbine engines.

Due their high strength and stiffness properties, their light weight and good environmental resistance, Polymer Matrix Composites (PMC) are considered to be a cost-effective alternative solution to conventional metals or alloys [13] [14]. PMC are composed of reinforcement fibers that are bounded together by a matrix of polymer made from polymer material. The fibers have high stiffness and strength to provide reinforcement and structure to the composite to support different loading conditions. On the other hand, the polymer matrix is usually of lower density than the fibers and provides load transfer mechanism and toughness to the fiber. When the fiber and the polymer matrix are bounded together its material properties will depend mainly on the fiber content, fiber orientation, fiber packaging (e.g., fabric, unidirectional tape, etc.), fiber length and the type of polymer matrix used. It is also possible to add core materials, fillers, functional groups on the fiber surface, and surface finishings to increase various material properties. [15]

While commercially available composites have many advantages and are already widely used in the aerospace industry, there are limitations regarding their usage in load-bearing situations [16] [17] [18]. When the load induces tensile stresses in the composite in the direction transverse to the

fibers, it often ends up failing due to delamination and/or fiber breakage [18] [19]. While quasi-isotropic composite laminates can be produced by alternating in-plane fiber orientations, there remains a deficiency in the normal to the surface direction (i.e., through-thickness or Z-axis direction). Thus, through-thickness reinforcement of the composite is necessary in order to improve its mechanical properties as well as its interlaminar damage tolerance [20] [21] [22]. Z-pinning, stitching technology, tufting technology are all pre-existing techniques that can be used to provide through-thickness reinforcement to a composite material [20] [23] [24] [25]. However, these techniques are slow and expensive in addition to the possibility of causing microstructural damages such as fibre crimping and waviness. [20] Additionally, these methods cannot be utilized to provide dense (i.e., >30% fiber content by volume) fiber reinforcement in the normal direction for bulk, local, or surfacing applications.

With the recent advancement in through-thickness reinforcement of composite materials, the Boston Materials ZRT™/PEEK film product has shown promising results to improve the tribological behavior. The ZRT film product is manufactured using a 60-inch-wide roll-to-roll process, Figure 3.1, in order to produce films of CF-PEEK with fiber oriented in the normal direction with a thickness that is typically 0.15mm [26]. Additionally, the ZRT film product is a cost-effective and environmentally benign method to impart through-thickness reinforcement in composite materials without the manipulation of hazardous chemicals, nanoparticles, or large mechanical processes. Consequently, by applying plies of ZRT film to conventional carbon fiber-reinforced polymer, it can maintain its in-plane performance while allowing an increase in its out-of-plane properties locally within the laminate [27]. This functionality shows promising results regarding its usage in harsh environments, especially in aerospace applications. [26]



Figure 3.1: 60"-wide ZRT film production line installed at Boston Materials' factory in Billerica MA, USA [26]

Previous studies have performed extensive characterization of carbon reinforced polymer composites and have demonstrated the impact of the parallel and anti-parallel orientation of the fibers on the mechanical properties and tribological behavior of composites [28] [29] [30] [31]. While polymer matrix composite with carbon fiber oriented in the normal direction have shown improved mechanical properties, the tribological behaviour of these systems have yet to be extensively characterized. The purpose of this study is to fully capture the tribological behavior of CF-PEEK with fiber oriented in the normal direction when compared to conventional unidirectional CF-PEEK and neat PEEK under various contact conditions for the purpose of long-lasting gas turbine engines.

3.3. Experimental procedure

3.3.1. Materials

During the course of this study, three different materials were used to produce samples for the tribological testing: Boston Materials ZRT/PEEK film, CF-PEEK unidirectional tape (Toray Cetex® TC1200) and pure PEEK. Boston Materials ZRT/PEEK film is developed by means of vertically orienting sub-millimeter carbon fibers using the roll-to-roll process to produce thin films of carbon fibers, aligned in the normal direction, in a PEEK polymer matrix. The reclaimed carbon fibers are being dispersed into water and subjected to a magnetic film in order to vertically align them. Once the fiber has been vertically aligned, the water is evaporated which leaves the ZRT film dry on top of the carrier film and ready to be processed based on the desired application. The ZRT film is then melt infiltrated with PEEK yielding a ZRT/PEEK film. A cross-section of this material is included in Figure 2.

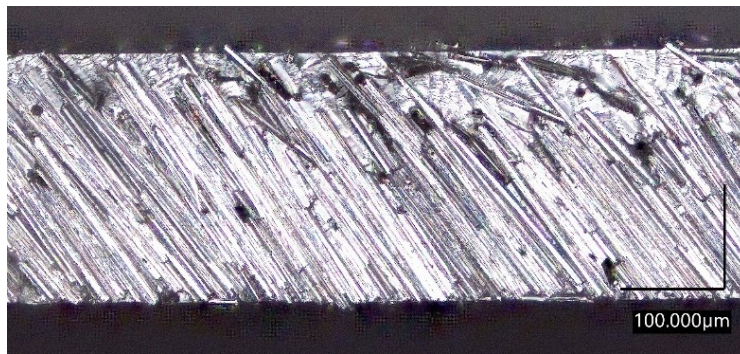


Figure 3.2: Cross-section of a ZRT composite film

For the samples with CF-PEEK normal to the in-plane fiber orientation, the composite laminate is composed of layers of CF-PEEK unidirectional tape, quasi-isotropically layered, and layers of ZRT/PEEK film material, symmetrically layered on the outside and consolidated together (using a compression molding process) to obtain the desired thickness. [32]

For the CF-UD-PEEK samples, unidirectional tape (Toray Cetex TC1200) used in this study is a commercially available thermoplastic composite [33]. Toray Cetex TC1200 is composed of a semi-crystalline polyether ether ketone (PEEK) matrix that bounds and aligns the continuously long carbon fibers together in order to produce the unidirectional tape which can then be processed based on the desired application. In this case, the CF-PEEK unidirectional tape is quasi-isotropically layered and consolidated (using a compression molding process) to obtain the desired thickness.

For the Pure PEEK samples, neat (unfilled) PEEK panels were sourced from Boedeker Plastics, a well-known online retailer of plastic films and shapes.

In order to obtain the tribological comparison of the different materials, four different square samples were produced. All the different samples were of 25x25mm of dimensions with a thickness of 2mm and a polished surface of obtained from automated polishing process:

- Sample 1: Boston Materials ZRT/PEEK film, CF-PEEK normal to the fiber direction
- Sample 2: CF-PEEK unidirectional tape (Toray Cetex TC1200) tested parallel to the fiber direction
- Sample 3: CF-PEEK unidirectional tape (Toray Cetex TC1200) tested anti-parallel to the fiber directions
- Sample 4: Pure PEEK

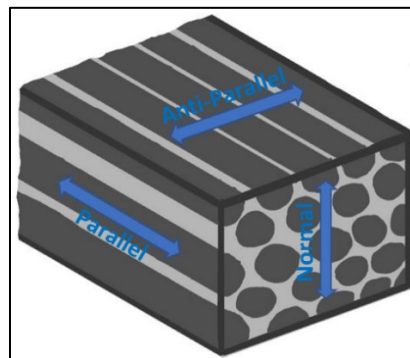


Figure 3.3: Samples Fiber Orientation

3.3.2. Characterization and Tribological Evaluation

The tribological testing were performed using a ball-on-disk linear tribometer (Anton-Paar TRB3 tribometer). In the ball-on-disk linear tribometer, Figure 3.4, a counterface, in this case Al_2O_3 , presses stationary on the surface of the samples which is displacing linearly by a rotating disk [34]. The tribometer is capable of varying the testing parameters such as the speed, the load, the distance and the counterface based on the study need, which will have significant effect on the result. The data from the testing is recorded on a modelization software which allow for easy data treatment and more importantly in this study, the obtention of the friction curve for each specific sample. [34]

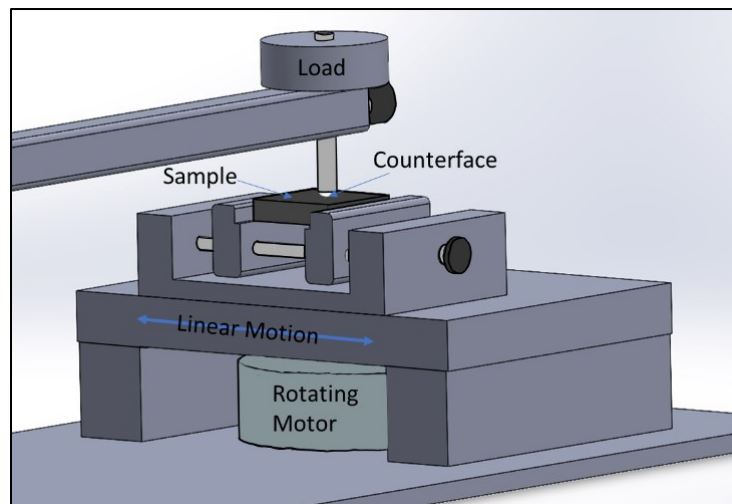


Figure 3.4: Schematic Representation of ball-on-disk linear tribometer

In the case of this study, testing parameters were preliminary determined based on prior tribological testing of the samples over a wide range of applied loading and distances in order to obtain a valid comparison of the frictional behaviour. To fully capture the performance of these systems in more extreme conditions, a higher contact stress and distance were chosen, as shown in Table 1. The testing was performed at room temperature (25–28°C). A total of three different tests were performed for each sample and the friction was reported as the average value of the three tests. The testing parameters that were predetermined are seen in Table 3-1.

Table 3-1: Tribometer Testing Parameters

PARAMETER	DESCRIPTION
Counterface Material	Al ₂ O ₃ (diameter of 6.35 mm)
Normal Load	18N
Velocity	3.1 cm/s
Frequency	1 Hz
Track Length	10mm
Distance	600M

Subsequently to the sliding tests, the wear depths were measured for each sample. The measurement was performed using a LEXT Confocal Laser Microscopy. The same instrument was used for optical images of the worn surfaces in order to provide a better understanding on the dominant wear mechanisms. were obtained for each different tribometer for the samples and their respective counterface in order to obtain the wear behaviour.

In addition characterization of the unworn surface and inside of the wear track of the samples as well as their counterface was also performed by means of Ex situ analysis to determine the principal wear mechanisms. In order to have a better understanding of the effect of the tribometer testing on the surface topography of the samples, Scanning Electron Microscopy (SEM) (Hitachi High Technologies America, Inc., USA) analysis was performed. This allows to get high precision images of the surface of the samples as well as the inside of the wear track of each sample and observe the change in the topography. Energy Dispersive X-ray Spectroscopy (EDS) (Pentafet Link, INCA X-sight, Oxford instruments, UK) analysis was also performed on the counterfaces to obtain their elemental distribution. Finally, Atomic Force Microscope (AFM) (Anton–Paar Tosca 400, Switzerland) analysis was performed for a total of 10 measurements on the surface and inside the wear track of each sample. AFM analysis was performed under contact mode and generated Force-Distance Curves (FDC) that were used to obtain the pull-off force (adhesion force) and the estimation of the hardness which can be obtained by measuring the deformation depth from the generated FDC and gives a better understanding of how the surface hardness of the samples has been affected after the tribological testing.

3.4. Results

3.4.1. Friction Behaviour

The coefficient of friction against the number of cycles is shown in Figure 3.5. Overall, it can be observed that the friction was evidently higher during the tribometer testing with the pure PEEK material compared to the other systems. The friction started significantly higher, at approximately 0.3, for the Pure PEEK sample and increases until it reaches 0.4. On the other hand, for all the CF-PEEK samples, the friction was equivalent within the first few cycles of the tests at 0.2. However, when performing the test for the CF-PEEK parallel to the fiber's directions, the coefficient of friction starts to increase at after 7000 cycles until it reaches 0.3 which showcases a lower friction than the Pure PEEK samples but higher friction than the other CF-PEEK samples. When the tests were performed on the CF-PEEK anti-parallel to the fiber's direction, the friction coefficient quickly stabilize and remains at about 0.23 during steady state. This behavior is also observed with the CF-PEEK normal to the fiber direction where the friction remains steady at around 0.25.

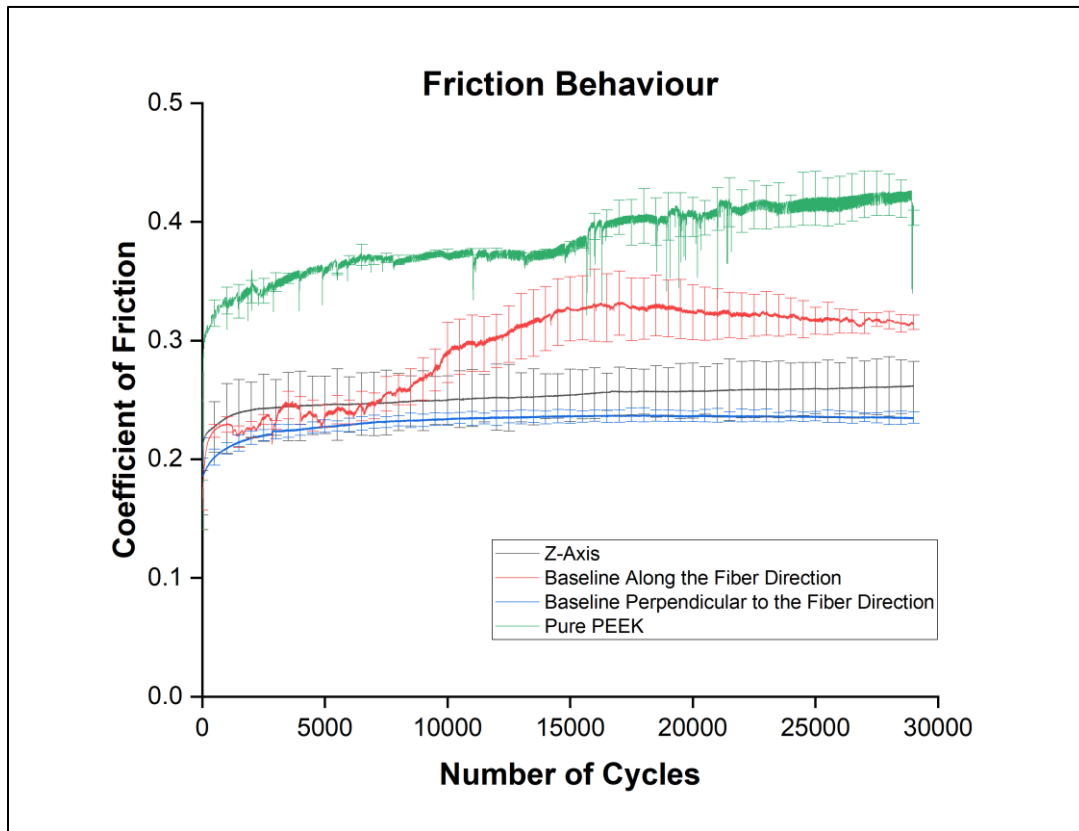


Figure 3.5: Friction Behaviour of the samples

3.4.2. Wear Behaviour

The wear measurements of each sample are shown in Figure 3.6. The wear depth is significantly higher for the Pure PEEK and the CF-PEEK parallel to the fiber direction samples, which can translate in a higher generation of debris particles. The highest recorded wear depth can be observed with the Pure PEEK sample reaching a maximum of $38\mu\text{m}$ following by the CF-PEEK parallel to the fiber direction which reaches a depth of $28\mu\text{m}$. On the other hand, the wear depth in Figure 3.6 is significantly lower in the case of the CF-PEEK normal to the fiber direction where a wear depth of $7\mu\text{m}$ was recorded. Finally, in the case of the CF-PEEK anti-parallel to the fiber direction, it is interesting to observe that no significant wear depth based on the measurements with the Confocal Laser Microscopy. This indicates that the lowest amount of wear is obtained from the CF-PEEK anti-parallel to the fiber direction sample.

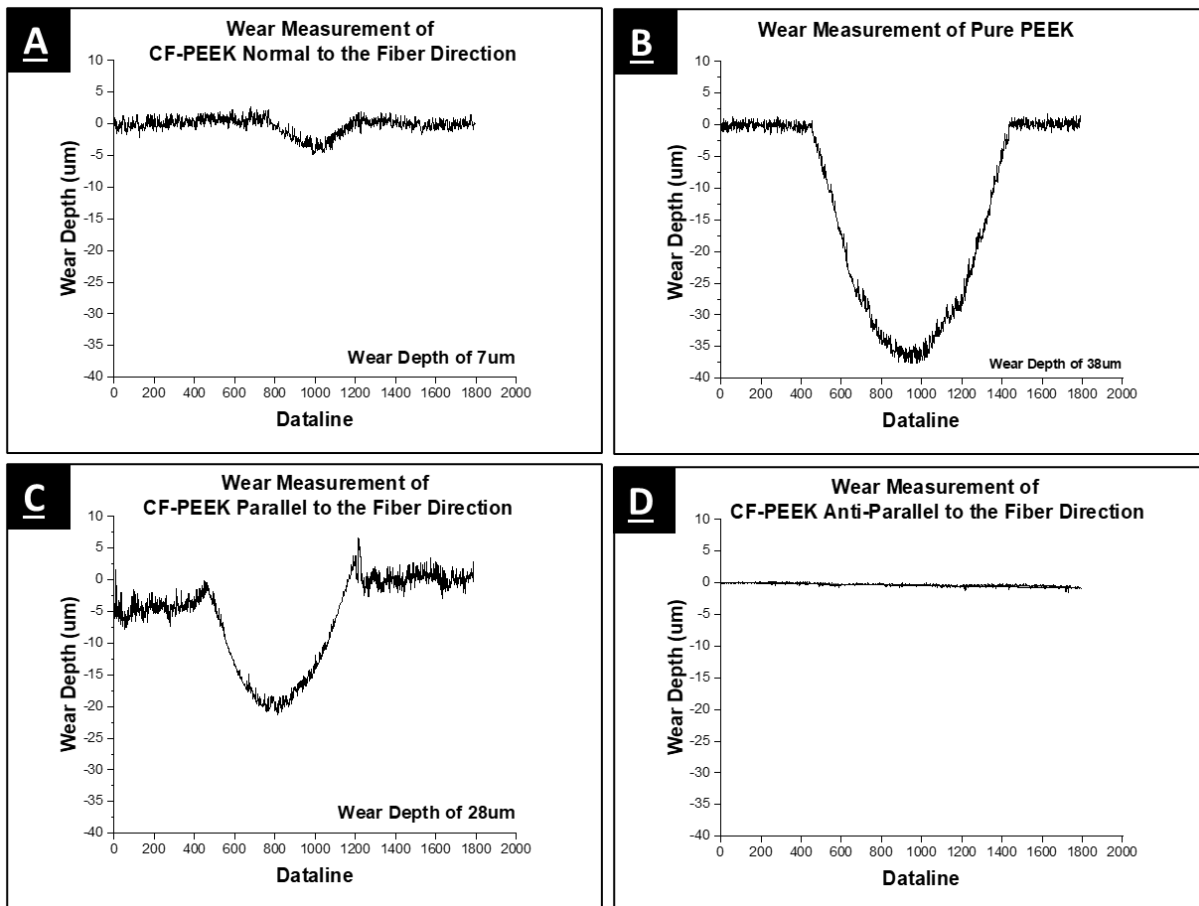


Figure 3.6: Wear Measurement for a 18N Load on A) CF-PEEK Normal to the Fiber Direction Sample B) Pure PEEK Sample C) CF-PEEK Parallel to the Fiber Direction Sample D) CF-PEEK Anti-parallel to the Fiber Direction Sample

In addition, the wear rate was also calculated for each of the samples based on the wear measurements found in Figure 3.6, which gives a more practical value to describe the amount of wear for each sample. The wear rate (K) is the ratio of the wear volume (V) divided by the applied load (w) and sliding distance (s) which can be seen in Equation 1 [35]:

$$K = \frac{V}{w*s} \quad (1) [35]$$

The wear rate for each of the sample is shown in Figure 3.7. From Figure 3.7, it is possible to observe that the Pure PEEK and CF-PEEK parallel to the fiber direction have first and second highest wear rate respectively which correlates with the results in Figure 3.6 since they showcase higher wear depth. Alternatively, the CF-PEEK anti-parallel to the fiber direction and CF-PEEK normal to the fiber direction samples has the lowest wear rate respectively in that order which also correlates with the lower wear depth measured from their wear track in Figure 3.6. Overall, the Pure PEEK exhibits the highest wear rate and the CF-PEEK anti-parallel to the fiber direction has the lowest wear rate.

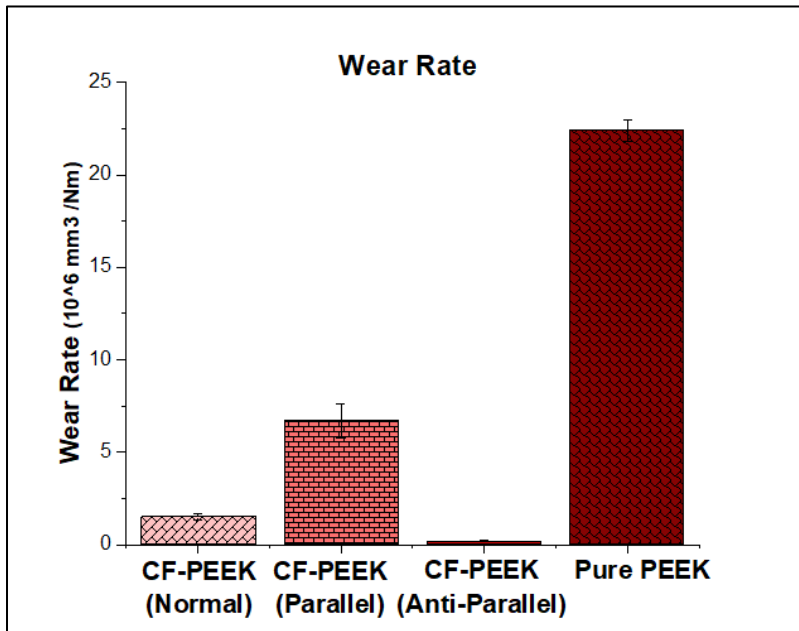


Figure 3.7: Wear Rate of the Samples

3.4.3. Ex Situ Analysis

3.4.3.1. Wear Track Analysis

Subsequently to the frictional and wear testing, the wear track of the samples was subjected to SEM analysis in order to have a better understanding of the wear mechanisms. SEM images were taken both outside and inside the wear track in order to showcase how the tribometer testing has affected the surface topography of the samples. Figure 3.8 represents the SEM images of each the samples taken outside the wear track where it is possible to get a better comparison of the surface topography of each different samples and especially when it comes to the orientation of the fibers. In Figure 3.8 A) it is possible to observe the cross-section of the fibers which shows clearly how the fibers have been oriented in the normal direction during the manufacturing whereas in Figure 3.8 C) and D) the fibers are oriented in the parallel and anti-parallel direction respectively. Figure 3.8 B) on the other hand shows a smooth and uniform surface which corresponds to the pure PEEK sample.

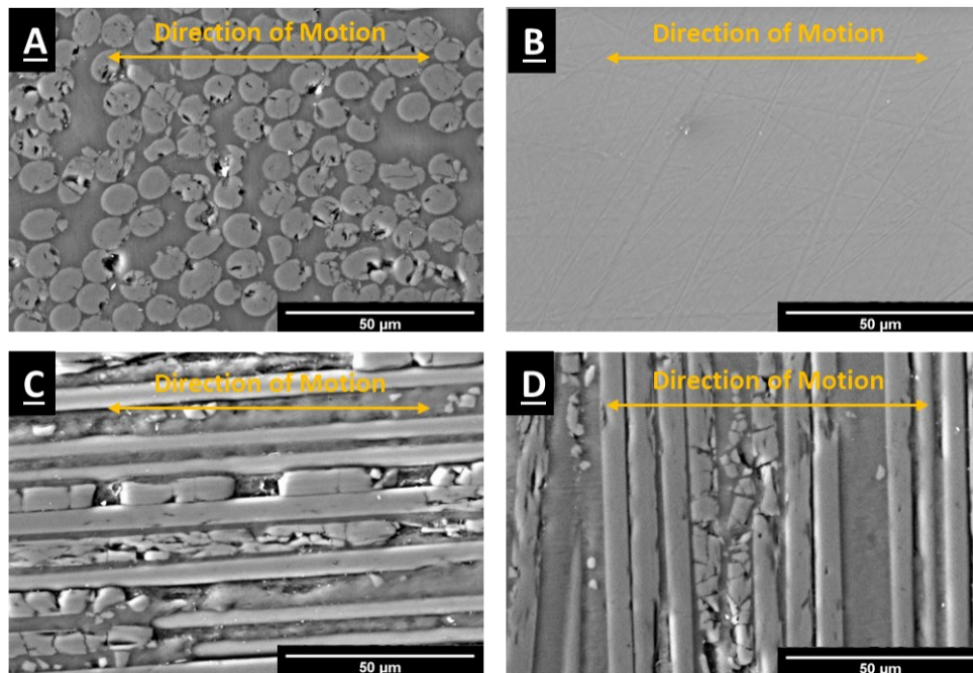


Figure 3.8: SEM Analysis of Sample Surface A) CF-PEEK Normal to the Fiber Direction Sample B) Pure PEEK Sample C) CF-PEEK Parallel to the Fiber Direction Sample D) CF-PEEK Anti-parallel to the Fiber Direction Sample

Figure 3.9 represents the SEM images of the samples taken inside the wear track where it is possible to observe how the sliding test has affected the topography of the surface of the samples.

In the case of the pure PEEK sample, shown in Figure 3.9 B), the sample has remained smooth but with the formation of large debris particles corresponding well with the sample highest recording wear in Figure 3.6. Furthermore, for the CF-PEEK samples, it is interesting to observe the influence the fiber direction on the topography of the inside of the wear track. From Figure 3.9 C) representing the CF-PEEK parallel to the fiber direction sample, a smooth surface without the presence of the fibers is observe. This indicates that during the tribometer testing, the fibers are being broken off in larger debris size and being pushed out of the wear track leaving a polymer-based interface resulting with a lower hardness and thus correlating to the higher wear observed in Figure 3.6. On the other hand, in the case of the CF-PEEK normal to the fiber direction and CF-PEEK anti-parallel to the fiber direction samples shown respectively in Figure 3.9 A) and D), it can be observed that the fibers have been crushed across the surface. This indicates that throughout the tribology testing, the fibers have been broken into smaller debris size that are staying in the wear track and being embedded into the polymer matrix to form a fiber-based interface resulting with higher hardness and thus correlating to the lower wear for both samples in Figure 3.6.

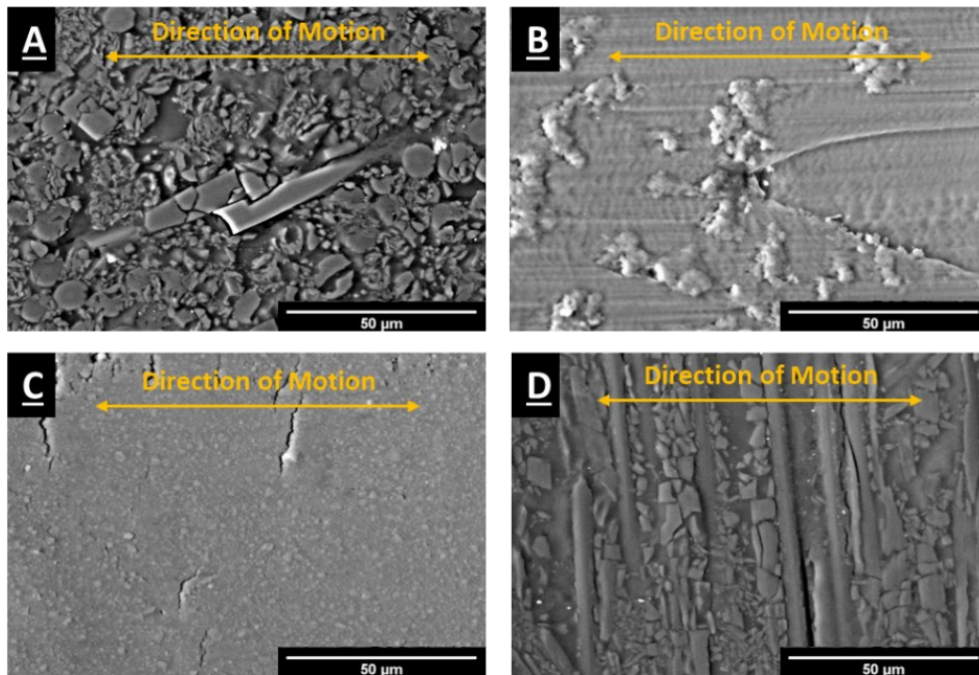


Figure 3.9: SEM Analysis of Sample Wear Track A) CF-PEEK Normal to the Fiber Direction Sample B) Pure Peek Sample C) CF-PEEK Parallel to the Fiber Direction Sample D) CF-PEEK Anti-parallel to the Fiber Direction Sample

Furthermore, ex situ analysis using AFM testing was also performed on the surface (unworn) and inside the wear track of each sample (worn), using a Force-Spectroscopy method, in order to have a better understanding on how the sliding test affect the adhesion force and the nano hardness of

the samples. The results of the average adhesion forces for the worn and unworn surfaces were obtained for each of the samples and are shown in Figure 3.10. It is interesting to initially observe the significant difference in pull-off force between the Pure PEEK sample and the CF-PEEK samples. When the adhesion force is high, in this case for the Pure PEEK sample, this indicates that it adheres better when in contact with another surface. This suggest that when performing the sliding test, the surface of the Pure PEEK sample adheres more to the alumina counterface and thus, pulling out larger debris particles which generates more friction and higher amount of wear. On the other hand, the CF-PEEK and CF-PEEK normal to the fiber direction sample have a lower in magnitude adhesion force and thus suggest that there is an easier sliding of the counterface on the surface of the samples, during sliding test, which would lead to lower friction and wear being generated than the Pure PEEK sample.

Additionally, it is also interesting to see how the adhesion force of the surfaces of the samples has been affected by the tribometer testing. More specifically, as shown in Figure 3.10, for the pure PEEK sample, the adhesion force has significantly decreased whereas for the CF-PEEK samples the opposite is happening, and the adhesion force is increased. It is also important to note that the adhesion force is directly related to the surface energy of the samples. When the adhesion force is increased, the surface energy is also increased since it is a function of the molecular attraction of the sample. In this case for the CF-PEEK sample, following the tribometer testing, it can be seen that there is an increased in the adhesion force inside the wear track which signifies that the surface energy of these samples has also increased. The highest increased can be observed for the CF-PEEK anti-parallel to the fiber direction which correlates with the wear results that were obtained in Figure 3.6.

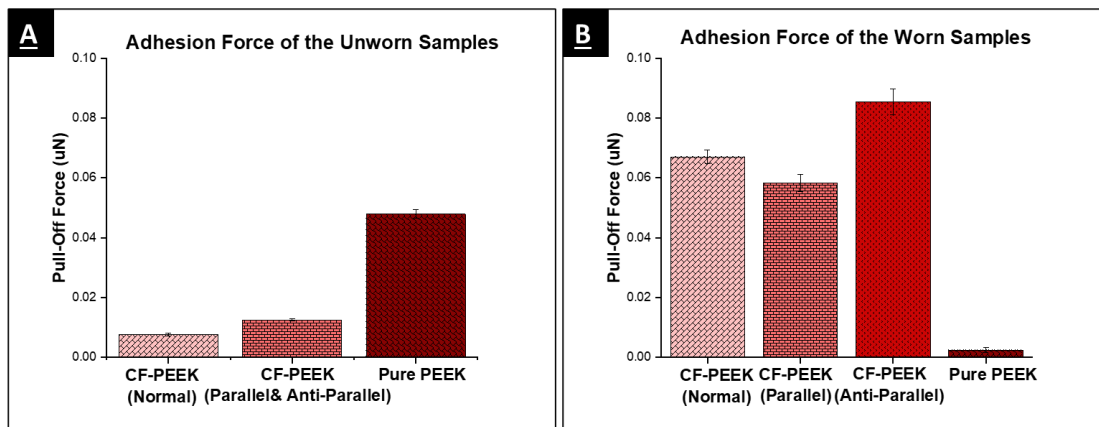


Figure 3.10: Adhesion Force of the A) Unworn Samples B) Worn Samples Using AFM Spectroscopy

The results of the estimated nano hardness, which is a function of the deformation depth, of the unworn and worn surfaces were obtained for each of the samples and are shown in Figure 3.11. In the case of the Pure PEEK and CF-PEEK parallel to the fiber direction, the increase in deformation depth of the worn samples indicates that the hardness of the surface has decreases following the sliding tests. Thus, it correlates with the results obtained in Figure 3.6 where it has the highest recorded wear depth and the observations done with the SEM analysis where the significantly increase in deformation depth indicates that the inside of the wear track is of lower hardness and thus produces more debris particles. On the other hand, for the CF-PEEK normal to the fiber direction and CF-PEEK anti-parallel to the fiber direction samples, the decrease in the recorded deformation depth indicates that the surface of the worn sample has increase in hardness. These observations also correlate with the observation made in Figure 3.6, where it has the lowest recorded wear depth, and the observations done with the SEM analysis where a fiber-based interface with higher hardness has been generated inside the wear track. Overall, the CF-PEEK anti-parallel to the fiber direction has the overall highest recorded decrease in deformation depth which would signify that the inside of the wear track is of highest hardness.

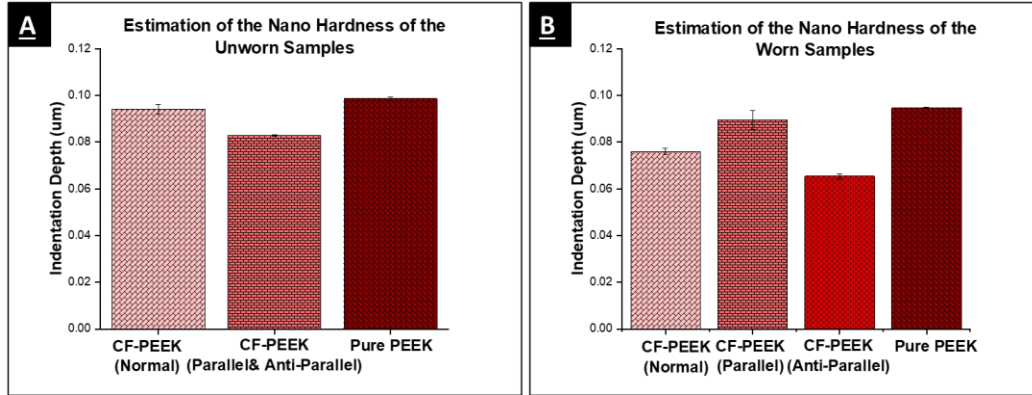


Figure 3.11: Estimation of the Nano Hardness of the Unworn (left) and Worn (right) samples Using AFM Spectroscopy

Optical images of the surface of the samples were also taken during the confocal analysis. An interesting observation that can be made from these pictures were form the CF-PEEK parallel to the fiber direction sample. During the three different tribological testing, all the samples were tested under the same applied load and for the same duration, however, in one of the testing's it was noticed from the optical images that it has failed. Figure 3.12 shows the surface of the CF-PEEK parallel to the fiber direction sample and its wear track where a significant crack can be observed and thus meaning there was a failure of the sample. In addition to the failure of the

sample, when using a higher magnification with the confocal, it is possible to observe the delamination of the fibers that was caused by the sliding of the counterface on the surface of the sample and thus being another cause of failure of the sample.

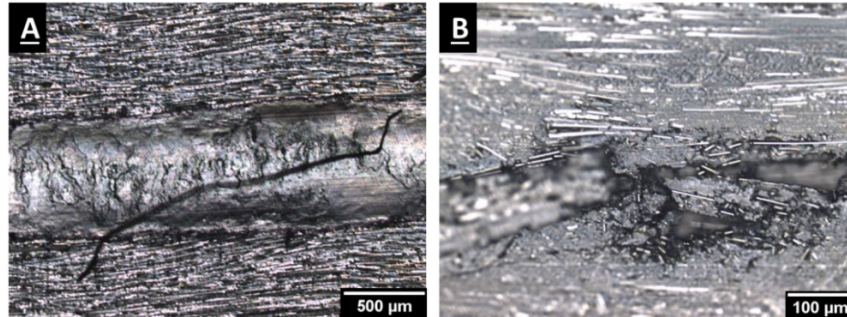


Figure 3.12: CF-PEEK Parallel to the Fiber Direction A) Failure due to a Crack on the Surface
B) Failure Due to Delamination

3.4.3.2. Counterface Analysis

Subsequently to the tribometer testing, it was possible to obtain images of the alumina counterfaces through Confocal Laser Microscopy in order to have a better understanding of the wear mechanism. Figure 3.13 shows the optical images of the portion of the counterfaces that was in contact with the surface of the samples during the testing.

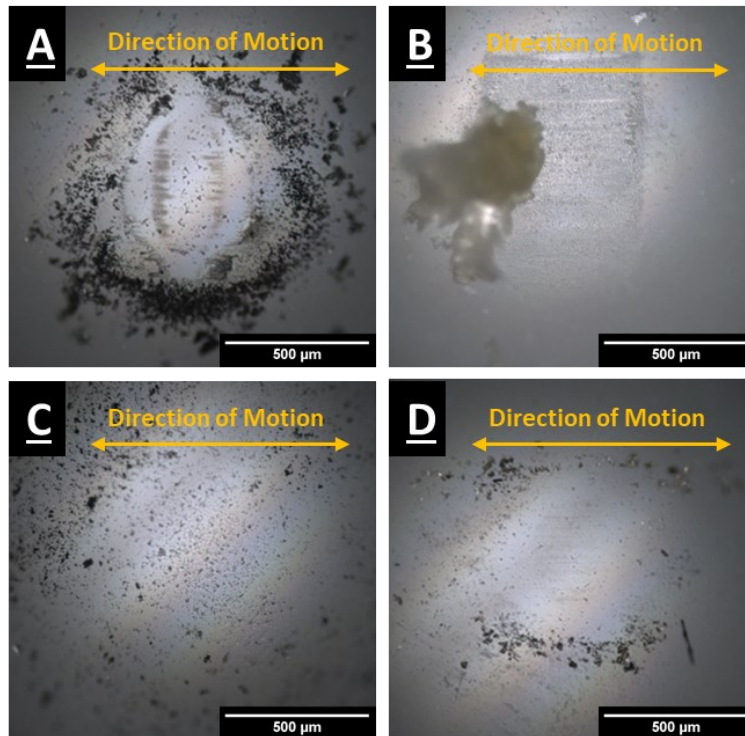


Figure 3.13: Confocal Images of Counterface for A) CF-PEEK Normal to the Fiber Direction Sample B) Pure Peek Sample
C) CF-PEEK Parallel to the Fiber Direction Sample D) CF-PEEK Anti-parallel to the Fiber Direction Sample

In these optical images, it is important to observe that in some cases there is a lack or presence of transfer film on the surface of the counterfaces. A transfer film on the alumina counterfaces gives a good idea of the adhesion of the sample and can help predict its wear and friction performance. The generation of transfer film between the sample and the counterface in Figure 3.14, can be caused by the generations of smaller debris particles and thus improves the wear performance of the sample.

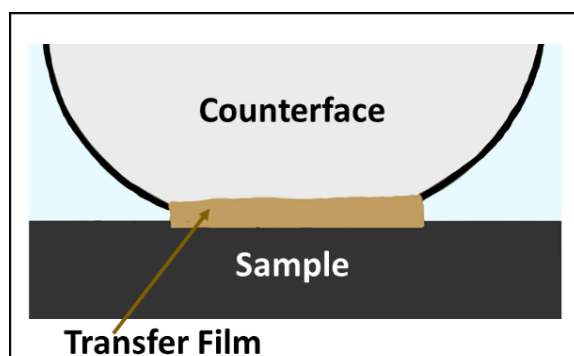


Figure 3.14: Transfer Film Formation

Figure 3.13 B) and C) represents the alumina counterfaces that were used during the testing of the pure PEEK and CF-PEEK parallel to the fiber direction samples respectively. These optical images revealed the absence of a transfer film on these samples which correlates to the higher amount of wear obtained in Figure 3.6. The lack of transfer can be explained by the higher amount of debris particle generation. Alternatively, Figure 3.13 A) and D) represents the alumina counterfaces used for the testing of the CF-PEEK normal to the fiber direction and the CF-PEEK anti-parallel to the fiber direction samples respectively. On these optical images, it is possible to observe that a thin and uniform transfer film has been generated on the counterfaces during the tribological testing. The presence of the transfer film in these images correlates with the low friction and wear that were observed on these samples.

Additionally, SEM images were also taken for the counterfaces used in each tribometer testing and are shown in Figure 3.15. From these images, EDS analysis was also performed on the counterfaces in order to obtain the elemental distribution present on their surfaces. The EDS analysis results in Figure 3.16, has revealed the presence of carbon and oxygen (coming from the samples itself) and of alumina (coming from the counterface) for all the samples however, in different amounts. In the case of the pure PEEK and the CF-PEEK parallel to the fiber direction

samples, where the higher amount of wear was observed, the counterfaces surface revealed the presence in higher quantity of carbon and a lower quantity of alumina and oxygen which correlates with the higher amount of debris generation. This also indicates that for these samples, the debris particles being generated are thicker and actual junk of materials coming out from the wear track. On the other hand, for the case of the CF-PEEK normal to the fiber direction and CF-PEEK anti-parallel to the fiber direction samples, it was revealed though the EDS that there was a lower quantify of carbon, when compared to the other two samples, present on the surface of the counterfaces and a higher amount of alumina and oxygen present. This also correlates with the observations made from the confocal images of the counterfaces of the two samples where there is formation of a transfer film on their surfaces. In this case, the transfer film is thin and formed from the low amount of transfer of material from the surface of the samples onto the surface of the counterfaces and is building up as a function of the applied load and time which explains the higher amount of alumina also detected since there is less debris particles being generated.

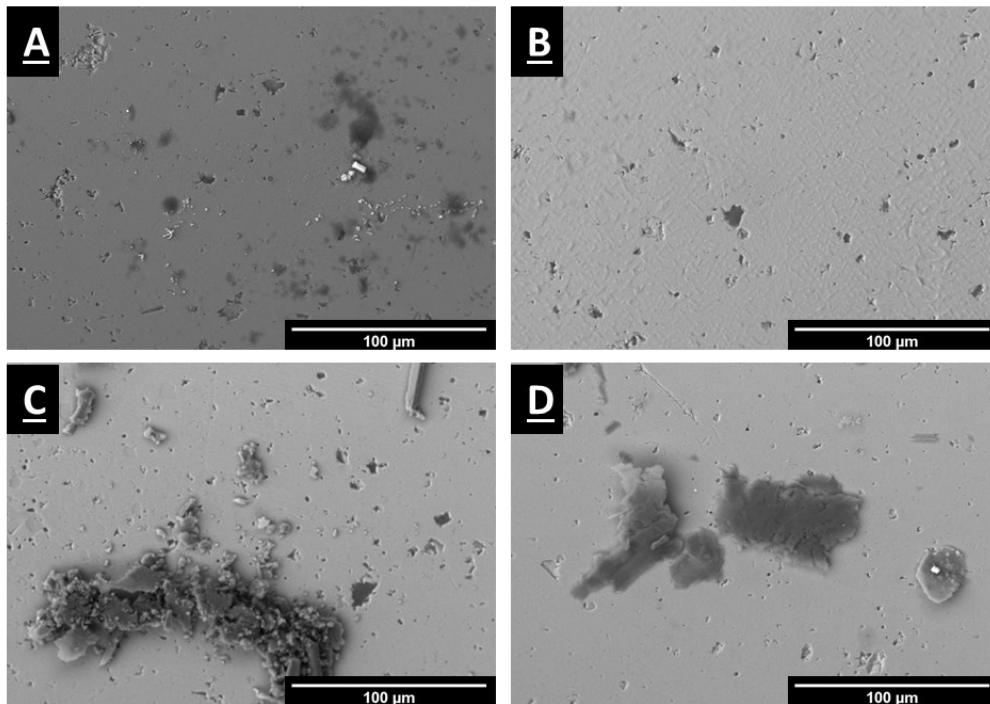


Figure 3.15: SEM Analysis of Samples Counterfaces A) CF-PEEK normal to the fiber direction Sample B) Pure Peek Sample C) CF-PEEK Parallel to the Fiber Direction Sample D) CF-PEEK Anti-parallel to Fiber Direction Sample

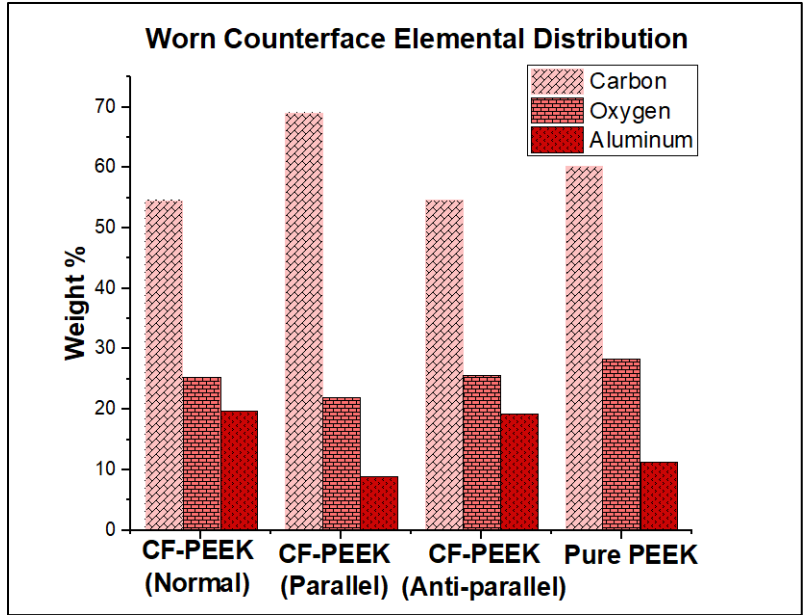


Figure 3.16: EDS Analysis on the Counterfaces

3.5. Discussion

The tribology testing that was performed for the purpose of this study has allowed to fully capture the tribological behavior of CF-PEEK with fiber oriented in the normal direction when compared to conventional unidirectional CF-PEEK and Pure Polyether ether ketone (PEEK) under various contact conditions and over time for the purpose of long-lasting gas turbine engines. The friction and wear behaviour, in Figure 3.5 and Figure 3.6 respectively, has revealed that the pure PEEK and CF-PEEK parallel to the fiber direction samples have higher coefficient of friction and have the surfaces that were the most worn off from the sliding of the counterface on their surface. Alternatively, the CF-PEEK normal to the fiber direction and CF-PEEK anti-parallel to the fiber direction have shown significantly lower coefficient of friction and wear on their surface and thus behaving more efficiently under an applied load and over time.

It has been determined from the different ex situ analysis that the samples follow the mechanism of adhesive wear when subjected to a sliding testing. The adhesive wear mechanism can be described as the adhesion on the surface of the samples to the surface of the counterface as it slides against it and thus pulls material away from it [35]. More importantly, the four different samples can be subcategorized into two different mechanisms: Ploughing and shearing. The pure PEEK and CF-PEEK parallel to the fiber direction samples follows the ploughing mechanism as illustrated in Figure 3.17. This mechanism is characterized by an increase in friction due to a

decrease in load-carrying capacity of the surface. In the case of these two samples, it has been revealed from the Ex-situ analysis that they are generating a greater number of debris particles when the counterface slides on its surfaces which is limiting the formation of a transfer film. The excessive generation of debris particle is thus directly affecting the load-carrying capabilities of the samples and thus when subjected to the constant applied load, it will generate a significantly higher wear rate and increase depth of the wear track.

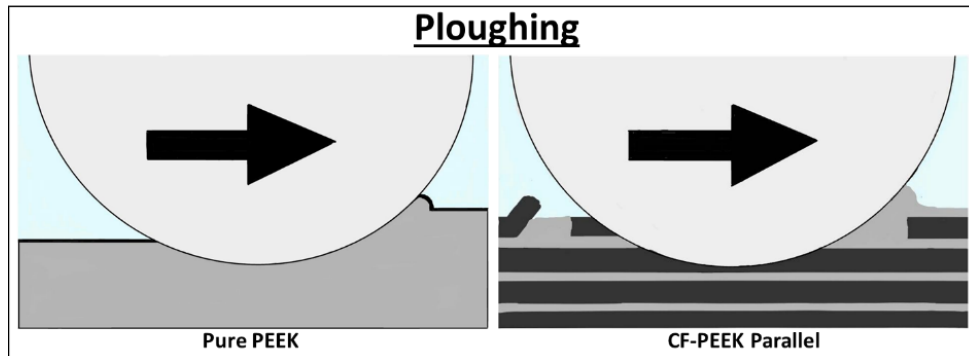


Figure 3.17: Ploughing mechanism

On the other hand, the CF-PEEK normal to the fiber direction and CF-PEEK anti-parallel to the fiber direction samples follows the shearing mechanism as illustrated in Figure 3.18. This mechanism can be characterized by a low number of debris particles being generated from the sliding of the counterface on the surface of the sample. In this case, the friction that is generated is significantly lower than when ploughing happens due the fact that the friction is directly proportional to the shear strength of the contact surface and related to its deformation properties [35]. In the case of the CF-PEEK normal to the fiber direction sample, since the fibers have been oriented upward in the normal direction, it has for effect to enhance the through thickness property of the material. Thus, since the fibers are normally oriented, as seen in Figure 3.8 A), the counterface is directly sliding across their cross-section which enhance the deformation properties of the CF-PEEK normal to the fiber direction material and thus procure that significantly lower friction and wear. On the other hand, for the CF-PEEK anti-parallel to the fiber direction, it is interesting to mention that the effect of the fiber direction is a decisive factor when it comes to its tribological properties. When the counterface slides in a motion anti-parallel to the fiber direction under the applied load, the fibers are at their full potential, being more stable, and thus have better deformation properties which again significantly lower the friction and wear compared to when sliding parallel to the fiber direction.

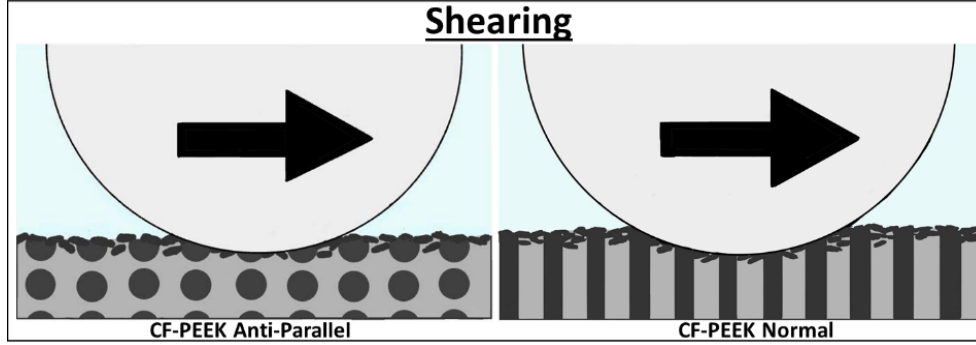


Figure 3.18: Shearing Mechanism

Theoretically, the coefficient of friction (μ) equation, Equation 2, that applies for fiber-reinforced polymer is a function of the ratio of the volume fraction of fiber (V_f) in the composite divided by the coefficient of friction component of the fiber (μ_f) and the ratio of the volume fraction of the matrix (V_m) in the composite divided by the coefficient of friction of the matrix (μ_m) [36]:

$$\frac{1}{\mu} = \frac{V_f}{\mu_f} + \frac{V_m}{\mu_m} \quad (2) [36]$$

Thus, Equation 2 can be directly related to the observations made from the SEM images of the inside of the wear track in Figure 3.9. In the case of the CF-PEEK normal to the fiber direction and the CF-PEEK anti-parallel to the fiber direction samples, the volume fraction of the fibers is increased and component of friction due to the fiber is reduced, due to the fibers being embedded in the matrix during the sliding test (shearing of the system), which has for effect of lowering the overall coefficient of friction of the system. The inverse is also true for the pure PEEK and CF-PEEK sample where the volume fraction of matrix is increased due to the generations of large debris particle (ploughing of the system) which in its turn increase the component of friction due to the matrix and thus increase the overall coefficient of friction.

Furthermore, the coefficient of friction (μ) of each component of the Equation 2 is also a function of the tangential frictional force (F) divided by the normal load (W) on the contact surface as seen in Equation 3 [35]. Subsequently the force (F) that is acting on the surface can be divided into two different components as seen in Equation 4: the force due to the adhesion (F_a) between the surfaces and the force due to the deformation (F_d) [35].

$$\mu = \frac{F}{W} \quad (3) [35]$$

$$F = F_a + F_d \quad (4) [35]$$

Where $F_a = \text{Friction due to adhesive}$

$F_d = \text{Friction due to deformation}$

This correlates with the friction behaviour that was observed in Figure 3.5 and explained above. Since the coefficient of friction is a function of the friction due to the deformation, it will make sense that for the pure PEEK and CF-PEEK parallel to the fiber direction samples it is significantly higher due to the ploughing which is directly causing a higher deformation of the surface. The inverse is also true for the CF-PEEK normal to the fiber direction and CF-PEEK anti-parallel to the fiber direction sample where its shearing mechanism is causes zero to little deformation of the sample surface and thus significantly decreasing/eliminating the friction due to deformation component in the equation and only leaving the friction due to the adhesive.

In addition, for the CF-PEEK normal to the fiber direction and CF-PEEK anti-parallel samples that are performing significantly better in terms or wear and friction, it can be observed when taking a closer look at the SEM images in Figure 3.8 that the fiber direction plays a substantial role. In the case of the CF-PEEK normal to the fiber direction sample in Figure 3.8 A), since the fibers are aligned in the normal direction, some areas on the surface will be denser in fibers than others where there is more PEEK material. When the counterface is sliding across the surface with higher volume ratio of fibers, its coefficient of friction decreases even more, as seen in Figure 3.5 with the error bars on the curve of the CF-PEEK normal to the fiber direction samples. The opposite is also true when the counterface is sliding in an area where the fiber volume ratio is smaller, and more resin material is exposed which brings the coefficient of friction up. On the other hand, in the case of the CF-PEEK anti-parallel to the fiber direction, when the counterface slides across the surface, it has for effect of pushing the fibers against one another and thus covering some of the resin material which has for effect of decreasing the friction generated.

When looking at the overall results for the wear and friction behaviour of the samples, it can be seen that the pure PEEK sample has the highest friction and wear followed by the CF-PEEK parallel to the fiber direction since they follow a ploughing mechanism. Alternatively, the CF-

PEEK normal to the fiber direction sample has a significantly better friction and wear behaviour due to the fibers being aligned in the z-direction. Finally, the CF-PEEK anti-parallel to the fiber direction is the sample that performed the best under tribological testing and providing the best wear and friction results.

However, it is important to note that for the purpose of this study, the same samples were taken for the CF-PEEK UD tape and was tested parallel to and anti-parallel to the fiber direction. In the case where the tribological testing was performed parallel to the fiber direction, the sample performed poorly compared to anti-parallel to the fibers which makes it fiber orientation dependent. Thus, this means that when manufacturing a component made of unidirectional carbon fiber (layered in the parallel & anti-parallel direction) an additional complexity is added since if not done in the right fiber direction, it could have the opposite effect and lower its tribological capabilities.

Finally, structures within gas turbine engines are often in contact and moving with a large number of complex mechanical assemblies where the tribological performance of the materials are crucial. Thus, in the case where the unidirectional carbon fiber would be chosen, an additional degree of difficulty regarding the assembly of the components within the engines would be added to ensure that the tribological properties are exerted to their maximum capabilities. On the other hand, the beauty of the CF-PEEK normal to the fiber direction is that it is not fiber dependent. Since the fibers are oriented in the z-direction, the direction of the sliding on the surface does not matter and allows to have as good tribological properties than the unidirectional carbon fiber when the sliding anti-parallel to the fiber direction. This would thus allow for structures to be integrated more easily within the engines and guaranteeing good tribological properties which thus makes it a better material option.

3.6. Conclusion

Through this study, it was possible to observe the impact of the direction of the fibers with regards to tribological properties in CF-PEEK. Three different orientations were tested for the CF-PEEK composite samples which are parallel, anti-parallel and normal direction and were also compared to pure PEEK material as a baseline. In order to obtain an accurate representation of the results, each different sample were tested under high applied loading and over time in order to simulate operating conditions for the purpose of long-lasting gas turbine engines. It was found through tribometer testing and Ex situ analysis (SEM, EDS, AFM, Confocal Laser Microscopy) that the pure PEEK and CF-PEEK parallel to the fiber direction samples, respectively in that order, generates the highest friction and wear. On the other hand, the CF-PEEK anti-parallel to the fiber direction and CF-PEEK normal to the fiber direction samples, respectively in that order, generates the lowest recorded friction and wear. Although the CF-PEEK anti-parallel to the fiber direction performed tribologically overall better, the analysis has revealed that it was not the case when parallel to the fiber direction which makes the CF-PEEK unidirectional tape orientation dependent. Thus, the CF-PEEK where the fibers are in the normal direction is a more advantageous options where it is orientation independent and can easily be integrated in designs as well as having competitive tribological performance to CF-PEEK when anti-parallel to the fiber direction. Methods to implement normal fiber orientation is commercially practical by using Boston Materials ZRT film product.

3.7. References

- [1] S. Kumar Thakur and D. L Deptowicz, "Technology Vision," *Surface Engineering*, vol. XXVII, no. 2, pp. 81-82, 2012.
- [2] X. Wu, W. Beres and S. Yandt, "Challenges in life prediction of gas turbine critical components," *Canadian Aeronautics and Space Journal*, vol. LIV, no. 2, pp. 31-39, 2008.
- [3] Z. Wei, S. Zhang, S. Jafari and T. Nikolaidis, "Gas turbine aero-engines real time on-board modelling: A review, research challenges, and exploring the future," *Progress in Aerospace Sciences*, vol. CXXI, no. 1, 2020.
- [4] M. Hughes, "Challenges for Gas Turbine Engine Components in Power Generation," *Procedia Structural Integrity*, vol. VII, pp. 33-35, 2017.
- [5] A. Misra, "Durability Challenges for Next Generation of Gas Turbine Engine Materials," NASA Glenn Research Center, Cleveland, 2012.
- [6] T. R. B. S. a. I. S. D. o. E. a. P. S. A. a. S. E. B. C. o. A. R. a. T. f. V. 2. National Research Council, *Securing the Future of U.S. Air Transportation: A system in Peril*, Washington: National Academies Press, 2003.
- [7] R. C. Reed, *The Superalloys Fundamentals and Applications*, United States of America: Cambridge University Press, 2006.
- [8] C. Sims, N. Stoloff and W. Hagel, *Superalloys II: High-Temperature Materials for Aerospace and Industrial Power*, London: Wiley, 1987.
- [9] S. A. Willey, "The Engines of Pratt & Whitney: A Technical History," *Air Power History*, vol. LVIII, no. 1, pp. 50-52, 2011.
- [10] C. DellaCorte and O. Pinkus, "Tribological Limitations in Gas Turbine Engines A Workshop to Identify the Challenges and Set Future Directions," NASA, Albany, 2000.
- [11] S. Schmidt, S. Beyer and H. Immich, "Ceramic Matrix Composites: A Challenge in SpacePropulsion Technology Applications," *International Journal of Applied Ceramic Technology*, vol. II, no. 2, pp. 85-93, 2005.

- [12] P. J. Bleau, "Elevated-temperature tribology of metallic materials," *Tribology International*, vol. XLIII, no. 7, pp. 1203-1208, 2010.
- [13] M. W. Hyer, *Stress Analysis of Fiber-Reinforced Composite Materials*, Lancaster: DEStech Publications, 2009.
- [14] I. M. Daniel and O. Ishar, *Engineering Mechanics of Composite Materials*, New York: Oxford University Press, 2006.
- [15] D. M. Knight, "Composite Materials," in *Encyclopedia of Physical Science and Technology (Third Edition)*, 2003, pp. 455-4698.
- [16] P. Mangalgiri, "Composite materials for aerospace applications," *Bulletin of Materials Science*, no. 22, pp. 657-664, 1999.
- [17] M. Bellonte, "Composite Materials in the Airbus A380," 2001.
- [18] D. F. Adams, L. A. Carlson and R. B. Pipers, *Experimental Characterization of Advanced Composite*, CRC Press, 2003.
- [19] E. S. Greenhalgh, *Failure Analysis and Fractography of Polymer Composites*, Woodhead Publishing Series in Composites Science and Engineering, 2009, pp. 107-163.
- [20] X. L. P. W. a. D. S. I Gnaba, "Through-the-thickness reinforcement for composite structures: A review," *Journal of Industrial Textiles*, vol. XLIX, no. 1, pp. 71-96, 2019.
- [21] K. Tan, N. Watanabe and Y. Iwahori, "Impact Damage Resistance, Response, and Mechanisms of Laminated Composites Reinforced by Through-Thickness Stitching," *International Journal of Damage Mechanics*, vol. XXI, no. 1, pp. 51-80, 2011.
- [22] G. Pappas, S. Joncas, V. Michaud and J. Botsis, "The influence of through-thickness reinforcement geometry and pattern on delamination of fiber-reinforced composites: Part I – Experimental results," *Composite Structures*, vol. CLXXXIV, pp. 924-934, 2018.
- [23] B. M'membe, M. Yasae, S. R. Hallett and I. K. Patridge, "Effective use of metallic Z-pins for composites' through-thickness reinforcement," *Composites Science and Technology*, vol. CLXXV, pp. 77-84, 2019.

- [24] G. Dell'Anno, J. Treiber and I. Patridge, "Manufacturing of composite parts reinforced through-thickness by tufting," *Robotics and Computer-Integrated Manufacturing*, vol. XXXVII, pp. 262-272, 2016.
- [25] L. K. Jain and Y.-W. Mai, "Mode I delamination toughness of laminated composites with through-thickness reinforcement," *Applied Composite Materials*, vol. I, pp. 1-17, 1994.
- [26] C. S. R. M. A. G. Dr. Rasam Soheilian, "Enhancing the Through-Thickness Modulus of Carbon Fiber Composites using Z-Axis Oriented Milled Carbon Fiber," Boston Materials, Inc., Billerica, 2020.
- [27] B. Materials, "ZRT Z-axis Aligned Carbon Fiber Films," Billerica, 2022.
- [28] D. Rajak, D. Pagar, P. Menezes and E. Linul, "Fiber-Reinforced Polymer Composites: Manufacturing, Properties, and Applications," *Polymers*, no. 11, p. 1167, 2019.
- [29] A. Abdelbary and Y. Mohamed, "Chapter 4 - Tribological behavior of fiber-reinforced polymer composites," in *Tribology of Polymer Composites*, Elsevier, 2021, pp. 63-94.
- [30] H. Parik and P. Gohil, "Tribology of fiber-reinforced polymer matrix composites—A review," *Journal of Reinforced Plastics*, vol. XXXIV, no. 16, pp. 1340-1346, 2015.
- [31] C. B., J. Gu, Z. Long, Z. Li, S. Ruan and C. Shen, "Effects of temperature and fiber orientation on the tensile behavior of short carbon fiber-reinforced PEEK composites," *Polymer Composites*, no. 42, pp. 597-602, 2021.
- [32] G. Gardiner, "Z-direction composite properties on an affordable, industrial scale," Veelo Technologies, 20 april 2021. [Online]. Available: <https://www.compositesworld.com/articles/z-direction-composite-properties-on-an-affordable-industrial-scale>. [Accessed 28 january 2022].
- [33] T. A. C. 'TORAY', "Toray Cetex® TC1200," 13 November 2019. [Online]. Available: <https://www.toraytac.com/product-explorer/products/ov14/Toray-Cetex-TC1200>. [Accessed 11 january 2022].
- [34] A. Paar, "Pin-on-disk tribometer: TRB3," Anton Paar, [Online]. Available: https://www.anton-paar.com/ca-en/products/details/trb3-pin-on-disk-tribometer/?utm_source=google&utm_medium=cpc&utm_campaign=CA_Dynamic.Search_EN

&utm_content=C-

00049741&gclid=CjwKCAiAlfqOBhAeEiwAYi43F4ZUMnEMxIBJnnZyr6y1ozwG0DrNGhfSi
nJM5r0NBcSqDRP97Z3wIRoC. [Accessed 10 01 2022].

[35] K. Holmberg and A. Matthews, *Coatings Tribology; Properties, Mechanisms, Techniques and Applications in Surface Engineering Second Edition*, Amsterdam: Elsevier, 2009.

[36] G. W. Stachowiak and A. W. Batchelor, *Engineering Tribology*, Burlington: ELSEVIER, 2005.

Chapter

4. Influence of temperature and fiber direction on the tribological behavior of carbon reinforced PEEK for applications in gas turbine engines

In this chapter...

The identification of the influence of temperature on the tribological behavior of carbon fiber PEEK will be presented.

4.1. Abstract

Next generations of gas turbine engines are required to significantly reduce their overall CO₂ emissions as well as reduce the noise pollution. In fact, by 2050, the aerospace industry has set a goal to reduce greenhouse gas (GHG) emissions to net zero which will consequently affect the conditions in which materials are expected to operate. Challenges will arise with the selection of materials in engines since they will be subjected to higher temperatures, pressures, and velocities which will limit the use of conventional metal or alloys due to their mechanical and tribological properties. Fiber-reinforced polymer (FRP) composites have been widely used in the aerospace industry but its usage in gas turbine engines has been limited due to the polymer matrix lower glass transition temperatures. However, many studies have showcased the tribological potential of FRP in the low temperature fan section of the engines, but little attention has been given to the potential of orienting the fibers in the normal direction of FRP. Thus, this study will focus on the effect of the fiber orientation on the tribological properties of carbon fiber/ PEEK (CF-PEEK) at high temperature. Three different CF-PEEK samples were chosen for the purpose of this study where the parallel, anti-parallel and normal direction were characterized as well as a fourth sample of pure PEEK in order to have a baseline material. Tribological testing was performed using a ball-on-disk tribometer where the samples were subjected to an elevated temperature of 200°C in order to obtain their wear and friction behavior. The characterization of the different worn surfaces and counterfaces to obtain the interfacial phenomena was done through Scanning Electron Microscopy (SEM), Energy Dispersive X-ray Spectroscopy (EDS) and confocal laser scanning microscopy (CLSM). Overall, it was found that the CF-PEEK with fibers oriented in the normal direction performed better at elevated temperature in terms of tribological behavior which makes it the most suitable orientation for implementation of CF-PEEK components in gas turbine engines.

4.2. Introduction

Within the structure of gas turbine engines, there exists a large number of complex and contacting moving mechanical assemblies [1] [2] [3]. These mechanical assemblies, as seen in Figure 4.1, are expected to operate in extremely harsh environment where the velocities are high, the operating temperatures are elevated, and the pressure is high [1] [4] [5] [6]. Thus, the proper selection of material for these engine components is crucial in order to ensure good efficiency and performance. Materials such as aluminum, titanium, steel, and nickel are currently used in specific regions of the engines [7] [8] [9] [10]. However, due to the current need to reduce the overall greenhouse gas (GHG) emissions within the aerospace industry [11] [12] [13], engines will need to increase their thermal efficiencies in order to achieve this challenge [14] [15]. The lifetime of many structures within the engines will be limited by the mechanical and tribological properties of the materials currently employed where degradation of these properties could lead to severe failures [16] [17] [18]. Thus, there exists a need in the aerospace industry to come up with a new generation of aerospace materials which would be able to fulfill the future operating requirements.

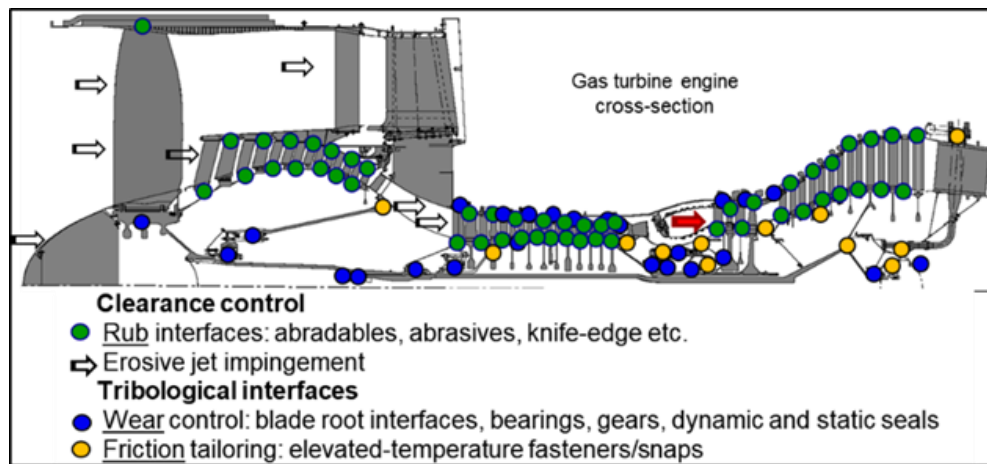


Figure 4.1: Contacting Mechanical-Assemblies in Cross-Section of Gas Turbine Engine [1]

Fiber-reinforced polymers (FRP) composites are already widely used in the aerospace industry and are considered to be an attractive alternative solution to conventional metals or unreinforced polymers [19] [20] [21] [22]. FRP have many different advantages since their properties can be customized based on specific applications and are generally lighter as well as having higher stiffness and strength properties [19] [23]. FRP are composed of a polymer matrix (ex: polytetrafluoroethylene, polyetheretherketone, etc.) and a reinforcement (ex: glass fibers, carbon

fibers, etc.) [20] [21] [22]. Thus, the choice of the matrix material, between a thermoplastic or thermosetting, and the choice of the fiber reinforcement is crucial for obtaining a competitive alternative material for structural applications [24] [25]. For the use of FRP in the aerospace industry, and more particularly for the purpose of gas turbine engines, the choice of the matrix material is a determining factor since the composite will be exposed to a harsh environment and more particularly to high operating temperatures [26] [25] [27]. There exists already a wide variety of polymer materials currently in use, as shown in Figure 4.2, but each of them operates at different temperature ranges [25] [28]. From Figure 4.2, the most common polymers normally operate between -250°C to 300°C which makes them a good option for operating in the front of the engines where temperature typically can range from -40°C to 300°C [7] [25] [29].

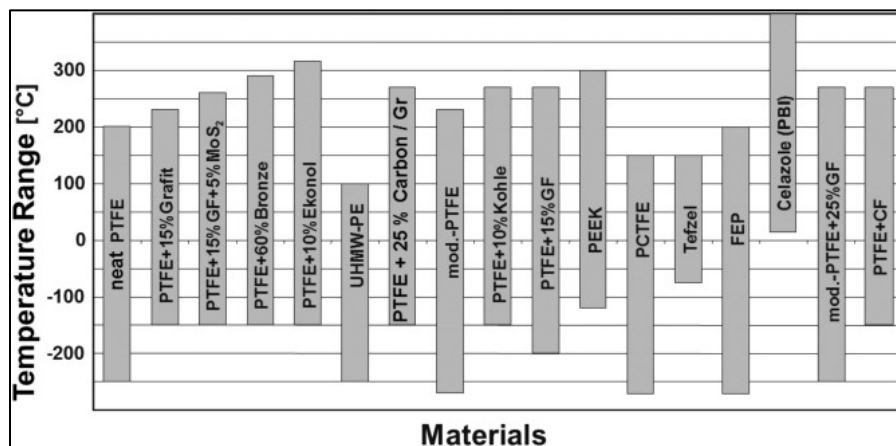


Figure 4.2: Temperature range for polymers materials currently in use [25]

Additionally, when considering FRP for the purpose of gas turbine engines, it is also important to take into consideration the orientation of the fibers [30]. Since there are a lot of moving and contacting mechanical assemblies in the engines, Figure 4.1, where a high quantity of elements such as bearings and seals are present [1] [29], the orientation of the fibers in FRP plays a crucial role in ensuring good tribological properties [30] [31]. Although studies have already been performed on the tribological characterisation of the fiber orientation in FRP at room temperatures [31] [32] [33], these studies have focuses more on the parallel and anti-parallel orientation of the fibers. However, little to no attention has been given on the characterization of the normal orientation of the fibers in FRP and its tribological properties when subjected to high temperatures. Thus, the purpose of this present study is to compare the tribological behavior of fiber-reinforced

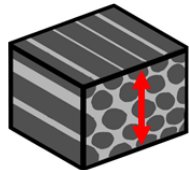
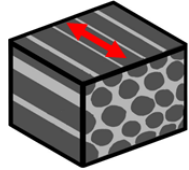
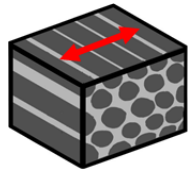
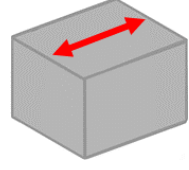
composite, in this case CF-PEEK, at high temperature and the effect of the fiber orientation (parallel, anti-parallel and normal direction) for the purpose of gas turbine engines.

4.3. Materials & methods

4.3.1. Materials

In this study, four different samples were subjected to high temperature tribometer testing for their characterization and to have a better understanding of the impact of the orientation the fibers in a reinforced composite. The materials that were chosen for the purpose of this study are carbon fiber/PEEK (CF-PEEK) composite and pure PEEK as a baseline for comparison. The CF-PEEK composite was tested in three different orientations: Parallel to the fiber direction, anti-parallel to the fiber direction and normal to the fiber direction, as illustrated in Table 4-1. The four different samples were polished through automated polishing process and were cut to dimensions of 25x25mm with a thickness of 2mm.

Table 4-1: Samples Descriptions

<i>Samples</i>	<i>Descriptions</i>	<i>Pictorial Representation</i>
Sample 1	CF-PEEK (ZRT/PEEK film) tested normal to the fiber direction <i>Sourced From: Boston Materials</i>	
Sample 2	CF-PEEK (unidirectional tape) tested parallel to the fiber direction <i>Sourced from: Toray Cetex</i>	
Sample 3	CF-PEEK (unidirectional tape) tested anti-parallel to the fiber directions <i>Sourced from: Toray Cetex</i>	
Sample 4	Pure Peek <i>Sourced from: Boedeker Plastics</i>	

The CF-PEEK unidirectional tape samples were obtained from Toray Cetex (Toray Cetex TC1200) and are composed of continuously long carbon fibers bonded and aligned by a semi-crystalline PEEK matrix [34] forming a unidirectional tape. The unidirectional tape is then isotropically layered up to the appropriate thickness using a compression molding process [34]. Alternatively, the CF-PEEK normal to the fiber direction sample was obtained from Boston Materials using their ZRT/PEEK film. The composite laminate is obtained from compression molding of quasi-isotropically layers of CF-PEEK unidirectional tape and layers of ZRT/PEEK film symmetrically layered on the outside. The ZRT/PEEK film is developed using a roll-to roll process, as illustrated in Figure 4.3, where reclaimed sub-millimeter carbon fibers are used and being vertically oriented in order to produce a ZRT film which is then melt infiltrated with PEEK yielding a ZRT/PEEK film. [35]

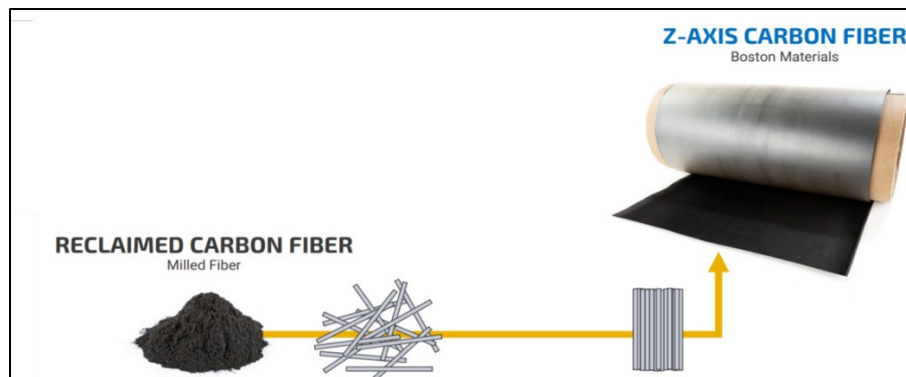


Figure 4.3: ZRT/PEEK film Manufacturing Schema

4.3.2. Tribological Evaluation & Characterization

Methods

For the purpose of this study, the tribological testing's were performed on a ball-on-disk linear tribometer with high temperature capabilities (Anton-Paar TRB3). Preliminary to performing tribological evaluation, testing parameters were determined in order to simulate more accurately the operating environment the samples would have to go through if they were operating in the front of a gas turbine engine. This includes an elevated testing temperature, a high loading, and a long distance to obtain a better representation of their performance over time. The determining tribological parameters are shown in Table 4-2.

Table 4-2: Tribological testing parameters

<i>Materials</i>	<i>Counterface</i>	<i>Normal load</i>	<i>Distance</i>	<i>Temperature</i>
CF-PEEK normal to the fiber direction	Al ₂ O ₃ (diameter of 6.35 mm)	18N	600m	200 Degree Celsius
CF-PEEK parallel to the fiber direction	Al ₂ O ₃ (diameter of 6.35 mm)	18N	600m	200 Degree Celsius
CF-PEEK anti-parallel to the fiber direction	Al ₂ O ₃ (diameter of 6.35 mm)	18N	600m	200 Degree Celsius
Pure PEEK	Al ₂ O ₃ (diameter of 6.35 mm)	18N	600m	200 Degree Celsius

*Other parameters: Track length (10mm), velocity (3.1cm/s), frequency (1Hz)

The tribometer testing results can yield to the obtention of the frictional behaviour of each different material. In order to obtain an accurate representation of the frictional behaviors and the variability in the data, three different testing's were performed for each different sample. Following the different tribometer testing's, it was possible to also analyse the wear tracks that were formed on the surface of the samples. The analysis of the wear tracks was performed using a Confocal Laser Microscopy (LEXT) from which optical images of the surface and cross-section measurement of the wear tracks can be obtained leading to the obtention of the wear behavior of the samples. A similar analysis can also be done for the counterfaces used during the tribometer testing using Confocal Laser Microscopy.

Ex Situ analysis was also performed in order to characterize the surface and wear track of the samples along with their corresponding counterfaces. Scanning Electron Microscopy (SEM) (Hitachi High Technologies America, Inc., USA) was performed to analyze the change in the topography of the surface following the tribometer testing which was possible by obtaining high precision images on the outside and the inside of the wear tracks. The topography of the

counterfaces was also obtained using SEM analysis. Following the obtention of the SEM images, it was also possible to perform Energy Dispersive X-ray Spectroscopy (EDS) (Pentafet Link, INCA X-sight, Oxford instruments, UK) analysis inside the wear track and on the surface of the counterfaces in order to obtain their elemental distribution which can give more insight on the wear of the counterface inside the wear track. Results

4.3.3. Friction Behaviour

The coefficient of friction against the number of cycles is shown in Figure 4.4. In order to obtain an accurate frictional behaviour for the four different samples, three tribometer test were performed for each of the samples and the average was plotted along with error bars every 500 cycles. In Figure 4.4, there is an obvious difference between the samples with fiber reinforcement and the pure PEEK sample where the coefficient of friction is significantly higher. In the case of the pure PEEK sample, the coefficient of friction starts a little under 0.35 and quickly stabilize and remain at steady state at 0.44 for the rest of the testing. On the other hand, for the samples with fiber reinforcement, the coefficients of friction at steady state in Figure 4.4 are significantly lower. For the CF-PEEK tested parallel to the fiber direction, the coefficient of friction increases rapidly at first until it reaches a maximum of 0.23 to then decrease and reach steady state at 8000 cycles. Similarly, for the CF-PEEK tested anti-parallel to the fiber direction, the coefficient of friction also rapidly increases to reach a maximum of 0.35 and then decreases and reach steady state at 15000 cycles. For both CF-PEEK parallel and anti-parallel to the fiber direction samples, it can be observed that at high temperature and over time, the influence of the fiber direction will have a low impact of the coefficient of friction once it reaches steady-state since for both samples it will remain at 0.1 until the end of the tribometer testing. When the tests were performed on the CF-PEEK normal to the fiber direction sample, the friction behavior follows a similar pattern to the CF-PEEK sample parallel and anti-parallel to the fiber direction but is significantly lower. The coefficient of friction rapidly increases to reach a maximum of 0.9 and will then decrease and attain steady state at 0.02 really early on in the testing at 5000 cycles.

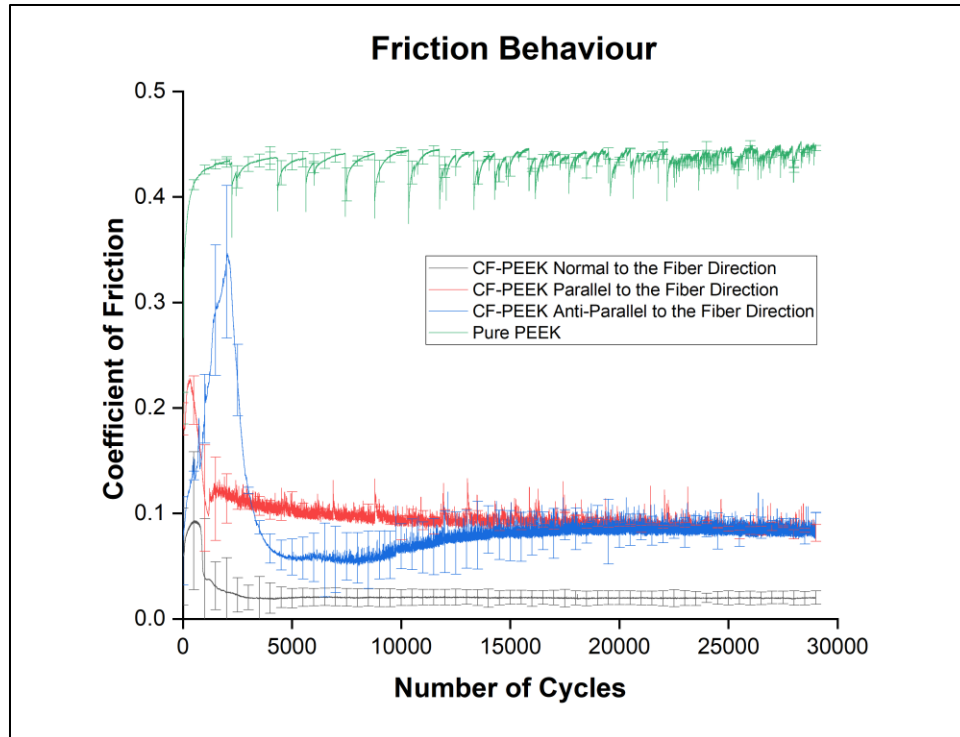


Figure 4.4: Friction Behaviour on Polished Samples at 200°C

4.3.4. Wear Behaviour

Following the tribometer testing, the wear track that was created on the surface of each sample were subjected to a Confocal Microscopy analysis in order to obtain an accurate representation of the cross-section of the wear track and obtain the maximum wear depth. The results of the wear measurements is shown in Figure 4.5 The maximum depth measurement, in Figure 4.5 B), is observed in the case of the pure PEEK sample, where it reaches a maximum of 45µm in the middle of the wear track. What is interesting to observe in the case of the samples that were reinforced with carbon fibers, is the significant difference that the fiber orientation has on the wear depth measurement. For the CF-PEEK anti-parallel and parallel to the fiber direction a maximum wear depth of 23µm and 17µm, respectively in that order, was measured in the middle of the wear track. On the other hand, for the CF-PEEK normal to the fiber direction sample, the lowest wear depth recorded in the center of the wear track is of 7µm, where there is the most contact with the counterface, and is significantly lower than any of the other samples subjected to the same testing parameters.

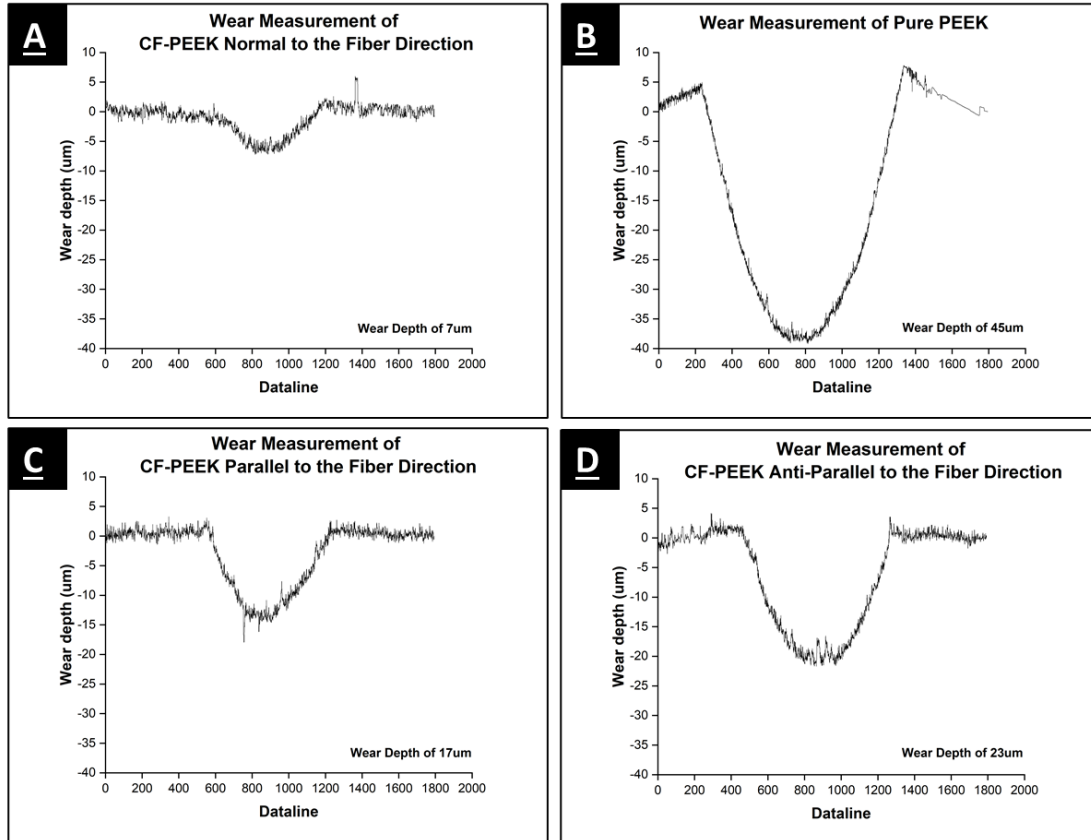


Figure 4.5: Wear Measurement at 200°C A) CF-PEEK Normal to the Fiber Direction Sample B) Pure PEEK Sample C) CF-PEEK Parallel to the Fiber Direction Sample D) CF-PEEK Anti-parallel to the Fiber Direction Sample

In addition to the measurement of the maximum wear depth from the confocal microscopy analysis, the wear rate was also calculated for each of the samples. From literature [37], the wear rate (k) can be calculated from the ratio of the wear volume (V), which can be obtained from Figure 4.5, over the multiplication of the applied load (w) and sliding distance (s) which are known parameter that were predefined to the tribometer testing. Thus, since the wear volume is a function of the depth of the wear track, the higher the depth measured in Figure 4.5, the higher the wear rate will be. The average wear rate for each of the four samples is represented in Figure 4.6 where it can be observed that the pure PEEK sample has the highest wear rate. In the case of the CF-PEEK samples, the wear rate is significantly lower and is the lowest for the CF-PEEK normal to the fiber direction sample. An interesting observation can be made from Figure 4.6 where for the CF-PEEK parallel to the fiber direction sample there is a large margin of error which indicates the instability of the sample since the results are not constant from testing to testing.

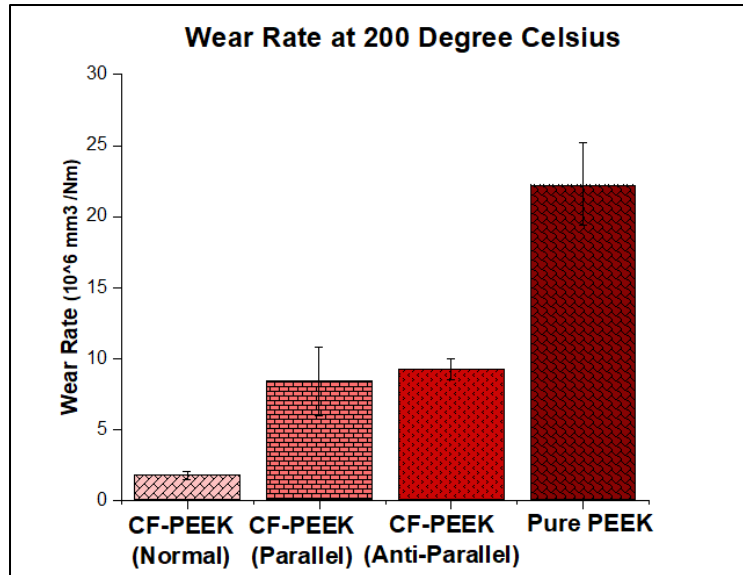


Figure 4.6: Wear Rate of the Samples at 200°C

4.3.5. Ex Situ Analysis

4.3.5.1. Wear Track Analysis

To begin the characterization of the wear tracks following the high temperature tribometer testing, SEM was performed on the surface of the samples. Figure 4.7 shows the images that were taken with a magnification of 1000x on the unworn surfaces after being subjected to a temperature of 200°C during the testing. For the pure PEEK sample, the surface is smooth however, with the presence of some random striation that can be explained by the polishing of the sample. Additionally, from Figure 4.7, it is also possible to observe more precisely the direction of the fibers in relation with the direction of the sliding. For the CF-PEEK tested normal to the fiber direction, in Figure 4.7A), the vertically aligned fibers can be observed as we clearly see their cross-section compared to the CF-PEEK unidirectional tape where we see long continuous fibers (Figure 4.7 C) and Figure 4.7B)). It is also important to note that for the case of the CF-PEEK unidirectional tape samples (parallel and anti-parallel), it can be observed that the continuous fibers have been broken at some places which can be due to the automated polishing process performed on the surfaces of the samples. The breaking of the continuous fibers can have for effect to weaken the upper surface laminate and increase the friction at the start of the tribometer testing which correlates with the results obtained in Figure 4.4.

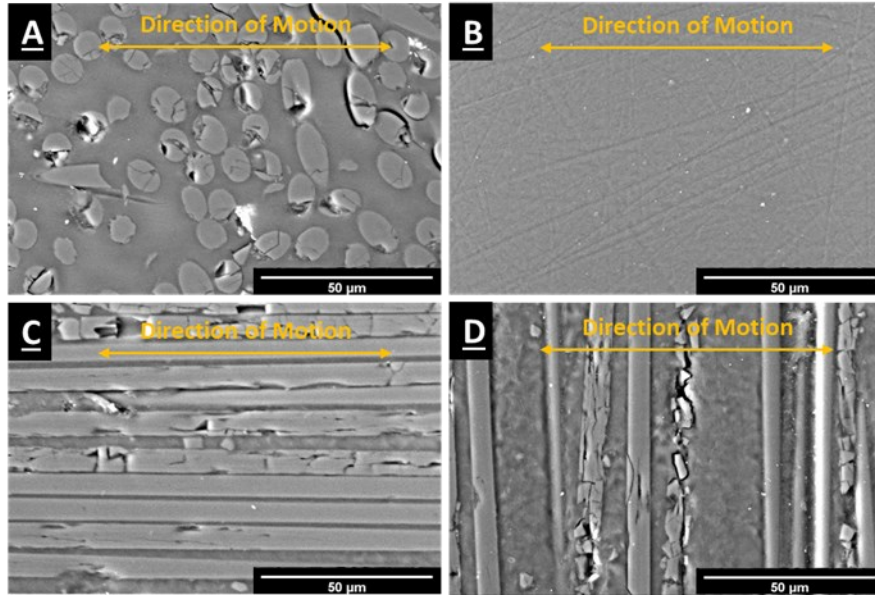


Figure 4.7: SEM Analysis of Sample Surface at 200°C A) CF-PEEK Normal to the Fiber Direction Sample B) Pure PEEK Sample C) CF-PEEK Parallel to the Fiber Direction Sample D) CF-PEEK Anti-parallel to the Fiber Direction Sample

Furthermore, SEM images of the inside of the wear track were also taken, as shown in Figure 4.8, with a magnification of 1000x in order to observe the change in topography. For the pure PEEK sample, in Figure 4.8 B), it can be observed that following the tribometer testing, large debris particles are being generated from the softening of the sample at higher temperature and are being pushed on both side of the track. With time, the large debris particles are pushed on the outside of the wear track which leaves the center of the wear track smoother and more prone to the formation of other large debris particles and thus increasing the wear of the surface. The observations made for the pure PEEK sample correlates well with the results obtained in Figure 4.6 where a higher wear rate is obtained compared to the other samples. On the other hand, when taking a closer look at the CF-PEEK reinforced samples, it can be observed that the fiber direction has a large influence on the topography of the inside of the wear track following the high temperature tribometer testing. In the case of the CF-PEEK tested anti-parallel to the fiber direction, the absence of fibers on the worn surface can be noticed when comparing Figure 4.7 D) and Figure 4.8 D) which implies that a more polymer based interface has been formed and is more prone to soften under the applied high temperature and thus increase the wear of the sample. A similar phenomenon can be observed in some regions of the worn surface of the CF-PEEK parallel to the fiber direction in Figure 4.8 C) where the upper region is left without the presence of fibers. On the other hand, the lower region of Figure 4.8 C) shows exposed continuous fibers which would signifies that at high temperature,

the CF-PEEK sample when tested parallel to the fibers is inconsistent and correlates with the high margin of error found the wear rate of Figure 4.6. The absence of fibers leaves a more softened polymer surface which increase the wear and the exposed section of the continuous fibers leaves a harder fiber base surface which lower the wear. Finally, when we compare the worn and unworn surfaces of the CF-PEEK tested normal to the fiber direction (Figure 4.7 A) VS Figure 4.8 A)) the opposite phenomenon to the CF-PEEK tested anti-parallel to the fiber direction is observed. Subsequently to the tribometer testing at high temperature, the fibers oriented in the normal direction have been broken and crushed in the softened PEEK matrix, which is leaving a more fiber-based interface of higher hardness resulting in a decrease in the wear of the surface.

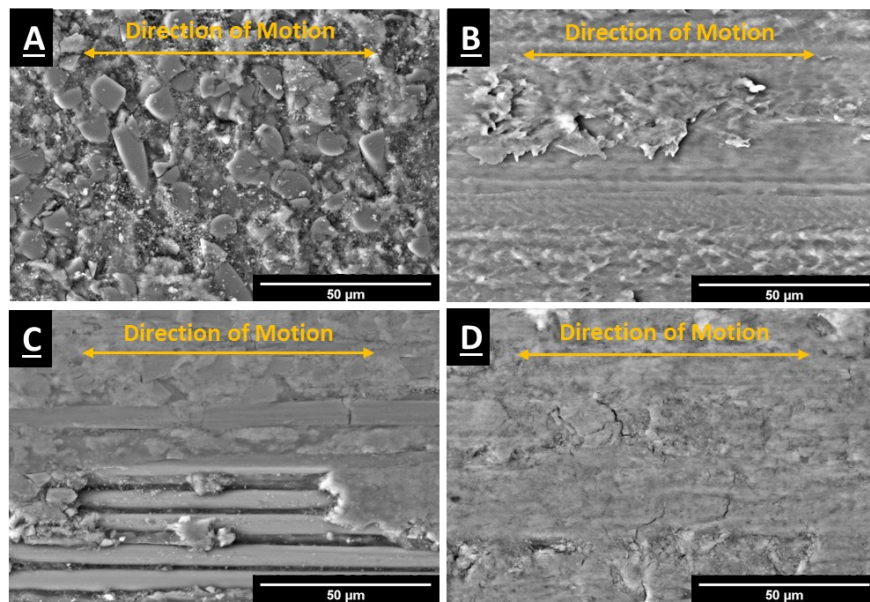


Figure 4.8: SEM Analysis of Sample Wear Track at 200°C A) CF-PEEK Normal to the Fiber Direction Sample B) Pure PEEK Sample C) CF-PEEK Parallel to the Fiber Direction Sample D) CF-PEEK Anti-parallel to the Fiber Direction Sample

Furthermore, a closer look at SEM image of the worn CF-PEEK parallel to the fiber direction sample was taken and more precisely the exposed continuous fiber area. Figure 4.9 shows a 2000x magnification of the exposed fiber region where it is possible to observe more clearly two regions of failure damages. In the upper right corner of Figure 4.9, a fiber break can be observed which can be due to the sudden rise in temperature of the sample and combination of high applied loading on the fiber. This phenomenon was also observed at many different places along the exposed fibers of the wear track. In addition, in the lower right corner of Figure 4.9 the delamination of the matrix can be observed and can be caused by the interlaminar stress being higher than the strength of the fiber reinforcement when subjected to the frictional force created by the sliding of the counterface

on its surface under high applied load. The fiber breaks and matrix delamination are both mechanics of damages that can lead to the failure of the CF-PEEK sample when subjected to frictional force parallel to the fibers.

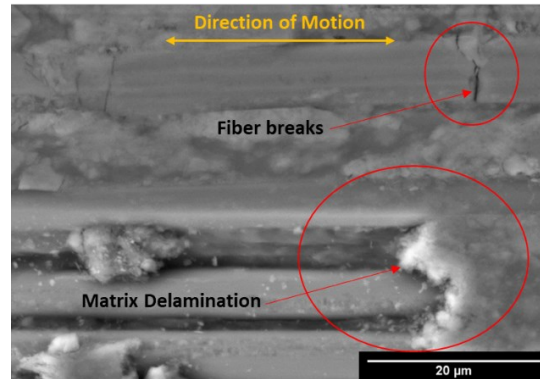


Figure 4.9: CF-PEEK Parallel to the Fiber Direction Mechanics of Damages at 200°C

Following the SEM analysis of the worn surfaces, a line type EDS was performed perpendicular to the wear track of the samples to determine the elemental distribution present. Results are shown in Figure 4.10. In the case of the CR-PEEK tested anti-parallel to the fiber direction, the elemental distribution in Figure 4.10 C) shows that there is a decrease of carbon in the middle of the wear track and by consequence an increase in oxygen and alumina which implies that the Al_2O_3 counterface has been worn off. Thus, for the CF-PEEK tested anti-parallel to the fiber direction, the surface is not only wearing off at a higher rate but at increase temperature with the softening of the PEEK matrix and the increase in debris size generated, it is also starting to wear off the counterface in the center of the wear track which is where the applied load is maximum. Similarly, for the CF-PEEK tested parallel to the fiber direction, the elemental distribution in Figure 4.10 B) also shows that in the region of the wear track where there is absence of fibers, there is a lower amount of carbon detected and a higher amount of oxygen and alumina present which correspond to a higher wear of the counterface in these regions of the wear track. On the other hand, in the regions where there are exposed continuous carbon fibers, it can be observed in Figure 4.10 B) that there is an increase in carbon and a decrease oxygen and alumina which implies that the Al_2O_3 counterface wears at a lower rate due to a decrease in debris particle in the wear track which also correspond to the lower wear rate results in Figure 4.6. Alternatively, for the CF-PEEK tested normal to the fiber direction, the elemental distribution in Figure 4.10 A) shows that the amount of carbon detected is more stable and significantly higher than the oxygen and alumina which corresponds well with the observation formulated from the SEM image of the wear track where a

more fiber based interface has been formed in the wear track since the small debris particle are being embedded in the soften PEEK matrix. Also, from Figure 4.10 A) for the CF-PEEK tested normal to the fiber direction it can be observed that on one side of the wear track there is a little more counts of alumina and oxygen and thus a decrease in carbon which would imply that in the center of the wear track where the point of contact of the counterface is maximum, more denser carbon fibers are present and on the side of the wear track where there is less applied pressure from the counterface a lower amount of carbon debris are embedded in the PEEK matrix. Finally, for the pure PEEK sample, the elemental distribution in Figure 4.10 D) remain stable across que wear track, as expected, since there is no fiber reinforcement in the sample.

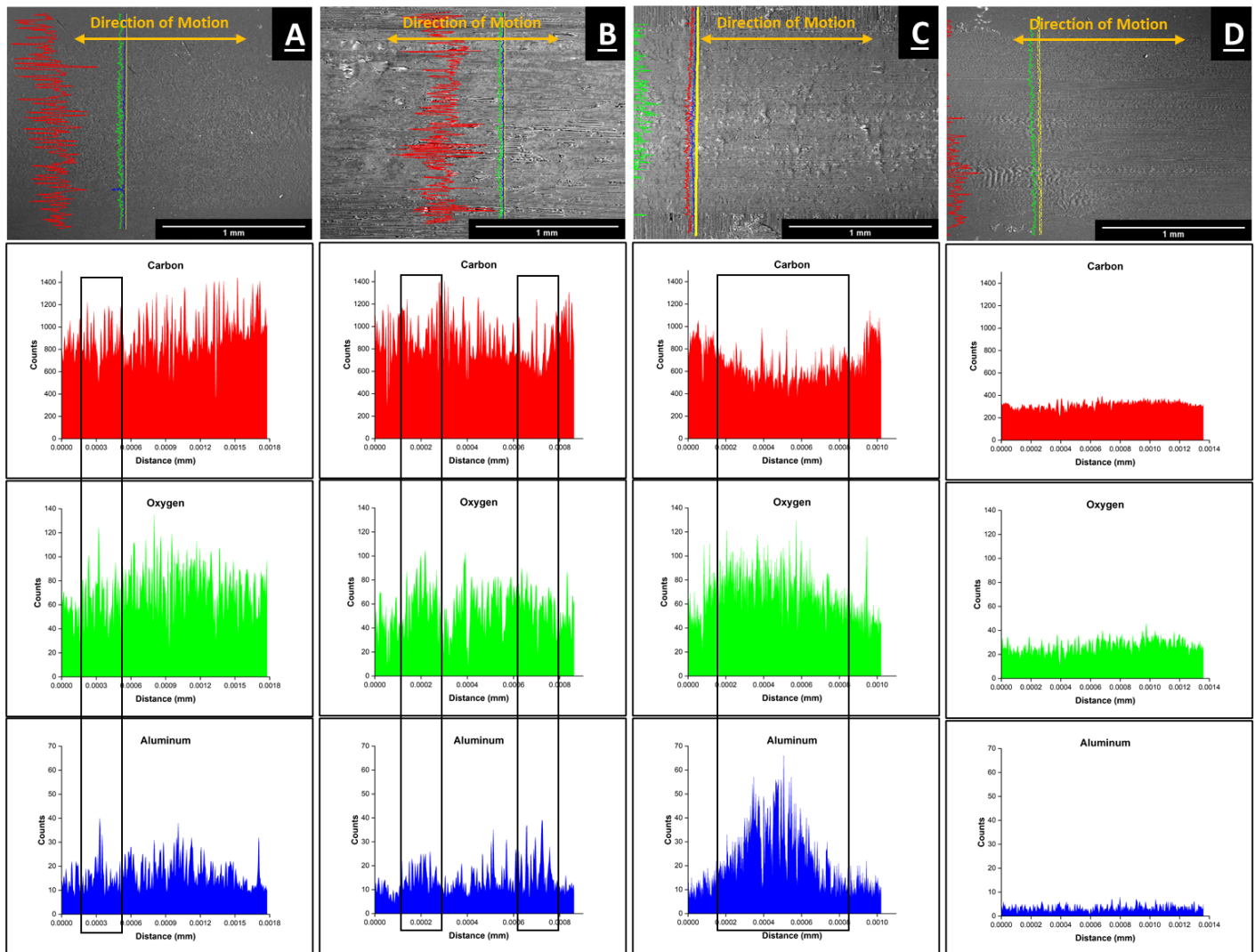


Figure 4.10: EDS Line Analysis of Sample Wear Track at 200°C A) CF-PEEK Normal to the Fiber Direction Sample B) CF-PEEK Parallel to the Fiber Direction Sample C) CF-PEEK Anti-parallel to the Fiber Direction Sample D) Pure PEEK Sample

4.3.5.2. Counterface Analysis

The ex situ analysis of the counterfaces used during the tribometer was also performed in the first place using Confocal Laser Microscopy. Images of the counterfaces contact surface with the samples were taken and are shown in Figure 4.11. From these images, it is possible to observe the presence of a transfer film on the contact surface of all the counterfaces, but the intensity of the transfer film varies based on the sample. In general the formation of a thick and uniform transfer film is caused by the generation of ultra-fine debris particle which leads to better wear performance as the friction between the sample and counterface is lower due to the formation of the film on its surface with similar compounds to the sample being tested. This phenomenon can be observed in the case of the counterface used for the CF-PEEK normal to the fiber direction sample where in Figure 4.11 A) a thick and uniform transfer film has been formed in the center where the applied pressure is maximum during the testing. Additionally, in Figure 4.11 A) for the CF-PEEK tested normal to the fiber direction, it can be observed that there is a lot more ultra-fine debris particles on the counterface which contribute to the formation of the thick and uniform transfer film and thus help to improve the wear performance of the sample. Similarly, on the counterface used for the CF-PEEK parallel to the fiber direction sample in Figure 4.11 C), there is also the presence of a uniform transfer film but of lower thickness than in Figure 4.11 A) which correlates for the higher wear rate observed in Figure 4.6. Alternatively, in the case of the counterface used CF-PEEK tested anti-parallel to the fiber direction samples, Figure 4.11 D), the transfer film is thinner and not as uniform in addition to a lower number of debris particles on the surface which implies that the transfer film is not helping as much in terms of wear performance leading to a significantly higher wear rate of the surface. In a similar manner, the counterface of the pure PEEK sample in Figure 4.11 B) shows a really thin and non uniform transfer film with little to no debris particles on the contact surface leading to lower wear performance explaining the highest wear rate measured in Figure 4.6.

An important observation can also be made from Figure 4.11 of the CF-PEEK samples, which is related to the area of focus on the confocal images. When performing confocal microscopy analysis in order to determine the wear of a surface, similarly to the analysis that was done for the wear track, the focus is made on a plane surface where the laser can measure the depth at different points from where a wear depth measurement can be extracted. In the case of the counterfaces, since they

are Al₂O₃ balls with a curved surface, the focus of the lens is harder to obtain for a full curved surface due to the significant change in depth along the surface which is a recurrent problem with confocal microscopy analysis of curved surfaces [38] [39]. However, since the focus on the ball is made on the flat surface, it can give more information on the wear of the counterface itself. If the width of the area of focus is large, it implies that there is a larger flat surface meaning that the surface of the counterface has been flattened and thus more worn during the tribological testing. This phenomenon can be observed in the case of the counterfaces used on the CF-PEEK parallel and anti-parallel to the fiber direction samples (Figure 4.11 C) and D)) where the area of focus is larger and thus translating in a higher wear of the counterface. On the other hand, the area of focus is smaller for the counterface, in Figure 4.11 A), tested on the CF-PEEK with fibers in the normal direction sample which correspond to a lower wear of the counterface since the surface has not been flattened out as much during the tribological testing.

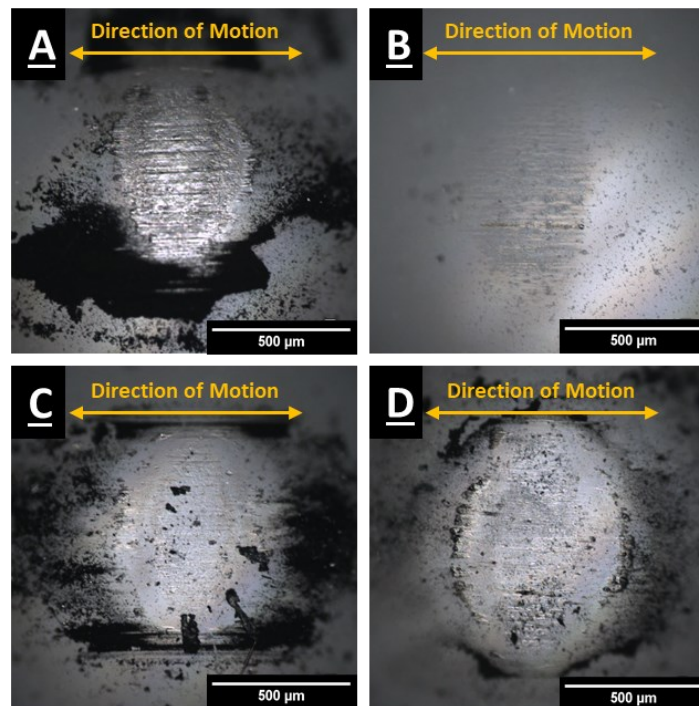


Figure 4.11: Confocal Images of Counterface at 200°C A) CF-PEEK Normal to the Fiber Direction Sample B) Pure Peek Sample C) CF-PEEK Parallel to the Fiber Direction Sample D) CF-PEEK Anti-parallel to the Fiber Direction Sample

Furthermore, SEM images were also taken of the surface of the counterfaces used during the tribometer testing and are shown in Figure 4.12. An interesting observation can be made on the counterface of the CF-PEEK sample tested normal to the fiber direction where it is possible to have a better look at the transfer film and how denser and uniform it is on the surface compared to

the other counterfaces. From the SEM images in Figure 4.12, it was also possible to perform an EDS analysis in order to obtain the elemental distribution of their surfaces and more particularly of the transfer films. The elemental distribution obtained for the different samples transfer films revealed the presence of carbon, oxygen, and aluminum, coming from the carbon fibers and Al_2O_3 counterface, but in different amounts. The results of the elemental distribution of the transfer films on each counterface for the different samples is shown in Figure 4.13. The interesting observation that can be made when comparing the elemental distribution of the different transfer films in Figure 4.13 is when looking at the carbon weight percent. The weight percent of carbon present on the transfer film of the counterface used in the testing of the CF-PEEK normal to the fiber direction sample is significantly higher which implies that the transfer film is denser in carbon and thus correlates with the observation made from the confocal images in Figure 4.11 A). A trend can also be observed in terms of the carbon weight percent present in the transfer films of the different counterfaces and the wear rate measured in Figure 4.6. When the carbon weight percent is highest in Figure 4.13, for the CF-PEEK tested normal to the fiber direction, the wear rate is the lowest in Figure 4.6, alternatively, when the weight percent is the lowest in Figure 4.13, for the pure PEEK, the wear rate is the highest in Figure 4.6 which confirms that a thicker and more uniform transfer film does in fact provides better wear performance.

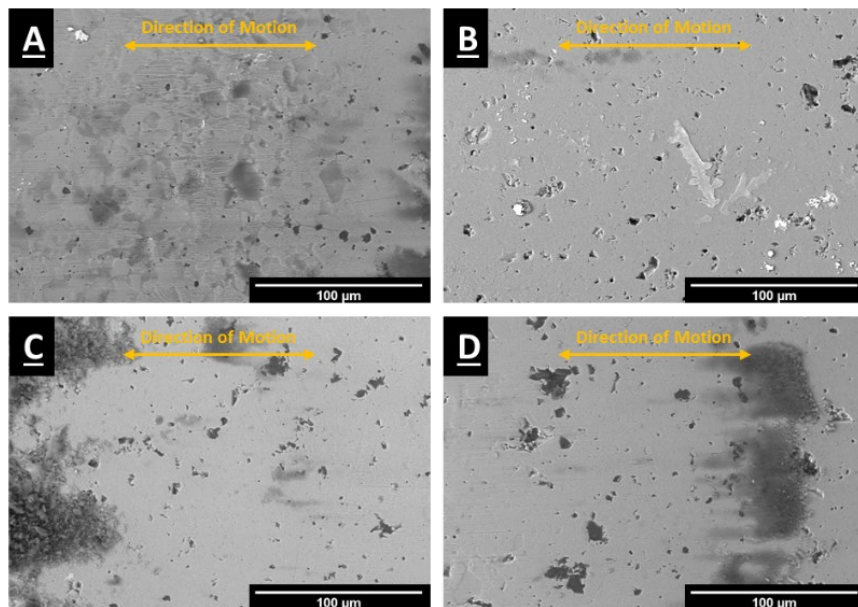


Figure 4.12: SEM Analysis of Samples Counterfaces at 200°C A) CF-PEEK normal to the fiber direction Sample B) Pure Peek Sample C) CF-PEEK Parallel to the Fiber Direction Sample D) CF-PEEK Anti-parallel to Fiber Direction Sample

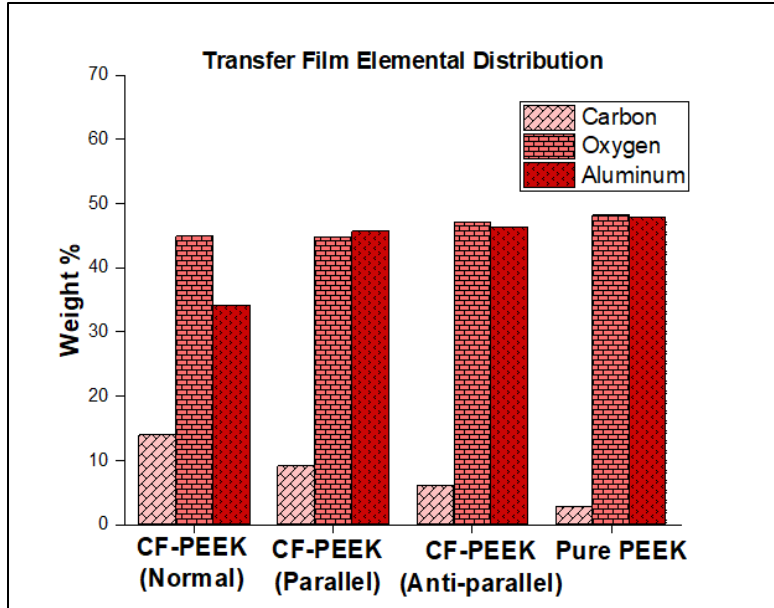


Figure 4.13: EDS Analysis on the Counterfaces at 200°C

4.4. Discussion

The high temperature tribological testing that were performed for the purpose of this study has allowed to fully capture the influence of temperature on the fiber orientation in CF-PEEK and its tribological behavior. To accomplish the purpose of this study, four different samples were tested where three of them were CF-PEEK composites with fibers oriented in the parallel, anti-parallel and normal direction and a pure PEEK sample in order to provide a baseline for the results. The different samples were tribologically tested at a high temperature, 200°C, under high applied loading, 18N, and over a long period of time in order to simulate harsh operating environments of the front of gas turbine engines. From the high temperature tribological testing, the wear and friction behavior were obtained, respectively in Figure 4.4 and Figure 4.6 where it has been revealed that the pure PEEK sample has the highest recorded coefficient of friction and wear rate. In the case of the CF-PEEK samples, the fiber orientation played a significant role in their friction and wear behavior. For the CF-PEEK tested parallel and anti-parallel to the fiber direction, their coefficient of friction at steady-state were equivalent but the average wear rate of the CF-PEEK tested anti-parallel to the fiber direction was higher. However, even if the average wear rate of the CF-PEEK tested parallel to the fiber direction was lower, there existed a large error hysteresis between the tests. Alternatively, the CF-PEEK tested normal to the fiber direction has show the

most potential regarding tribological behaviour and its usage in elevated temperature. From the friction and wear behavior in Figure 4.4 and Figure 4.6, it has been shown that its coefficient of friction is significantly less than the CF-PEEK samples tested parallel and anti-parallel to the fiber direction, but its wear rate is also significantly lower and thus behaving more efficiently.

Furthermore, from literature, PEEK polymers have a glass transition temperature of 143°C where once heated passed this temperature, the amorphous regions in the PEEK polymer gain mobility and secondary intermolecular forces can cause movement and flow of the polymer chains [40]. Due to the samples being subjected to 200°C during the testing, passed the glass transition temperature, it has for effect to soften the PEEK polymer matrix and by consequence to decrease the strength of the matrix creating a weaker surface that when exposed to the repetitive sliding of a counterface would thus increase the wear rate. This phenomenon can be especially observed in the case of the CF-PEEK tested anti-parallel to the fiber direction, where the SEM analysis images have revealed that the fibers have been broken-off in big debris particles during the tribometer testing and pushed outside the wear track leaving a more polymer-based interface and correlating with the higher wear rate obtained in Figure 4.6. Moreover, the breaking-off of the fibers in large debris particles for the CF-PEEK tested anti-parallel to the fiber direction sample limits the formation of a thick and uniform transfer film on the surface of the counterfaces which would typically help reduce the wear and friction. A similar observation can be made for the CF-PEEK tested parallel to the fiber direction where the matrix is exposed, and fibers are absent from the worn surface. Alternatively, for the CF-PEEK reinforced in the normal direction sample, the counterface slides directly across the cross-section of the fibers which limits the formation of large debris particles and thus produces small debris particles. Since the PEEK matrix is softening when subjected to 200°C, the small debris particles get embedded into the matrix to form a fiber-based interface. The fiber-based interface causes strain hardening of the worn surface which limits the deformation of the surface and makes it more resistant to local shear. Consequently, when the counterface repeatedly slides on the surface of the CF-PEEK reinforced in the normal direction, it creates a three bodies abrasion where a thick and uniform transfer film is formed in between the worn surface and the counterface. The transfer film is developed by the transfer of ultra-fine debris particles layering-up during the run-in of the two hard surfaces together to form a thick and uniform transfer film as represented in Figure 4.14. The presence of the transfer film on the surface of the

counterface contributes to a lower wear, in Figure 4.6 of the CF-PEEK reinforced in the normal direction sample.

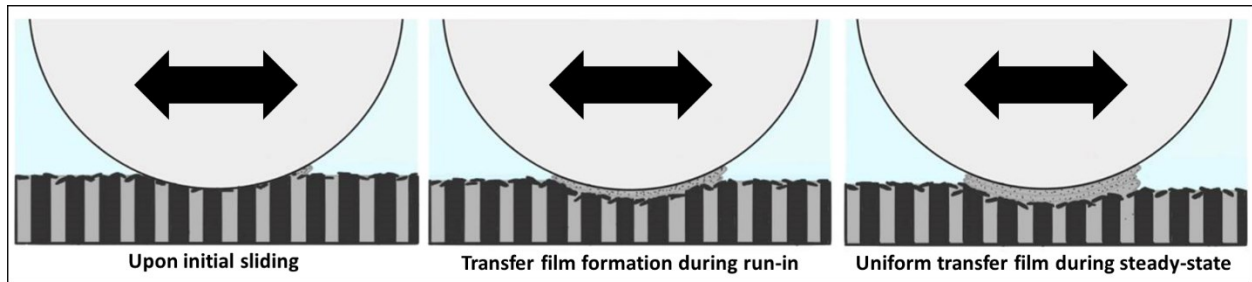


Figure 4.14: Pictorial representation of a transfer film formation on a counterface

Moreover, from the EDS analysis of the transfer films present on the surface of the counterfaces and the EDS analysis of the wear track of the samples, it was possible to observe a correlation concerning the present elemental distribution. In the case of the CF-PEEK tested normal to the fiber direction, the wear track revealed really low presence of alumina and the transfer film revealed a high presence of carbon which confirms that the transfer film is thicker and more uniform and contributes to the lower wear. On the other hand, for the CF-PEEK tested anti-parallel to the fiber direction, there was a high presence of alumina in the center of the wear track and a low presence of carbon on the transfer film. Similarly, for the CF-PEEK tested parallel to the fiber direction, the wear track revealed a higher presence of alumina in polymer-based interface regions and an overall lower quantity of carbon present in its transfer film compared to the CF-PEEK tested normal to the fiber direction. Based on the optical and elemental analysis on the counterfaces, it appears that the counterface wear is higher for the CF-PEEK unidirectional tape sample (ie. Anti-parallel and parallel direction) when compared to the CF-PEEK with fibers oriented in the normal direction. It is also important to consider that since components within the engines are part of moving assemblies, not only the wear of the component made of CF-PEEK is important to consider, but also the wear of the contacting part. The premature wear of the contacting part could lower the lifetime of a moving assembly within the engines by increasing the risk of unpredictable failures.

Additionally, it is important to observe the high instability of the CF-PEEK tested parallel to the fiber direction from the results obtained in the wear behavior and ex-situ analysis. A large deviation in the wear rate results obtained in Figure 4.6 combined with the mechanics of damages (delamination and fiber cracks) found inside the wear track, makes the wear behaviour of the CF-PEEK tested parallel to the fiber direction sample not reliable since there is a large hysteresis error

between one the results obtained from one test to another. The reliability of a material is important in the aerospace industry and especially when it comes to gas turbine engines. There exists a large number of complex contacting moving assemblies in the engines where the reliability of each component is extremely important in order to ensure good operations of the engines. Thus, there cannot exits an uncertainty in the behavior of a material used for the manufacturing of components within the engines and especially with tribological interfaces, such as bearing and seals, where low friction and wear of the components is essential. The premature wear could decrease the lifetime of components leading to failure and thus increase the operational and maintenance cost. Hence, due to the unreliability at high temperatures of CF-PEEK tested parallel or anti-parallel to the fiber direction, this material would not be suitable for aerospace applications. On the other hand, the high reliability and good tribological properties at high temperatures, 200°C, of CF-PEEK reinforced in the normal direction makes it a competitive alternative to more conventional metals or alloys for the manufacturing of components operating in the front of the engines as well as permitting an easy integration since the direction of sliding of moving components on its surface does not matter.

4.5. Conclusion

In conclusion, through this study it was possible to obtain a better understanding of the effect of fiber orientation in FRP, more specifically in CF-PEEK, and its tribological behavior when subjected to high temperatures. The parallel, anti-parallel and normal fiber orientation in CF-PEEK were tribologically tested and compared to pure PEEK as a baseline for comparison. The wear and friction behavior as well as the ex situ analysis (SEM, EDS, AFM, Confocal Laser Microscopy) of the worn surfaces and counterfaces has allowed the accurate characterization of each sample. The pure PEEK and CF-PEEK tested anti-parallel to the fiber direction have showcased the first and second higher, respectively in that order, wear rate due to worn surface being more a polymer-based interface limiting the formation of a transfer film. The CF-PEEK tested parallel to the fiber direction had a lower wear rate but the hysteresis in the results obtained between the different testing makes it an unreliable material and thus would not be suitable for aerospace applications within the engines where the reliability of components is essential. Finally, the CF-PEEK sample that showcased the lowest wear rate and most suitable tribological properties at high temperatures was the CF-PEEK sample with fibers oriented in the normal direction. Thus, the CF-PEEK where the fibers are in the normal direction is a more advantageous options since it is not fiber orientation dependent and can easily be integrated as well as having competitive tribological performance to current conventional metal or alloys present in components of the front of the gas turbine engines.

4.6. References

- [1] P. Stoyanov, K. Harrington and A. Frye, "Insights into the Tribological Characteristic of CU-Based Coatings Under Extreme Contact Conditions," JOM, vol. LXXII, p. 2191–2197, 2020.
- [2] A. Komshin and V. Pronyakin, "Modern Diagnostics of Aircraft Gas Turbine Engines," in IOP Conference Series: Materials Science and Engineering, Moscow, 2019.
- [3] A. El-Sayed, Aircraft Propulsion and Gas Turbine Engines, Boca Raton: CRC Press, 2017.
- [4] P. Stoyanov, A. Wusatowska-Sarnek and T. Kaspro, "International Conference on Metallurgical Coatings and Thin Films," in ICMCTF, San Diego, 2018.
- [5] W. Cullinane and R. Strange, "Gas turbine engine validation instrumentation: measurements, sensors, and needs," Proceedings, vol. MMMDCCCLII, no. Harsh Environment Sensors II, 1999.
- [6] L. Amoo, "13 - On a selection of the applications of thermodynamics," in Applications of Heat, Mass and Fluid Boundary Layers, Woodhead Publishing Series in Energy, 2020, pp. 383-412.
- [7] P. Spittle, "Gas Turbine Technology," Physics Education, vol. XXXVIII, no. 6, pp. 504-511, 2003.
- [8] E. Benini, Advances in Gas Turbine Technology, Rijeka: InTech, 2011.
- [9] G. Kear and E. Thompson, "Aircraft Gas Turbine Materials and Processes," SCIENCE, vol. CCVIII, no. 4446, pp. 847-856, 1980.
- [10] G. Meetham, "High temperature materials in gas turbine engines," Materials & Design, vol. VIII, no. 4, pp. 213-219, 1988.
- [11] T. Canada, "CANADA'S ACTION PLAN to Reduce Greenhouse Gas Emissions from Aviation," Public Works and Government Services Canada, Ottawa, 2012.
- [12] E. a. C. C. Canada, "2030 EMISSIONS REDUCTION PLAN Canada's Next Steps for Clean Air and a Strong Economy," Gatineau, 2022.

- [13] U. D. o. Transportation, "United States 2021 Aviation Climate Action Plan," 2021.
- [14] N. Yilmaz and A. Atmanli, "Sustainable alternative fuels in aviation," *Energy*, vol. CXL, no. 2, pp. 1278-1386, 2017.
- [15] M. Hasan, A. Mamun, S. Rahman, K. Malik, M. Al Amran, A. Khondaker, O. Reshi, S. Tiwari and F. Alismail, "Climate Change Mitigation Pathways for the Aviation Sector," *Sustainability*, vol. XIII, no. 7, p. 3656, 2021.
- [16] X. Wu, W. Beres and S. Yandt, "Challenges in life prediction of gas turbine critical components," *Canadian Aeronautics and Space Journal*, vol. LIV, no. 2, pp. 31-39, 2008.
- [17] R. Kurz and K. Brun, "Degradation in Gas Turbine Systems," *J. Eng. Gas Turbines Power*, vol. CXXIII, no. 1, pp. 70-77, 2001.
- [18] H. Bernstein, "Materials Issues For Users Of Gas Turbines," in *Turbomachinery Symposium 35th*, Texas, 2006.
- [19] S.-J. Park and M.-K. Seo, "Chapter 7 - Types of Composites," *Interface Science and Technology*, vol. XVIII, pp. 501-569, 2011.
- [20] C. Soutis, "Fibre reinforced composites in aircraft construction," *Progress in Aerospace Sciences*, vol. XLI, no. 2, pp. 143-151, 2005.
- [21] C. Soutis, "Carbon fiber-reinforced plastics in aircraft construction," *Materials Science and Engineering: A*, vol. CDXII, no. 1-2, pp. 171-176, 2005.
- [22] B. Wang and H. Gao, "Fibre Reinforced Polymer Composites," *Advances in Machining of Composite Materials*, pp. 15-43, 2021.
- [23] S. Das, "Life cycle assessment of carbon fiber-reinforced polymer composites," *The International Journal of Life Cycle Assessment*, vol. XVI, pp. 268-282, 2011.
- [24] F. Bassani, G. L. Liedl and P. Wyder, *Encyclopedia of Condensed Matter Physics*, Academic Press, 2005.
- [25] K. Friedrich, "Polymer composites for tribological applications," *Advanced Industrial and Engineering Polymer Research*, vol. I, no. 1, pp. 3-39, 2018.

- [26] S. Aliukov, K. A.V. and A. Nikonov, "Polymer composite materials and their application in designs of gas turbine engine," in 4th International Conference on Condensed Matter and Materials Physics, London, 2018.
- [27] P. Balakrishnan, M. John, L. Pothen, M. Sreekela and S. Thomas, "12 - Natural fibre and polymer matrix composites and their applications in aerospace engineering," in *Advanced Composite Materials for Aerospace Engineering*, Woodhead Publishing, 2016, pp. 365-383.
- [28] X. Pei, W. Han, G. Ding, M. Wang and Y. Tang, "Temperature effects on structural integrity of fiber-reinforced polymer matrix composites: A review," *Journal of Applied Polymer Science*, vol. CXXXVI, no. 45, p. 48206, 2019.
- [29] X. Centrich, E. Shehab, P. Sydor, T. Mackley, P. John and A. Harrison, "An Aerospace Requirements Setting Model to Improve System Design," *Procedia CIRP*, vol. XXII, pp. 287-292, 2014.
- [30] C. B., J. Gu, Z. Long, Z. Li, S. Ruan and C. Shen, "Effects of temperature and fiber orientation on the tensile behavior of short carbon fiber-reinforced PEEK composites," *Polymer Composites*, no. 42, pp. 597-602, 2021.
- [31] A. Abdelbary and Y. Mohamed, "Chapter 4 - Tribological behavior of fiber-reinforced polymer composites," in *Tribology of Polymer Composites*, Elsevier, 2021, pp. 63-94.
- [32] P. Sarath, R. Reghunath, J. Haponiuk, S. Thomas and S. George, "Tribology of Fiber-reinforced Polymer Composites: Effect of Fiber Length, Fiber Orientation, and Fiber Size," in *Tribological Applications of Composite Materials*, Springer, 2021, pp. 99-117.
- [33] H. Parikh and P. Gohil, "Tribology of fiber-reinforced polymer," *Journal of Reinforced Plastics*, pp. 1-7, 2016.
- [34] T. A. C. 'TORAY', "Toray Cetex® TC1200," 13 November 2019. [Online]. Available: <https://www.toraytac.com/product-explorer/products/ov14/Toray-Cetex-TC1200>. [Accessed 11 January 2022].

- [35] G. Gardiner, "Z-direction composite properties on an affordable, industrial scale," Veelo Technologies, 20 april 2021. [Online]. Available: <https://www.compositesworld.com/articles/z-direction-composite-properties-on-an-affordable-industrial-scale>. [Accessed 28 january 2022].
- [36] Nanosurf, "Nanomechanical Indentation Measurements with Force Spectroscopy," AZO NANO, 05 11 2020. [Online]. Available: <https://www.azonano.com/article.aspx?ArticleID=5579>. [Accessed 04 2022].
- [37] K. Holmberg and A. Matthews, *Coatings Tribology; Properties, Mechanisms, Techniques and Applications in Surface Engineering Second Edition*, Amsterdam: Elsevier, 2009.
- [38] M. Rahlves, B. Roth and E. Reithmeier, "Systematic errors on curved microstructures caused by aberrations in confocal surface metrology," *Opt Express*, vol. XXIII, no. 8, 2015.
- [39] J. Béguelin, T. Scharf, W. Noell and R. Voelkel, "Correction of spherical surface measurements by confocal microscopy," *Measurement Science and Technology*, vol. XXXI, no. 7, 2020.
- [40] S. Kurtz, *PEEK biomaterials handbook*, Elviser and William Andrew Applied Science Publishers, 2019.
- [41] G. W. Stachowiak and A. W. Batchelor, *Engineering Tribology*, Burlington: ELSEVIER, 2005.

Chapter

5. Conclusion & Future Work

In this chapter...

The final conclusions and proposal for future work regarding the use of carbon fiber-reinforced PEEK in the aerospace industry is presented.

5.1. Conclusion

Fiber-reinforced polymer (FRP) composites have been widely used in the aerospace industry but their use in gas turbine engines has been limited due to, among other reasons, the effect of temperature and fiber orientation on their tribological properties. In the past, tribological studies has been performed on the impact of fiber orientation on the tribological properties of FRP, especially in in the parallel and anti-parallel direction, but little studies have focused on the impact of the normal orientation and temperature on FRP. This study was divided into two different sections. Firstly, the influence of fiber direction on the tribological behavior of carbon reinforced PEEK for application in gas turbine engines and secondly, the influence of temperature and fiber orientation on the tribological behavior of carbon reinforced PEEK for application in gas turbine engines.

In the first part, it was demonstrated that aside from the pure PEEK, the CF-PEEK tested parallel to the fiber direction had the highest wear rate followed by the CF-PEEK tested normal to the fiber direction. The CF-PEEK tested anti-parallel to the fiber direction showed the lowest wear rate. However, for applications in gas turbine engines, and more specifically due to the large amount of contacting and moving assembly, a material such as CF-PEEK unidirectional tape (parallel and anti-parallel) would not be the most suitable option since it is anisotropic and its tribological properties are greatly impacted by the orientation of the fibers. Consequently, this adds a complexity for its integration withing the engines. Thus, CF-PEEK with fibers oriented in the normal direction would be the optimal option for implementation within gas turbine engines due to its competitive tribological properties and ease of integration withing contacting and moving assemblies since it is not fiber orientation dependent.

In the second part, it was demonstrated that at an elevated temperature, 200°C, the tribological performance of the CF-PEEK unidirectional tape (parallel and anti-parallel) was not sufficient for applications in the hotter section of gas turbine engines (e.g. LPC). More specifically, the CF-PEEK tested anti-parallel to the fiber direction showed the highest wear rate and the CF-PEEK tested parallel to the fiber direction had a high hysteresis error between the different tests, making it an unreliable option as well. In addition, since the precision in the operations of components is

high within the aerospace industry, and especially in gas turbine engines, the premature wear of components cannot be left unknown. Consequently, CF-PEEK reinforced with fibers in the normal direction is the most suitable option for tribological interfaces within the engines at higher temperatures since it provides excellent tribological properties and a good reliability.

A final observation can be made concerning the effect of the fiber orientation on FRP, and in this case for CF-PEEK, relating the findings made in the first and second part of this study. Throughout the tribological evaluation, it has been found with SEM analysis that certain wear tracks have more of a polymer-based interface whereas others have fiber-based interface. It has been shown through prior studies that with increasing temperatures, [1]. This indicates that when the PEEK matrix has been heated above its glass transition temperature, which is the case in this study, fiber pullout is bound to happen, which weakens the sample material and increase fracture strains [1]. Consequently, the fibers of a unidirectional CF-PEEK composite, when subjected to a temperature above its glass transition, the anisotropy of CF-PEEK unidirectional tape (parallel and anti-parallel) is matrix dominated are broken-off and being pulled out which is decreasing the amount of support the fibers are providing to the composite, decreasing the overall strength, against the applied load of the counterface and thus increasing the wear. Alternatively, for CF-PEEK reinforced with fibers in the normal direction, since the counterface is sliding on the cross-section of the fibers, it is lowering the risk of fiber pullout and strain fractures by creating a fiber-based interface with small debris particles being embedded in the matrix and thus ensuring the structural integrity of the composite and good strength properties since the support of the fibers is maintained.

In conclusion, for the purpose of long-lasting gas turbine engines, there is a clear benefit of using CF-PEEK reinforced with fibers in the normal direction since it showcases better tribological properties, a higher reliability and higher potential of integrations within the engine.

5.2. Future work

Subsequently to the tribological evaluation of the effect of fiber orientation in CF-PEEK, and more precisely after obtaining the results from AFM analysis regarding the adhesion force (Figure 3.10), an additional analysis of contact angle measurement was performed. The contact angle measurement analysis was performed to have a better understanding of the effect of the fiber orientation in CF-PEEK composite in relation to the hydrophobicity of a surface. From the AFM analysis, the CF-PEEK tested normal to the fiber direction had a significantly lower adhesion force than the CF-PEEK tested parallel & anti-parallel to the fiber direction. A lower adhesion force indicates that materials or substances adheres less to the surface and thus could lead to a surface that is more hydrophobic.

Contact angle measurement analysis is performed by dropping a droplet of water on the surface of a sample, using a tube, in order to wet it and then sucking back the water inside the tube in order to de-wet the surface. The angle the water droplet makes with the horizontal plane after it has stopped moving on the surface can give a better idea of surface energy of the sample and thus how hydrophobic the surface is. From literature, when the droplet of water makes an angle above 90 degrees with the horizontal plane, the surface is said to be more hydrophobic whereas when the droplet of water makes an angle below 90 degrees with the horizontal plane, the surface is said to be more hydrophilic [2] [3].

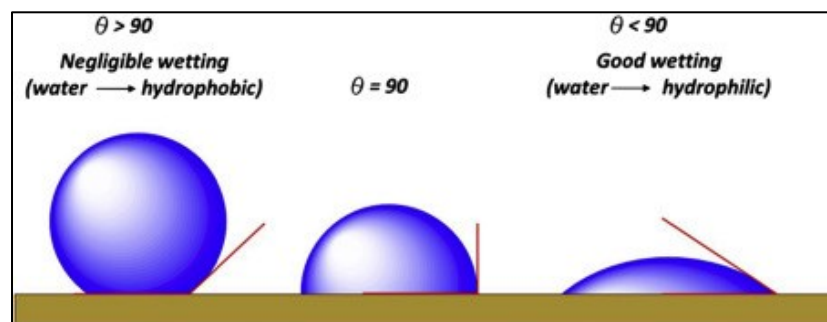


Figure 5.1: Interpretation of contact angle measurement results for hydrophobicity [2]

In addition, while performing a contact angle measurement, the advancing and receding angles can be measured and used to measure the critical force for line contact movement [4] [5]. The advancing angle is the angle the droplet of water makes with the horizontal plane during the wetting of the sample once the water stops moving on the surface [4]. On the other hand, the

receding angle is the angle the droplet of water makes with the horizontal plane during the de-wetting of the sample once the water starts moving back on the surface [4].

The contact angle measurement was performed on the CF-PEEK normal to the fiber orientation sample and the CF-PEEK parallel & anti-parallel (unidirectional) sample. The results of the advancing contact angles measurement, circled in red, are shown in Figure 5.2. It can be observed that the advancing angle for the Cf-PEEK parallel & anti-parallel to the fiber direction sample is larger than the advancing angle of the CF-PEEK normal to the fiber direction sample. For both samples, the advancing contact angle is above 90 degrees which showcases hydrophobicity properties. In addition, the results of the receding contact angle measurement, circled in red, are shown in Figure 5.3. In this case, the receding angle of the CF-PEEK normal to the fiber direction sample is larger than the CF-PEEK parallel and anti-parallel to the fiber direction sample which indicates that the water has started to move back faster on the surface of the sample.

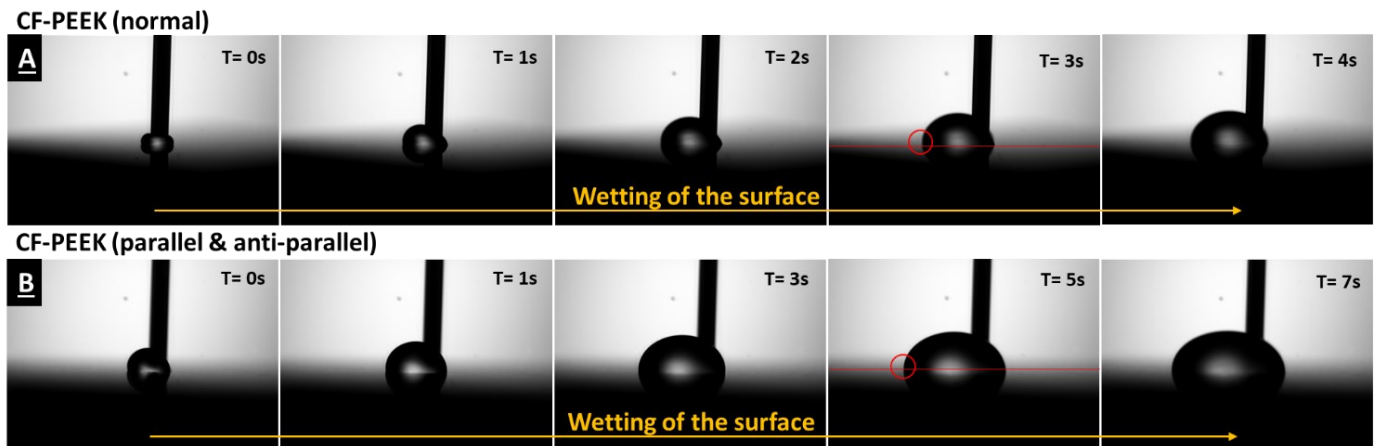


Figure 5.2: Advancing angle measurement A) CF-PEEK (normal) sample B) CF-PEEK (parallel and anti-parallel) sample

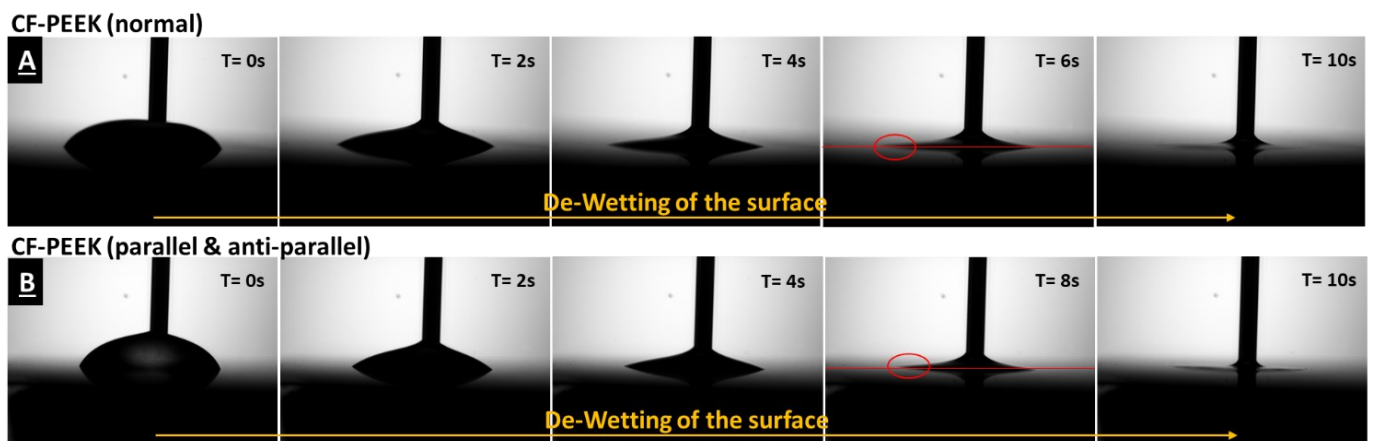


Figure 5.3: Receding angle measurement A) CF-PEEK (normal) sample B) CF-PEEK (parallel and anti-parallel) sample

From the advancing and receding contact angle measurement obtained in Figure 5.2 and Figure 5.3, the critical force for contact line movement can be obtained. The critical force for contact line movement is defined as the force required to start moving a droplet of water on a surface [4]. The critical force for contact line movement (F) is a function of the liquid surface tension (γ_{lv}), the receding contact angle (θ_R) and the advancing contact angle (θ_A) which can be seen in Equation 1 [4]:

$$F = \gamma_{lv}(\cos \theta_R - \cos \theta_A) \quad (1) [4]$$

Since for both samples the contact angle measurement analysis was performed with the same liquid (water), the ratio of the force over the liquid surface tension was calculated and is shown in Figure 5.4. The ratio of the force over the liquid surface tension is significantly lower for the CF-PEEK normal to the fiber direction sample compared to the CF-PEEK parallel and anti-parallel to the fiber direction sample. This indicates that the surface of the CF-PEEK with fibers oriented in the normal direction is a more hydrophobic surface since it requires less force to move the water on the surface and relates back to the lower adhesion force measured for this sample.

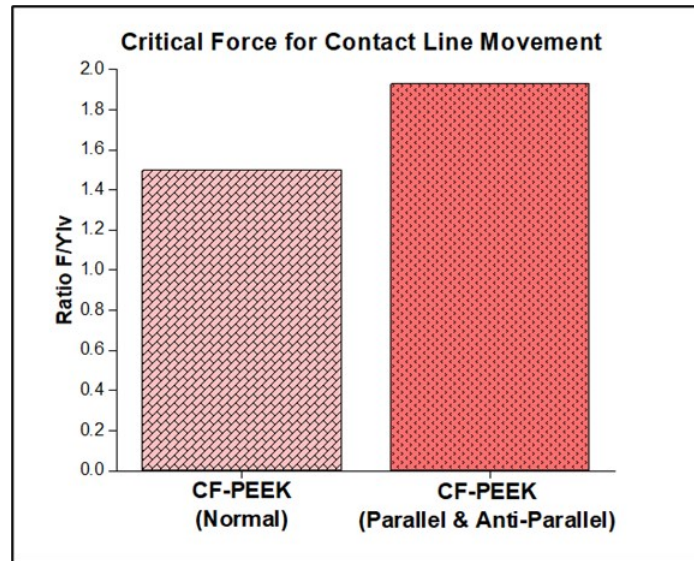


Figure 5.4: Critical force for contact line movement

Overall, the finding made concerning the CF-PEEK normal to the fiber direction sample showcases a potential regarding aircraft icing problems since it leads to believe that ice could adhere less to surfaces made out of this material. Additional tribological evaluations at low icing temperatures and ice adhesion testing could be performed in the future on the CF-PEEK with fibers oriented in the normal direction in order to examine more closely its potential regarding aircraft icing.

5.3. References

- [1] B. Chang, J. Gu, Z. Long, Z. Li, S. Ruan and C. Shen, "Effects of temperature and fiber orientation on the tensile behavior of short carbon fiber-reinforced PEEK composites," *Polymer Composites*, no. 42, pp. 597-607, 2020.
- [2] R. Hebbar, A. Isloor and A. Ismail, "Chapter 12 - Contact Angle Measurements," in *Membrane Characterization*, Elsevier, 2017, pp. 219-255.
- [3] A. C. Society, "Definitions for Hydrophilicity, Hydrophobicity, and Superhydrophobicity: Getting the Basics Right," *Physical Chemistry Letters*, vol. V, pp. 686-688, 2014.
- [4] A. Rudawska, "9 - Assessment of surface preparation for the bonding/adhesive technology," in *Surface Treatment in Bonding Technology*, Academic Press, 2019, pp. 227-275.
- [5] H.-G. Wei, H.-K. Tsao and K.-C. Chu, "Slipping moving contact lines: critical roles of de Gennes's 'foot' in dynamic wetting," *Journal of fluid dynamics*, vol. DCCCLXXIII, pp. 110-150, 2019.